Spring 2024

Dissecting The Tissue-Specific Contributions To Seizures, Cardiorespiratory Dysfunction, And Sudden Death In The Kv1.1 Mouse Model Of Epilepsy Using Conditional Knockout Approaches

Kelsey Paulhus
kpaulhus@smu.edu

DISSECTING THE TISSUE-SPECIFIC CONTRIBUTIONS TO SEIZURES,

CARDIORESPIRATORY DYSFUNCTION, AND SUDDEN DEATH

IN THE KV1.1 MOUSE MODEL OF EPILEPSY USING

CONDITIONAL KNOCKOUT APPROACHES

Approved by:

_____

Dr. Edward Glasscock
Associate Professor
Prothro Distinguished Chair
Graduate Director
Southern Methodist University

_____

Dr. Amy Brewster
Associate Professor
Southern Methodist University

_____

Dr. Franck Kalume
Associate Professor, Neurological Surgery
Adjunct Associate Professor, Global Health
Adjunct Associate Professor, Pharmacology
University of Washington

_____

Dr. Adam Norris
Assistant Professor
Southern Methodist University
University of California Riverside

DISSECTING THE TISSUE-SPECIFIC CONTRIBUTIONS TO SEIZURES, CARDIORESPIRATORY DYSFUNCTION, AND SUDDEN DEATH IN THE KV1.1 MOUSE MODEL OF EPILEPSY USING CONDITIONAL KNOCKOUT APPROACHES

A Dissertation Presented to the Graduate Faculty of the

Dedman College

Southern Methodist University

in

Partial Fulfillment of the Requirements

for the degree of

Doctor of Philosophy

with a

Major in Molecular and Cellular Biology

by

Kelsey Paulhus

B.S., Biology, Texas Christian University
M.S., Biology, Texas Christian University

May 11, 2024

ACKNOWLEDGMENTS

There would be no dissertation without the people I have been surrounded with during my time at SMU. To my mentor Dr. Glasscock, I do not have the right words to thank you for everything you have done. When I came into your lab via “unique” circumstances, I had nearly given up on science. You helped me find my love for research again and become a better writer, scientist, and person. Fallon, you are an elite human being and someone who has made me laugh more times in lab than I can count. I appreciate you always being willing to help me and be a listening ear when I desperately needed one. Man Si, we have been together since day one when the lab moved to SMU, and I am so grateful I got to work with you! Sayumi and Ayesha, you both came into my lab journey a little more recently, but all the same I could not have done this without you. You both are fantastic scientists, and I cannot wait to see what you both accomplish in the future. Lastly, to my intelligent and wildly talented group of undergraduate girls Maxine, Frederica, Ellen, Regina, and Amy. You are all so incredibly brilliant, and I could not have asked for harder working people to help me accomplish parts of my work.

To my family, there truly are not enough words. To my mom who kept my life outside the lab together during the dissertation chaos and who has been by my side since I started my science career. To my brother, Scott, who has read everything I have ever published and who set the sibling bar so high. To my husband, Austin, who has been my emotional support, listening ear, sounding board, and best friend. I love you all more than an acknowledgement can express. This dissertation is as much yours as it is mine.

Paulhus, Kelsey B.S., M.S., Biology, Texas Christian University

Dissecting the Tissue -Specific Contributions to Seizures
Cardiorespiratory Dysfunction, and Sudden Death
In the Kv1.1 Mouse Model of Epilepsy Using
Conditional Knockout Approaches

Advisor: Dr. Edward Glasscock

Doctor of Philosophy conferred May 11, 2024

Dissertation completed May 3, 2024

Sudden unexpected death in epilepsy (SUDEP), the primary cause of mortality in epilepsy, remains poorly understood. Studies suggest seizures may trigger dangerous signals affecting the heart and lungs leading to collapse and death. The Kv1.1 deficiency mouse model mirrors clinical SUDEP cases, showing spontaneous seizures, cardiorespiratory issues, and premature death. However, this model lacks regional specificity in Kv1.1 deletion, hindering insights into SUDEP's mechanisms and anatomical substrates.

This dissertation employs three distinct conditional knockout (cKO) techniques to investigate the individual roles for the forebrain, brainstem, and heart in SUDEP related phenotypes. The findings reveal that the forebrain alone can trigger spontaneous seizures and premature death. Additionally, the brainstem may play a significant role in regulating blood oxygen levels and may show gender differences in respiratory measures. Lastly, Kv1.1 in the heart is essential for cardiomyocyte action potential repolarization but does not significantly impact overall cardiac function measured in mice. This research highlights how distinct brain circuits contribute to SUDEP mechanisms, providing insights specifically for researchers using the Kv1.1 deficiency model as to where the crucial anatomical substrates may be found in future studies.

TABLE OF CONTENTS

LIST OF FIGURES

LIST OF TABLES

For my dad, who loved me harder than anyone. We did it.

CHAPTER 1

INTRODUCTION

1.1 Epilepsy

A quick PubMed search for "seizure" will pull up results dating back to 1849 and searching "epilepsy" results in publications even farther back into our history to 1781. These dates don't even get close to the real origins of epilepsy though as this disorder has been documented since ancient times. The first mention of epilepsy can be traced back to Mesopotamia where a 4000-year-old tablet holds a record of what is now known as a seizure (Kaculini et al., 2021; Labat, 1951). The Babylonians were the next to have documentation of seizures, and this record was more comprehensive including categorizing different kinds of seizures and mentions of outcomes based on seizure type (Kaculini et al., 2021). In these most ancient times, these episodes were believed to be the work of spirits or gods so caring for individuals with seizures mainly boiled down to spiritual or religious intervention (Kaculini et al., 2021; Reynolds, 2005a). This belief stood for a long time and generated a negative stigma around those with epilepsy, but Hippocrates began the line of thinking to change this stigma around the 5th century BC when he suggested epilepsy was a heritable disease of the brain (Kaculini et al., 2021; Magiorkinis et al., 2010). Electrical activity in the brain became part of the discussion in the mid-1800s, but not until Hans Berger invented the human electroencephalogram in 1924 was this confirmed and the true underpinning of epilepsy discovered (Binder et al., 2011; Kaculini et al., 2021; Reynolds, 2005a). Despite the work of Hans Berger showing that evil spirits were not in fact the cause of seizures, people with epilepsy face unfair hardships even into the modern day. Marriage restrictions, suggestions for sterilization, and

refusal of service from public restaurants were common in the Unites States until the mid-20th century (Epilepsy Foundation of America, n.d.; Kaculini et al., 2021; Reynolds, 2005b, 2005a).

Today, we know epilepsy as being one of the most common neurological disorders impacting more than 3 million adults and 450,000 children in the US alone (Zack & Kobau, 2017). Epilepsy is defined as having at least two unprovoked seizures occurring more than 24 hours apart, one unprovoked seizure with the probability of further seizures (at least 60%) over the next 10 years, or a diagnosis of an epilepsy syndrome (Fisher et al., 2014). Epilepsy can arise from a number of different causes including genetic/familial causes, brain injury, brain infection, metabolic disorder, tumors, and even idiopathic causes. Idiopathic epilepsy, which by definition has no known cause, is prevalent, and in the US alone accounts for at least 150,000 new cases annually (Feigin et al., 2021).

Epilepsy is defined as a chronic disorder of recurrent and unprovoked seizures, but what are seizures? Seizures are the behaviors underlying epilepsy and result from synchronous and inappropriate electrical signals in the brain. These signals can lead to transient behaviors such as loss of consciousness, body tremors, hallucinations and more. The brain is made up of more than 80 billion neurons that participate in various neurocircuits which, when properly functioning, reach a homeostatic balance of excitation and inhibition (Azevedo et al., 2009; Helmuth, 2001; Nishiyama et al., 2005; Williams & Herrup, 1988). When the balance shifts and excitation is greater than inhibition, seizures can manifest (Scharfman, 2007). At the cellular level, this shift can arise from a variety of sources including depression of inhibitory GABAergic synapses, facilitation of excitatory glutamatergic synapses, alteration of neurotransmitter release and reuptake, and dysregulation of ionic concentrations both inside and outside the cell (Bracci et al., 2001; Deng et al., 2014; Jane et al., 2009; Lazarevic et al., 2013; Letts et al., 1998; Rajakulendran

et al., 2012; Staley, 2015; Veeramah et al., 2013; Yokoi et al., 2012). While the list appears comprehensive, we still do not completely understand the cellular underpinnings of epilepsy.

Much of epilepsy research has focused on treatment, and at least half of those with epilepsy benefit from this with partial or full remission of seizures. Significantly, however, at least 1/3 of those with epilepsy will fail to find one or a combination of drugs that can provide seizure freedom. In fact, a Centers for Disease Control (CDC) progress report for the years 2012-2022 showed that in the United States less than half of people taking epilepsy medication were wholly seizure free (Centers for Disease Control and Prevention, 2022). As epilepsy has a myriad of causes, there is no "one size fits all" treatment. Both pharmacological treatments and non-pharmacological strategies, such as vagal nerve stimulation and deep brain stimulation, seek to restore the electrical imbalances in the brain (Riva et al., 2021). Antisense oligonucleotides (ASOs) are another incredibly promising avenue for treating genetic epilepsies by fine-tuning control and restoration of proper gene expression (Dias & Stain, 2002; J. Kim et al., 2019; Matos et al., 2018). Ultimately, the gold standard for epilepsy treatment would be to specifically tailor therapeutics to a patient's genetics and environment, while also considering their comorbidities, but research is currently not yet capable of this.

1.2 SUDEP

Epilepsy can be lethal and epilepsy-related death can take many forms. For example, epilepsy can cause death due to accidental drowning/suffocation during a seizure, status epilepticus, or seizure-related fatal injury. There is also a version of epilepsy-related death in which a person with epilepsy, who is otherwise healthy, dies with no other cause of death revealed by autopsy (Nashef

et al., 2012). This type of death, known as sudden unexpected death in epilepsy (SUDEP), is the primary cause of mortality among individuals with epilepsy (Harden et al., 2016; Ryvlin et al., 2019; Thurman et al., 2014). In fact, the risk of sudden death in people with epilepsy is 20 times greater than the age-matched general population (Mesraoua et al., 2022; Thurman et al., 2014; Whitney & Donner, 2019). Despite focused efforts towards understanding SUDEP, clinicians are unable to stratify risk between different people with epilepsy nor do they have any viable biomarkers which could help towards this effort. Furthermore, as the brain is a complex organ with billions of neurons and synapses, research also seeks to understand the anatomical substrates which may be playing central roles in SUDEP mechanisms and therefore could be specifically targeted by therapeutics. While research has not been able to completely describe the pathological events underlying SUDEP, several risk factors have been revealed. These include the presence of frequent generalized tonic-clonic seizures, intractable epilepsy, seizures at night, young onset of seizures, long seizure duration, and a long history with epilepsy (DeGiorgio et al., 2018; Shankar et al., 2017).

While there is a gap in the understanding of SUDEP mechanisms, there is knowledge of SUDEP risk genes. These genes are largely, but not all, ion channels and include *SCN1A*, *SCN1B*, *SCN8A*, *SCN2A*, *KCNA1*, *GNB5*, and *DEPDC5* (Bagnall et al., 2017). Importantly, there are instances of SUDEP which do not share these genes, but in understanding how these genes contribute to SUDEP, we can better our understanding of the mechanisms that may be shared across different etiologies. For the ion channel genes that are known as risk factors, mutations in the sodium channel genes (*SCN1A*, *SCN1B*, *SCN8A*, *SCN2A*) tend to increase hyperexcitability of neurons which either directly leads to aberrant glutamatergic signaling or may lead to altered interneuron firing which can tip the excitation-inhibition balance in the brain (Catterall, 2012). In

the case of *KCNA1*, mutations lead to dysfunctional repolarization which typically helps the neurons return to rest for the appropriate time before firing again (Jan & Jan, 2012). Mutations in this gene facilitate more continuous firing which can lead to seizures and potentially SUDEP. It is important to note that there is no single genome wide significance for any one gene, and SUDEP is likely incredibly complex and heterogenous (Kearney, 2012).

The 2013 Mortality in Epilepsy Monitoring Units Study (MORETMUS) provided a strong initial hypothesis into the cascade of events during the terminal seizure. In people with epilepsy who succumbed to SUDEP, there was a consistent pattern of a generalized tonic-clonic seizure which ended in generalized EEG suppression (Ryvlin et al., 2013). Additionally, it was noted that terminal apnea preceded terminal asystole suggesting a heightened role for respiration in SUDEP pathology (Ryvlin et al., 2013). Furthermore, it has been reported that post-convulsive central apnea may be important in SUDEP pathophysiology as it is also present in near-SUDEP and possible SUDEP cases (Vilella et al., 2019). Despite the "respiration first" hypothesis for SUDEP, the heart is also playing a vital role and simply takes longer to cease functioning as there are pacemaker cells which can continue to facilitate beats in the absence of a neural signal. The MORTEMUS study, while invaluable to the SUDEP field, has its drawbacks. These limitations include the patients being weaned off anticonvulsant drugs at the time of death and the monitoring of respiration by visual inspection of chest movement only (Ryvlin et al., 2013). Collectively, however, these studies indicate the importance of brain-heart-lung dynamics in SUDEP.

There are several working hypotheses surrounding SUDEP mechanisms, one of which is the adenosine hypothesis. Proposed by Shen et al in 2010, this hypothesis suggests that seizure induced elevations in adenosine are a primary contributor to SUDEP (Shen et al., 2010). Adenosine, a brain neurotransmitter, is produced from the breakdown of adenosine triphosphate during periods when

the brain is utilizing a high level of energy such as during a seizure (Boison, 2012; Peng et al., 2020). During a seizure, the production of adenosine acts as an anticonvulsant to help terminate the epileptic event and prevent ongoing seizures from occurring (Boison, 2011, 2012; Lado & Moshé, 2008; B. S. Purnell et al., 2023; Shen et al., 2010). Adenosine is able to travel across the brain through paracrine transmission and act on A1 presynaptic receptors to facilitate seizure termination(Agnati & Fuxe, 2014; Canas et al., 2018). Adenosine can also act on A2A receptors which produces a proconvulsive response (Canas et al., 2018). Furthermore, adenosine has been shown to contribute to the postictal respiratory depression seen in animal models and people with epilepsy following a generalized seizure event (Moseley et al., 2012; B. Purnell et al., 2021; Seyal et al., 2012). There are several pieces of clinical evidence linking adenosine and SUDEP. Firstly, there is clinical evidence linking increases in adenosine levels in real time with seizures (During & Spencer, 1992). Both adenosine receptors and the enzyme which breaks down adenosine triphosphate into adenosine (adenosine kinase; ADK) have altered expression levels in people with epilepsy (Aronica & Crino, 2011; Barros-Barbosa et al., 2016; Weltha et al., 2019). Thus, adenosine can be seen as a "double-edged sword" which must be properly balanced for people with epilepsy to benefit from the anticonvulsant effects and prevent the proconvulsant and respiratory depressive activity.

The serotonin hypothesis is another proposed mechanism of SUDEP and suggests that SUDEP prevention can be attained through increasing the bioactivity of serotonin (5-hydroxytryptamine; 5HT) (Tupal & Faingold, 2006). A large proportion of the literature suggests serotonin acts as a natural anticonvulsant; however, it should be noted that research also exists supporting its role as a proconvulsant (Dailey & Naritoku, 1996; Gilliam et al., 2021; Jobe & Browning, 2005; Johannessen Landmark et al., 2016; Kanner, 2016; Kondziella & Asztely, 2009; Petrucci et al.,

2020). As suggested from the MORETEMUS study, respiratory failure is one of the initiating events in the SUDEP pathological cascade, suggesting that SUDEP can also be viewed as a failure to restart proper respiration (Ryvlin et al., 2013). Physiologically, there are three primary mechanisms which should initiate in response to attenuated respiration. These include autoresuscitation (gasping) to quickly increase blood oxygen levels, the hypercapnic ventilatory response that enhances respiration in response to increased blood CO_2 levels, and the hypoxic ventilatory response which increases respiration due to decreased blood oxygen levels (Corcoran & Milsom, 2009; Dosumu-Johnson et al., 2018). Interestingly, all of these mechanisms involve serotonin to mediate these responses (Corcoran & Milsom, 2009; Dosumu-Johnson et al., 2018). Clinically, it has been shown that people with epilepsy taking selective serotonin reuptake inhibitors (SSRIs) for comorbid depression showed significantly less respiratory depression than those people with epilepsy who are not on SSRIs (Bateman et al., 2010; Lacuey et al., 2019). Furthermore, postmortem SUDEP cases exhibit both reduced numbers of brainstem serotonergic neurons and a reduction in the enzyme which synthesizes serotonin (Patodia et al., 2021, 2022). Collectively, this hypothesis suggests that preemptively increasing serotonin in people with epilepsy may be able to reduce SUDEP risk.

It is critically important to stress that there is no single SUDEP hypothesis that is universally accepted, or which explains all elements of SUDEP discovered thus far. In addition to adenosine and serotonin, postictal generalized electroencephalographic suppression (PGES), autonomic dysfunction (mentioned below), and cardiac arrhythmias are also proposed SUDEP mechanisms (Devinsky et al., 2016; Singh et al., 2023). Beyond seizure-induced respiratory arrest, apnea can be caused by laryngospasm-induced mechanisms which have been associated with cardiorespiratory abnormalities and mortality in animal seizure models (Irizarry et al., 2020;

Stewart et al., 2020), as well as oxygen desaturation and cardiac dysfunction in people (Lacuey et al., 2018; Murray et al., 2010; Tavee & Morris III, 2008). PGES occurs when there is postictal reduction of cerebral activity which can increase SUDEP risk by shutting down communication in important cardiorespiratory regions (Lhatoo et al., 2010; Peng et al., 2017; Poh et al., 2012). PGES has been shown to last longer in people who ultimately die from SUDEP (Lhatoo et al., 2010). Lastly, cardiac dysfunction is heavily associated with both seizures and SUDEP. People with epilepsy are at a 2.8-fold increased risk of cardiac arrhythmias compared to the general population (Verrier et al., 2020). Furthermore, those with high risk of SUDEP due to intractable epilepsy and those who have experienced near SUDEP often display significant cardiac arrhythmias (Espinosa et al., 2009; Serdyuk et al., 2021; Sivathamboo et al., 2022; van der Lende et al., 2015). Ultimately, SUDEP appears heavily linked to the brain, heart, and lungs and these systems all have to be taken into account when trying to understand SUDEP mechanisms.

1.3 Autonomic Nervous System

Research has emphasized cardiac and respiratory dysfunction and eventual failure as two of the leading pathological events in SUDEP. The autonomic nervous system (ANS) is known to be the master regulator of the heart and lungs which suggests it may play an important pathological role in SUDEP. The ANS is comprised of sympathetic, parasympathetic, and enteric systems which project to nearly every part of the body (Wehrwein et al., 2016). The vagus nerve (part of the parasympathetic system) alone runs from the brain down into the reproductive organs highlighting the vast expanse and influence of the ANS. The role of the ANS is to internally detect changes in the body and transmit signals to and from the brain through sensory and motor fibers, with the goal of prompting responses that address the body's immediate requirements (Wehrwein

et al., 2016). The traditional ANS circuitry resides in the brainstem where it receives sensory inputs that are relayed to the appropriate brain regions in order to achieve the proper response. The brainstem is comprised of the midbrain, pons, and medulla and the ANS circuity runs throughout all three regions (Benarroch, 2020). Importantly, the nucleus of the solitary tract (NTS), which lies in the medulla, is the primary nuclei which receives inputs from the body (Holt & Rinaman, 2022). The brainstem is not, however, the only important region for the ANS as there are many regions in the forebrain which can communicate with the brainstem to regulate how the system responds to inputs. These connections can be both direct and indirect, and include regions such as the cortex, hippocampus, and amygdala (Allen et al., 2019; Mueller et al., 2014, 2018). Together, the ANS can be loosely broken down into the classical brainstem circuitry and forebrain limbic circuitry which work together to ultimately maintain proper regulation of the body.

The forebrain and brainstem regions of the ANS are known to communicate heavily with one another, as well as show alterations in epilepsy and SUDEP. Firstly, there is evidence supporting communication between the amygdala and rostral ventrolateral medulla in the brainstem showing the amygdala's role in respiratory control (Feinstein et al., 2022; Ritz et al., 2020; Yang et al., 2020). Furthermore, the periaqueductal gray (PAG) in the midbrain acts as a central "suffocation alarm" and has anatomical connections to the amygdala furthering this respiratory link (Huang et al., 2019; Schimitel et al., 2012). Imaging studies revealed that SUDEP cases with temporal lobe epilepsy (TLE) show more severe and widespread mesencephalic volume loss in the PAG, dorsal pons, and upper medulla oblongata compared to TLE patients alone (Mueller et al., 2014). In fact, widespread brainstem volume loss is present in the final scan for people who died from SUDEP, and the degree of damage correlates with survival time (Mueller et al., 2018). Not only is the regional brain volume reduced, but this is functionally linked to reduced heart rate variability

(HRV) in epilepsy patients (Mueller et al., 2018). Furthermore, these autonomic brainstem regions share communication with the forebrain, including the hippocampus, amygdala, and prefrontal cortex (Mueller et al., 2014; Nieuwenhuys et al., n.d.). TLE patients with a high risk of SUDEP exhibit functional connectivity differences between these key autonomic brain regions (Allen et al., 2019). Additionally, at rest functional connectivity differences are prevalent in the thalamus-brainstem circuit of those at high risk for SUDEP (Tang et al., 2014). Collectively, this evidence demonstrates that brain volume alterations have functional consequences in regions which are vital for cardiorespiratory function and recovery that may augment SUDEP risk and aid in understanding anatomical substrates of SUDEP pathomechanisms.

1.4 Modeling SUDEP

Preclinical animal models have allowed for better understanding of the anatomical substrates and mechanisms contributing to SUDEP and SUDEP risk (R. Li & Buchanan, n.d.). Cardiorespiratory dysfunction is one shared phenotype across several mouse models. In the DBA1/2 audiogenic seizure model, seizures induced respiratory arrest followed by cardiac arrest and death mimicking phenotypes seen in the MORTEMUS study (Feng & Faingold, 2017; Ryvlin et al., 2013). The *RyR2* R176Q point mutant mouse has rare spontaneous seizure and sudden death events, associated with apnea, cardiorespiratory collapse, and death (Aiba et al., 2016). This respiratory-then-cardiac dysfunction phenotype is also shared with the genetic *Kcna1* knockout (KO) preclinical mouse model during spontaneous seizures, and this model also shows cardiac abnormalities that increase in prevalence during the ictal period (H. Dhaibar et al., 2019; Glasscock et al., 2010; K. A. Simeone et al., 2018). Importantly, the *Kcna1* model is especially advantageous because the seizures are spontaneous and do not have to be provoked in order to see

cardiorespiratory dysfunction. Another genetic model, the *Scn1a* mouse (both the R1407X point mutant and heterozygous knockout), displays ictal bradycardia leading to SUDEP, and death can be prevented through respiratory rescue by mechanical intervention and the drug atropine (Auerbach et al., 2013; Kalume et al., 2013; Y. Kim et al., 2018). This model also shows interictal cardiac arrhythmias and HRV abnormalities (Auerbach et al., 2013; Kalume et al., 2013). Interestingly, the *Kcna1* mouse model also displays similar interictal deficits (H. Dhaibar et al., 2019). The *Scn1a* model has also provided insights into the timing of events, as both nonfatal seizures and SUDEP were observed to occur more in the dark phase, and seizure frequency increased the day before death (Teran et al., 2019). Another sodium channel mutant, *Scn8a* N1768D point mutant mice, also show spontaneous seizures and death which is both dependent on gene dose and region of the brain that the mutant channel is expressed (Lopez-Santiago et al., 2017; Wagnon et al., 2015). Lastly, SUDEP research can be performed in higher order animal models. In a sheep model of status epilepticus, it was shown that the mechanisms of death shared substantial overlap with proposed SUDEP mechanisms (Simon, 1997). There is also research using an epileptic baboon and sudden unexpected death in these animals presented with a similar pathology to SUDEP (Ákos Szabó et al., 2009). Importantly, there is no perfect model for SUDEP, and research uses a combination of genetic and acquired epilepsy models to try to understand the complex multisystem failure in SUDEP. Many models share similar phenotypes and characteristics, however, which suggests the information gathered from one model may be applicable across many models and ultimately may translate to the clinic. The work in this dissertation uses the preclinical *Kcna1* mouse model, and the gene and model are further described in the subsequent sections.

1.5 KCNA1

*The content in this section is adapted from my two first-author reviews (Paulhus et al., 2020; Paulhus & Glasscock, 2023)

The *KCNA1* gene encodes the 495 amino acid (aa) Kv1.1 voltage-gated potassium (Kv) channel α-subunit (Choi & Choi, 2016; D'Adamo et al., 2015). *KCNA1* is one of 40 human Kv α-subunit genes that are spread across 12 different gene subfamilies (Kv1–12) (Ranjan et al., 2019). Kv channels, such as Kv1.1, play important roles in regulating neuronal excitability by controlling the action potential shape, repolarization, and firing properties (Jan & Jan, 2012). Kv1.1 is uniquely suited for counterbalancing depolarizing inputs and preventing excessive neuronal excitation because it has a much lower activation threshold and faster onset rate than other members of the Kv1 family, which includes Kv1.1–Kv1.8 (Ovsepian et al., 2016). Kv channels are comprised of four α-subunits which associate as homo- or hetero-tetramers to form a functional transmembrane pore (Parcej D.N. et al., 1992; V. E. S. Scott et al., 1994; H. Wang et al., 1993). To form a complete channel complex, α-subunit tetramers also associate with up to four accessory β-subunits that can impact channel gating, assembly, and trafficking (Pongs & Schwarz, 2010). In the brain, Kv1.1 associates with Kv1.2 and/or Kv1.4 α-subunits to form heterotetramers, but evidence is lacking for the presence of Kv1.1 homotetramers in the central nervous system (CNS) (Coleman et al., 1999). In fact, biochemical experiments isolating Kv1.1 have shown that this subunit is nearly always in combination with Kv1.2 in central neurons, whereas it assembles with Kv1.4 or possibly as homotetramers in peripheral non-myelinated axons (Ovsepian et al., 2016). Although Kv1.1, Kv1.2, and Kv1.4 subunits are all abundant in the brain, their expression and channel composition vary depending on the brain region, cell type, and subcellular localization (Robbins & Tempel, 2012). Interestingly, Kv1.1 levels are lowest in the cerebellum and

hippocampus, implying a low copy number in heterotetramers in these brain regions (Ovsepian et al., 2016). The relatively low representation of Kv1.1 in these brain structures combined with its distinctive biophysical characteristics, which cannot be completely compensated for by other Kv1 subunits, has been hypothesized to cause a low functional reserve that renders the cerebellum and hippocampus especially vulnerable to Kv1.1 deficits (Ovsepian et al., 2016). *KCNA1* is also expressed in the heart where it has been shown to be an important mediator of action potential repolarization in the atria, ventricles, and sinoatrial cells.

Each Kv α-subunit has six transmembrane (TM) spanning segments (helices S1–S6) joined by alternating extra- and intracellular linkers (Figure 1). The S1-S6 TM helices comprise the functionally critical voltage-sensing and pore domains. Helices S1–S4 form the voltage-sensing domain of the protein, with S4 playing a specifically important role as the voltage sensor (Miceli et al., 2015). Evenly spaced positive charges across S4 allow this helix to acutely sense changes in voltage across the membrane; together with S3, these helices form a voltage sensor paddle that can change conformation to alter the state of the channel (Bezanilla, 2000; Bhuyan & Seal, 2015; Miceli et al., 2015). The pore region of the channel, which allows ion flux through the membrane and acts as a K^+ selectivity filter, is formed by S5 and S6 (Ranjan et al., 2019). The S4–S5 intracellular linker communicates changes in the voltage-sensing domain to the pore domain and thus can initiate a shift between the open and closed states of the pore (Bhuyan & Seal, 2015; Miceli et al., 2015). The intracellular N- and C-terminal domains of each Kv α-subunit also regulate channel function. While the mechanisms are not fully understood, evidence suggests that the C-terminus influences channel tetramerization and membrane targeting (Rea et al., 2002), while the N-terminus participates in both channel inactivation and subunit assembly (Hoshi et al., 1990; M. Li et al., 1992).

At least 65 different pathogenic mutations have been identified in the human *KCNA1* gene and they are implicated in a number of different clinically relevant disorders. The first disease attributed to *KCNA1* was the movement disorder episodic ataxia type 1 (EA1). EA1 was first identified in 1975 by Van Dyke and colleagues when they described a family with a movement disorder accompanied by myokymia, which is characterized by muscle rippling (Van Dyke, 1975); however, it was not until much later, in 1994, that Browne et al. identified *KCNA1* as the genetic cause of EA1 (Browne et al., 1994). In addition to EA1, over the years mutations in *KCNA1* have also been implicated in myokymia, epilepsy, hypomagnesemia, paroxysmal kinesigenic dyskinesia, as well as comorbidities such as intellectual disability and respiratory abnormalities. Furthermore, mutations in *KCNA1* are primarily loss-of-function (LOF) or dominant negative, but more recently there have been two gain-of-function mutations described clinically (Miceli et al., 2022; Müller et al., 2023; Yuan et al., 2020).

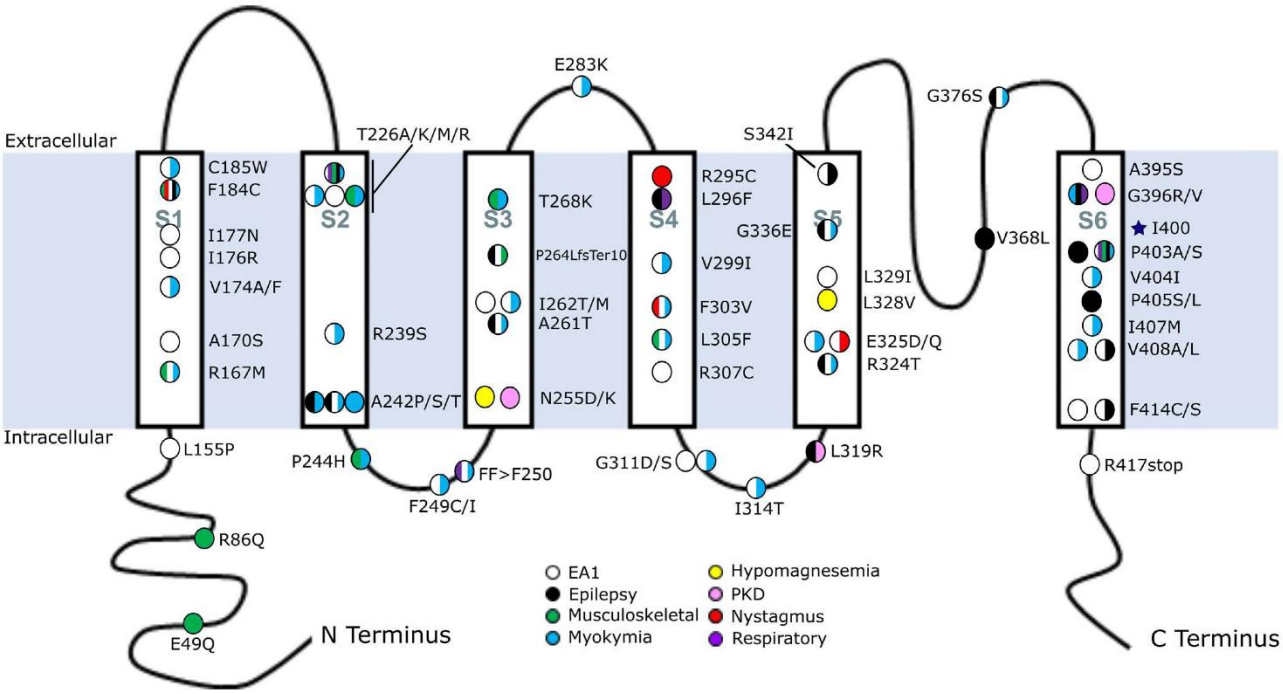

Figure 1.1. Map of *KCNA1* mutations associated with human disease. Human mutations in *KCNA1* were mapped across the protein and color-coded to indicate their clinically documented disease association. Circles with multiple colors represent mutations with multiple phenotypes. Multiple circles at a given amino acid position represent different amino acid substitutions at that location (e.g., A242P/S/T) and their associated disease manifestation. The blue star indicates the RNA editing position. The identity of the various transmembrane domains is indicated as S1–S6. Abbreviations: EA1, episodic ataxia type 1; PKD, paroxysmal kinesigenic dyskinesia.

Understanding genotype–phenotype correlations for *KCNA1* channelopathy is challenging because mutations can result in a variety of different diseases, which often occur in combination (Figure 1). Historically, three diseases have been predominantly associated with *KCNA1* mutations, namely episodic ataxia type 1 (EA1), myokymia, and epilepsy. Among these, the most common is EA1, a rare genetic paroxysmal movement disorder that can be triggered by stress resulting in impaired voluntary movements such as walking (Choi & Choi, 2016; Graves et al., 2014; Imbrici et al., 2017). Out of the approximately 65 known pathogenic or likely pathogenic *KCNA1* mutations, 69% cause EA1 (Table 1). Myokymia is the second most common, linked to 52% of *KCNA1* variants and usually occurring in combination with EA1. Myokymia is

characterized by episodes of involuntary muscle rippling arising from abnormal peripheral nerve activity (Chen et al., 2007). The third most common phenotype associated with *KCNA1* variants is epilepsy or seizures, accounting for approximately 32% of mutations. Clinical case reports often describe patients experiencing seizures without stating an official epilepsy diagnosis, so this category comprises patients with either documented epilepsy or seizures. Although not traditionally recognized, it is now becoming increasingly apparent that musculoskeletal abnormalities and nystagmus can also be features of *KCNA1* channelopathy, occurring in 17% and 6% of KCNA1 mutations, respectively (Paulhus & Glasscock, 2023). Importantly, at least 60% of *KCNA1* mutations cause more than one type of disease (Paulhus & Glasscock, 2023). This high degree of comorbidities complicates simple genotype–phenotype correlations.

The location of the mutation within the protein apparently plays a role in determining the type of disease that manifests. Epilepsy-causing mutations are most common in the S5–S6 pore domain, with the most severe forms of the disease associated with the PVP motif of S6. EA1 and myokymia, the most common diseases associated with *KCNA1* variants, show relatively even mutation distributions across the various protein domains. However, mutations in the S1 domain and in S2 and S2–S3 linker domains appear to have particularly high associations with EA1 and myokymia, respectively.

Protein	No.	Disease or Symptom					
Domain	Mutations	EA1	Myokymia	Epilepsy	MSk	Respiration	Nystagmus
N	3	33%	0%	0%	67%	0%	0%
S1	8	100%	63%	13%	25%	0%	13%
S1–S2	0	0%	0%	0%	0%	0%	0%
S2	8	63%	88%	38%	25%	13%	0%
S2–S3	4	75%	100%	0%	25%	25%	0%
S3	7	57%	43%	29%	29%	0%	0%
S3–S4	1	100%	100%	0%	0%	0%	0%
S4	6	67%	50%	17%	17%	17%	33%
S4–S5	4	75%	50%	25%	0%	0%	0%
S5	7	86%	43%	43%	0%	0%	14%
S5–S6	2	50%	50%	100%	0%	0%	0%
S6	14	57%	36%	57%	7%	21%	0%
C	1	100%	0%	0%	0%	0%	0%
Total	65	69%	52%	32%	17%	9%	6%

Table 1. Disease rates for pathogenic or likely pathogenic *KCNA1* variants in different protein domains. The values shown represent the percentage of mutations in each Kv1.1 protein domain associated with the listed disease or phenotype. The individual cells of the table are color-coded in a heat map where white is the lowest value, and the darkest shade of blue is the highest. Percentages were calculated by dividing the number of mutations associated with the listed disease or symptom in the designated domain by the total number of mutations in that domain. Abbreviations: EA1, episodic ataxia type 1; MSk, musculoskeletal abnormalities.

1.6 Kcna1 Mouse Models

The *Kcna1* KO mouse model was created in 1998 by Smart and colleagues when they used electroporation of embryonic stem cells to insert a vector which, through homologous recombination, replaces the entire Kv1.1 open reading frame with a neomycin cassette (Smart et

al., 1998). These mice were generated on a 129Sv x N:NIHS-BC genetic background and exhibited spontaneous seizures with approximately 50% of the mice dying between the third and fifth week of life (Smart et al., 1998). The seizure and premature mortality phenotypes were extremely penetrant, exhibiting similar degrees of severity in three other mouse genetic backgrounds (Smart et al., 1998). Not only is this model useful for the study of spontaneous seizures and SUDEP-related mechanisms, but research also suggests this model has applicability for understanding developmental epilepsies. *Kcna1* KO mice exhibit enhanced seizure susceptibility beginning at a young age around day P10 before the onset of spontaneous seizures (Rho et al., 1999). Early in life, *Kcna1* is also critical in the regulation of postnatal neurogenesis by maintaining proper membrane potential in neural progenitor cells to prevent aberrant proliferation (Chou et al., 2021).

Kcna1 mouse models have been valuable for understanding the influence of genetic modifier mutations that exacerbate or suppress disease penetrance or expressivity. In support of this, several gene mutations that modify epilepsy phenotypes in *Kcna1* KO mice have been identified. The first genetic modifier identified was the mouse *tottering* (*tg*) mutation, a partial LOF allele of the P/Q-type calcium channel α-subunit *Cacna1a*, which was crossed into *Kcna1* KO mice. The *tg* mice display spike-wave absence-like seizures as well as ataxia (Fletcher et al., 1996; Noebels & Sidman, 1979). Double mutant $Kcna1^{-/-}$; $Cacna1a^{tg/tg}$ mice exhibit reduced seizure frequencies and drastically improved survival (Glasscock et al., 2007). Thus, a partial LOF mutation in a gene implicated in EA2 (i.e., *Cacna1a*) alleviates abnormalities due to the absence of the gene responsible for EA1 (i.e., *Kcna1*). Another study identified *Mapt* as a modifier of *Kcna1* (Holth et al., 2013). *Mapt* encodes the microtubule binding protein tau, which is known to regulate microtubule stability and axonal trafficking and is implicated in Alzheimer's disease (Dixit et al., 2008; J. Z. Wang & Liu, 2008). $Kcna1^{-/-}$ mice carrying $Mapt^{-/-}$ mutations exhibit reductions in

seizures and improved survival (Holth et al., 2013). The BCL2-associated agonist of cell death (*Bad*) gene has also been identified as a third genetic modifier of *Kcna1* (Foley et al., 2018). *Kcna1*$^{-/-}$; *Bad*$^{-/-}$ mice outlive *Kcna1*$^{-/-}$ mice and exhibit reduced seizure severity (Foley et al., 2018). Heterozygosity for a deletion in the *Scn2a* voltage-gated sodium channel α-subunit gene acts as a protective modifier in *Kcna1* KO mice, decreasing the seizure burden while improving lifespan and brain–heart dynamics (Mishra et al., 2017). Furthermore, doubly heterozygous *Scn2a*$^{+/-}$; *Kcna1*$^{+/-}$ mice exhibit ameliorated autism-like phenotypes compared to singly heterozygous *Scn2a* and *Kcna1* mice alone (Indumathy et al., 2021). *Scn8a* and *Slc7a11* are the two most recently identified genes that can modify aspects of epilepsy in *Kcna1* KO mice. In a study exploring the efficacy of ASO therapy for the treatment of epilepsy, a reduction in *Scn8a* brain expression levels by ASO was found to extend the lifespan of and delay SUDEP onset in *Kcna1* KO mice; however, seizure burden was not significantly improved (Hill et al., 2022). In a second study, *Slc7a11*; *Kcna1* double KO animals were generated to investigate mechanisms of neurogenesis and epileptogenesis (Aloi et al., 2022). Genetic knockout of *Slc7a11* was found to have unique modifying effects in *Kcna1* KO mice, improving the megencephaly phenotype associated with *Kcna1* deletion but not significantly changing seizure severity or SUDEP incidence (Petersson et al., 2003). Thus, the *Slc7a11* mutation seems to have beneficial effects on aberrant postnatal neurogenesis in *Kcna1* KO mice without significantly altering epileptogenesis. These genetic interactions demonstrate that *Kcna1*-related phenotypes can be dramatically modified by second-site gene mutations.

Further evidence of potential genetic modifiers can be observed by the presence of phenotypic differences between *Kcna1* KO mice maintained on different genetic backgrounds. While all *Kcna1* KO mice exhibit epilepsy and sleep deficits, they can also manifest differences in

mortality and respiratory deficits depending on the genetic background of the mouse strain. *Kcna1* KO mice with a C3HeB/FeJ genetic background begin seizing and dying at about 5 to 7 weeks old, leading to a mortality rate of 100% (Moore et al., 2014; K. A. Simeone et al., 2016). In contrast, *Kcna1* KO mice with a Black Swiss genetic background exhibit seizures and death with an earlier onset of 2 to 3 weeks old, but only about 75% of animals die prematurely, usually by the 6th week of life (Glasscock et al., 2007; Smart et al., 1998). The two strains also exhibit potential differences in respiration. C3HeB/FeJ-strain knockout mice display increases in apnea frequency, whereas Black Swiss-strain knockout mice show a decrease (H. Dhaibar et al., 2019; K. A. Simeone et al., 2018). These examples of strain variation provide additional evidence that genetic modifiers can alter the penetrance and expressivity of phenotypes associated with *Kcna1* mutations. However, environmental factors may also influence phenotypic differences between *Kcna1* KO strains since the mice are maintained in different laboratory facilities.

The importance of cardiorespiratory dysfunction to SUDEP mechanisms has been shown by various labs using the *Kcna1* mouse model. Cardiorespiratory profiling using simultaneous electroencephalogram-electrocardiogram-plethysmography (EEG-ECG-pleth) showed that *Kcna1* KO mice have frequent cardiorespiratory abnormalities during seizures with respiratory deficits preceding cardiac dysfunction similar to what was reported in the MORTEMUS study (H. Dhaibar et al., 2019; Ryvlin et al., 2013). Furthermore, this study reported substantial interictal respiratory dysfunction including increases in respiratory variability and a unique generalized absence of apneas (H. Dhaibar et al., 2019). One lab reported that respiratory dysfunction in *Kcna1* KO mice progressively worsens closer to sudden death and that young mice that die following chemically-provoked seizures exhibit respiratory patterns resembling the older KO mice that die naturally (K. A. Simeone et al., 2018). *Kcna1* KO mice at high risk for SUDEP show higher degrees of

intermittent bradycardia and administering the cardiorespiratory modulator Orexin (a dual orexin antagonist) improves oxygen saturation, decreases heart rate variability, and increases longevity in these mice (Iyer et al., 2020). Importantly, one study showed the presence of Kv1.1 in nearly every cardiorespiratory and chemosensory center in the brain solidifying the importance of this gene to heart and lung function (H. A. Dhaibar et al., 2021). In fact, this paper also showed that *Kcna1* KO mice had significant gliosis in these regions linking the absence of Kv1.1 to seizures and pathological disturbances in these vital cardiorespiratory regions (H. A. Dhaibar et al., 2021). Furthermore, a different study showed that restricting *Kcna1* deficiency specifically to neurons of the brain largely recapitulated both ictal and interictal phenotypes seen in global *Kcna1* KO mice, suggesting these phenotypes are specifically driven by the brain and not due to intrinsic dysfunction of the heart or lungs (Trosclair et al., 2020).

Kcna1-KO mice have been utilized to test potential therapeutic strategies towards both seizure reduction and protection from premature mortality. In *Kcna1* KO mice, the evaluation of pharmacoresponsiveness for epilepsy treatment was aided by administering already approved drugs such as carbamazepine, levetiracetam, phenytoin, and phenobarbital (Deodhar et al., 2021). Only phenobarbital confers seizure freedom across all mice treated, while the other drugs are only partially effective (Deodhar et al., 2021). Treating *Kcna1* KO mice with the KCNQ channel activator, retigabine, reduces spontaneous seizures by 60% (Vanhoof-Villalba et al., 2018). Adrenocorticotropic hormone treatment in *Kcna1* KO mice prevents impairment of long-term potentiation and restores spatial learning and memory in the Barnes maze test without altering the frequency of seizures (Scantlebury et al., 2017). Though the seizures remained, drugs which can prevent the comorbid learning and memory deficits are just as important and can help people with epilepsy live more neurotypical lives. Interestingly, more recent work has focused on the

generation of highly selective potassium channel openers derived from glycine which has successfully produced an opener that is specific for Kv1.1 and not its closest relative Kv1.2 (Manville & Abbott, 2020). Future work implementing these sorts of therapies into mice such as the *Kcna1* KO model will be a critical step towards seeing if these novel drugs could be translatable to the clinic.

There is a substantial portion of *Kcna1* KO mouse literature devoted to testing the efficacy of the high fat, low carb ketogenic diet as a potential therapeutic. Treating mice with this diet has been shown to get rid of seizure periodicity and restore rest-activity rhythm values to wildtype levels (Fenoglio-Simeone et al., 2009). Comparing the effects of the ketogenic diet to the antiseizure drug phenobarbital showed both were effective in reducing seizures, but the ketogenic diet was uniquely able to preserve cell numbers in the hippocampus (K. A. Simeone et al., 2021). Importantly, there is evidence that the time of treatment factors into the ketogenic diet's efficacy as merely the difference in treating at P30 versus P25 results in greater lifespan at the earlier therapeutic point (Chun et al., 2018). Also, this same research showed that females on the ketogenic diet live longer than the males in their same treatment cohort, suggesting sex is also a critical factor to therapeutic efficacy (Chun et al., 2018).

The *Kcna1* KO mouse model has been pivotal in showing that Kv1.1 is both present and functionally active in the heart. Original studies of *Kcna1* believed that the gene was only expressed in the brain, but more current research has shown its presence in multiple areas in the heart. Global *Kcna1* knockout mice were shown to have prolonged atrial action potential repolarization which was most notable in the right atria (Si et al., 2019). Furthermore, applying the Kv1.1-specific blocker dendrotoxin-K (DTX-K) to wildtype atrial cells reproduced this repolarization deficit showing the prolongation is due to the lack of Kv1.1 (Si et al., 2019). The

ventricles were also shown to be impacted by Kv1.1 deficiency. *Kcna1* KO mice displayed features of cardiac contractile dysfunction including decreased ejection fraction and fractional shortening (Trosclair et al., 2021). Electrophysiology of *Kcna1* knockout ventricles also showed prolonged action potentials similar to atrial cells (Trosclair et al., 2021). Significantly, histological evidence has also shown the presence of Kv1.1 in human ventricular cells suggesting the work done in mice is translatable to humans (Trosclair et al., 2021). To date, there remains no research into the consequences of heart-specific *Kcna1* deficiency at the whole animal level, nor is there published research into the contributions of *Kcna1* in the sinoatrial node. The final chapter of my dissertation (Chapter 4) comprises contributions I have made towards helping to answer these questions alongside other members of the lab.

In addition to the more heavily studied *Kcna1* global KO mouse model, there are other *Kcna1* mutant models which have aided studies into the gene's function. Likely the second most common *Kcna1* mouse model is the *Kcna1*$^{V408A/+}$ mouse which was generated to match the human V408A mutation that was identified as causing EA1 (Herson et al., 2003). This model has been useful in understanding how mutations in *Kcna1* can mechanistically lead to the stress-induced motor incoordination typical of EA1, as well as serve as a model to test potential therapeutics (Herson et al., 2003). Another mouse model, the *megalencephaly* (*mceph*) mouse, carries a truncation early in the *Kcna1* gene at amino acid 230 and uniquely presents with both epilepsy and unsteady gait? properties bridging phenotypes between EA1 and epilepsy (Persson et al., 2005; Petersson et al., 2003; Rae Donahue et al., 1996). Using N-ethyl-N-nitrosurea mutagenesis, a rat model was generated with a S309T mutation in *Kcna1* which phenotypically presents with myokymia, neuromyotonia, seizures, and premature death, which are relevant phenotypes seen in clinical cases with *KCNA1* mutations (Ishida et al., 2012). More recently, CRISPR/Cas9 was used

to generate zebrafish that were homozygous for a null allele of the homologous *Kcna1a* gene mutant, causing them to exhibit features of both EA1 and epilepsy (Dogra et al., 2023). This model is extremely useful, as it can be used as a more high throughput system for drug testing as it has already been shown that carbamazepine is able to suppress hyperexcitability in these fish (Dogra et al., 2023)**.** Ultimately, there is no perfect model of SUDEP, but utilizing models that capture different critical aspects of SUDEP allows researchers to piece together SUDEP pathomechanisms and better understand the anatomical substrates and markers of risk.

1.7 Hypothesis and Aims

Overall Hypothesis

The primary aim of this research was to gain deeper insights into the distinct tissue-specific roles contributing to epilepsy and cardiorespiratory dysfunction associated with SUDEP. SUDEP is the leading cause of epilepsy-related death, but despite this, research efforts still struggle to understand the mechanisms which underlie this devastating phenomenon. One prominent hypothesis is that epilepsy somehow leads to a breakdown in communication between the brain, heart, and lungs leading to cardiorespiratory failure and death. However, there remains a significant lack of understanding regarding the precise mechanisms occurring before and during the terminal event, as well as the anatomical structures responsible for these characteristics.

The autonomic nervous system (ANS) is commonly referred to as the primary regulator of the heart and lungs, and for this reason it is a strong candidate for being one of the primary anatomical pathways contributing to SUDEP mechanisms. The classical ANS circuitry lies in the brainstem (comprised of the midbrain, pons, and medulla), and includes vital nuclei such as the

nucleus of the solitary tract (NTS), nucleus ambiguus (NA), dorsal motor nucleus of the vagus (DMNX), and the retrotrapezoid nucleus (RTN). The NTS lies in the medulla and receives inputs for many sensory afferents including those which are involved in chemoreception and mechanoreception from the heart, lungs, and airways. The NTS has afferent projections into both the forebrain and other brainstem nuclei to form autonomic regulatory circuits. The NA is specifically important in cardiac regulation as it houses parasympathetic neurons which innervate the heart and receive heavy influence from glutamatergic neurons in the forebrain. The DMNX houses the cell bodies of pre-ganglionic parasympathetic neurons which extend throughout the viscera including the heart and lungs, and the RTN is the primary central chemoreceptor which influences breathing regulation. In anesthetized global *Kcna1* KO mice, treating with a potassium channel blocker leads to seizures which coincide with respiratory depression leading to spreading depolarization in the brainstem and culminating in death from cardiorespiratory arrest (Aiba & Noebels, 2015). This evidence shows that seizures can lead to altered brainstem electrophysiology which can lead to cardiorespiratory collapse and death. The second part of my dissertation (Chapter 3) focuses on how Kv1.1 deficiency in the brainstem alone contributes to SUDEP-related phenotypes such as cardiorespiratory dysfunction and the risk of seizure-induced death.

The forebrain is another vital region for ANS regulation as it has extensive connections with the brainstem circuitry and has known roles in cardiac and respiratory function. These important forebrain regions include corticolimbic circuitry such as the cortex, hippocampus, and amygdala. Importantly, post-ictal FOS labeling reveals activation of both the hippocampus and amygdala in *Kcna1* KO mice which suggests that the cardiorespiratory dysfunction characterized in these mice may be driven by similar regions that are activated during a seizure (Gautier & Glasscock, 2015). Seizure spread and direct stimulation of the amygdala, hippocampus, or

temporal lobe can result in apnea and/or respiratory depression linking the forebrain to respiratory regulation (Nobis et al., 2018, 2019). Discrete stimulation of the CA1 region of anesthetized rats reveals hippocampal control of both cardiovascular and respiratory control (Ajayi et al., 2018). Also, the amygdala has known connections with the hypothalamus, rostral ventrolateral medulla, and NTS and can influence autonomic signaling to cause alterations in cardiac function and blood pressure (Saha, 2005). Human imaging shows that the hippocampus and amygdala have connections with nuclei in the brainstem, and research in rats demonstrates a direct connection between the hippocampus and NTS showing the heavy influence of the corticolimbic circuit on autonomic regulation. The first part of my dissertation (Chapter 2) tests how *Kcna1* deficiency specifically in the corticolimbic circuit contributes to seizures, cardiorespiratory dysfunction, and sudden death phenotypes which have been characterized in SUDEP models.

In addition to potential contributions by autonomic neural circuits, intrinsic dysfunction in the heart may also facilitate seizure-related cardiorespiratory collapse. Chronic epilepsy is known to negatively alter cardiac electrophysiology and ion channel remodeling (Ravindran et al., 2016). Furthermore, these changes can lead to arrhythmia development which may predispose SUDEP risk (Ravindran et al., 2016). More recent research has shown that Kv1.1 is present in atrial and ventricular cardiomyocytes and plays an important role in action potential repolarization. However, the sinoatrial myocytes are responsible for intrinsic cardiac pacemaking, and the presence and function of Kv1.1 protein has not yet been studied in this region. Furthermore, genetically and pharmacologically manipulating Kv1.1 in atrial and ventricular cells has revealed its role in action potential repolarization, but how Kv1.1 contributes to whole animal cardiac function is not known. Chapter 4 of this dissertation utilizes genetic strategies to knock out Kv1.1 in the heart to first evaluate the presence of Kv1.1 in the pacemaker cells of the sinoatrial node,

and then to evaluate how heart-specific Kv1.1 deletion impacts whole animal cardiac health. These studies will help to reveal how the heart contributes to cardiac dysfunction and seizure-related death in the preclinical Kv1.1 deficiency mouse models.

Current research using the preclinical *Kcna1* deficiency model has utilized global and neuron-specific deletion of Kv1.1 to better understand SUDEP mechanisms, but there has not been work discerning how specific neural circuits or the heart may act as substrates for SUDEP phenotypes and overall risk of sudden death. Both the *Kcna1* global KO and the neuron-specific *Kcna1* conditional knockout (cKO) models display spontaneous seizures, cardiorespiratory abnormalities, and sudden death which indicates that these phenomena are brain derived. Limiting *Kcna1* deletion to corticolimbic or brainstem circuits will inform how specific autonomic circuits may be directly contributing to SUDEP mechanisms. Though the characterized phenotypes in the Kv1.1 deficiency mouse model are largely believed to be brain-derived, the neuron-specific cKO mice did display attenuated phenotypes suggesting regions outside the brain may also be contributing. Kv1.1 is not expressed in the lungs but is present in the heart and may be contributing to basal cardiac dysfunction which may increase risk of seizure-related death. Lastly, research into other SUDEP mouse models, such as *Scn1a* mice, have elucidated the specific cellular substrates contributing to their classified phenotypes, but this has never been done for the *Kcna1* mouse model to highlight areas for more intensive future research in this model.

Therefore, the overall hypothesis is that the forebrain and brainstem circuits, as well as the heart, make unique contributions to SUDEP pathology, and Kv1.1 deficiency in these regions may contribute to overall SUDEP risk.

Specific Aims

Aim 1: To determine how Kv1.1 deficiency in the corticolimbic circuit contributes to seizures, cardiorespiratory abnormalities, and sudden death.

Rationale. Brain-driven mechanisms have been strongly implicated in epilepsy, cardiorespiratory, and sudden death phenotypes due to Kv1.1 deficiency in mouse models, but the contributions of specific circuits and brain regions remain unknown. Based on expression studies and seizure behaviors, limbic circuits (including the hippocampus and amygdala) likely play a role in the neural and cardiorespiratory phenotypes of *Kcna1* KO mice, but this has never been tested directly. Kv1.1 transcripts and protein are known to be expressed in limbic regions such as the hippocampus and amygdala, as well as in cortex (H. Wang et al., 1994). Furthermore, spontaneous seizures in *Kcna1* global KO mice exhibit behavioral features of rearing and falling that are indicative of limbic origin (Glasscock et al., 2010; Smart et al., 1998). Additionally, mapping of seizure-induced neuronal activity in *Kcna1* KO mice by measuring FOS activation shows increased activity in the basolateral amygdala and dentate hilus of the hippocampus, further supporting limbic involvement during seizures (Gautier & Glasscock, 2015). Finally, both the amygdala and hippocampus play an upstream regulatory role in autonomic signaling which can influence cardiac and respiratory function through known connections with the periaqueductal grey and ventral tegmental areas of the midbrain, the locus coeruleus (LC) of the pons, and the nucleus of the solitary tract (NTS) of the medulla (Arrigo et al., 2017; Deboer et al., 1999; García-Medina & Miranda, 2013; Gasbarri et al., 1994; Kahn & Shohamy, 2013; Liddell et al., 2005; Rizvi et al., 1991). Thus, we hypothesize that deletion of *Kcna1* in forebrain corticolimbic circuits will be sufficient to cause seizures, cardiorespiratory abnormalities, and sudden death.

Experimental Methods. To test this hypothesis, we will generate corticolimbic-specific cKO mice using the *Emx1* (*empty spiracles homeobox 1*)-Cre driver. *Emx1*-Cre is commonly used to modify gene expression in various mouse models of epilepsy (Bunton-Stasyshyn et al., 2019; H. T. Wang et al., 2021). The *Emx1*-Cre allele targets 88% of excitatory neurons in the neocortex and hippocampus, the olfactory bulb, and regions of the amygdala (Briata et al., 1996; Gorski et al., 2002; Kohwi et al., 2007). Amygdalar cre expression has been confirmed in the basolateral, basomedial, and lateral amygdala as well as in the posterolateral cortical amygdaloid nucleus and posteromedial amygdaloid nucleus which collectively process environmental stimuli to elicit emotional and physiological responses (Gorski et al., 2002). To generate this cKO strain, we will cross our floxed *Kcna1* mice to *Emx1*-Cre (JAX 005628) mice. Currently, all required mouse lines are established and breeding in our colony. $Cre^{+/-}$, $Kcna1^{flox/-}$ mice are being generated as cKOs. Control animals will be the following: 1) $Cre^{-/-}$, $Kcna1^{+/+}$ (labeled WT); 2) $Cre^{-/-}$, $Kcna1^{flox/-}$ (labeled fl/-); 3) $Cre^{+/-}$, $Kcna1^{+/+}$ (labeled Cre). The breeding scheme is highlighted in Figure 2.

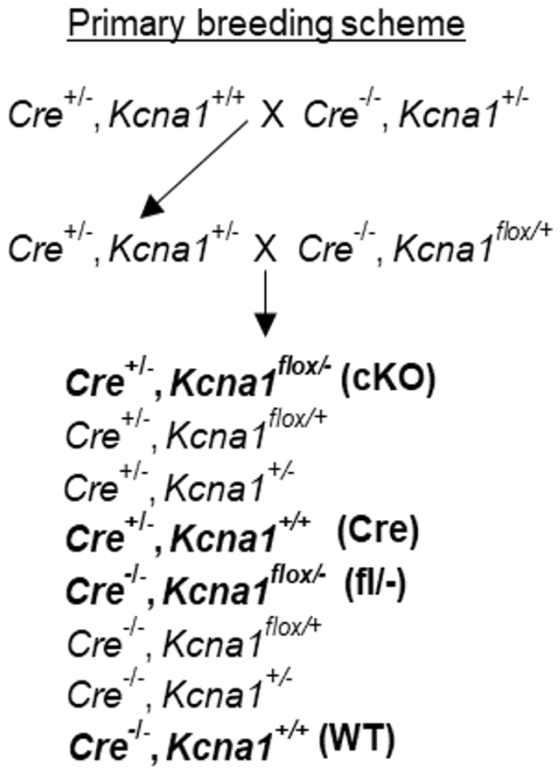

Figure 1.2. Primary Breeding scheme to generate conditional knockout (cKO) mice. For *Kcna1*, - indicates the global KO allele, and *flox* indicates the presence of the floxed allele. For Cre, + indicates the presence of a Cre allele.

We will assess neural and cardiorespiratory function in corticolimbic cKOs in the following subaims: 1) lifespan (measurement of premature/sudden death phenotype); 2) video-EEG-ECG and video-EEG-ECG-Plethysmography (to record spontaneous neural, cardiac, and respiratory function). For all experiments, animals will be age- and sex-matched. For the *in vivo* recordings mice will be tested at approximately 30-d old to make the measurements comparable with our previous studies in global KO and neuron-specific cKO mice which focused on this age since it corresponds to the median survival of global KO mice (Trosclair et al., 2020; Vanhoof-Villalba et al., 2018).

Subaim 1.1: We will generate Kaplan-Meier survival curves for cKO mice to test whether corticolimbic ablation of Kv1.1 is sufficient to cause premature death. We will measure lifespans up to 100 days for WT, Cre, and fl/- littermates as controls (15-20 per genotype). Survival curves will be analyzed using the Kaplan-Meier log-rank (Mantel-Cox) test.

Subaim 1.2: We will measure the contribution of corticolimbic-specific loss of Kv1.1 to neural and cardiorespiratory function by performing 24-h simultaneous video-EEG-ECG and 6-h video-EEG-ECG-Plethysmography recordings in 4-6 week old freely-moving, conscious mice (6-12 per genotype), as done previously (H. Dhaibar et al., 2019; Mishra et al., 2018). Briefly, mice will be anesthetized using an anesthetic cocktail (80-100 mg/kg Ketamine; 6-10 mg/kg Xylazine; 1-2 mg/kg Acepromazine, i.p.) and implanted with bilateral silver wire electrodes (0.005-inch diameter) attached to a microminiature connector. EEG electrodes will be implanted in the subdural space through cranial burr holes made above the parietotemporal cortex for recording electrodes and above the frontal cortex for ground and reference electrodes. ECG electrodes will be tunneled into the subcutaneous thoracic space and sutured in to record cardiac activity. Mice will be allowed to recover for 2 d before recordings. Mice will first undergo 24 h of continuous EEG-ECG recording in a tethered recording configuration using a Data Sciences International (DSI) digital EEG/video monitoring system with Ponemah software to capture and analyze data. Then mice will be placed in an unrestrained whole-body plethysmography chamber with a modified lid allowing for tethered EEG-ECG recording lasting 6 h using the same system and software. EEG, ECG, and Plethysmography data will be analyzed manually, as done previously (H. Dhaibar et al., 2019; Trosclair et al., 2020), to compare the following seizure and cardiorespiratory phenotypes: 1) seizure characteristics (frequency, duration, and behavior); 2) cardiac conduction blocks (ie, skipped beats due to atrioventricular or sinus blocks); 3) heart rate

variability (HRV, measured as RMSSD, SDNN, CV, and pNN6, as done previously (Trosclair et al., 2020)); 4) apnea frequency (ie, breathing cessation of ≥2 cycles, usually ~0.8 s); 5) sighs (augmented breaths of ≥25% higher amplitude and ≥125% higher tidal volume compared to the preceding 10 s); 6) respiratory variability (calculated as coefficient of variance as done previously (H. Dhaibar et al., 2019; Trosclair et al., 2020). Figure 3 shows sample waveforms for these measurements. Statistical comparisons will be made using a 1-way analysis of variance (ANOVA) followed by Tukey post-hoc tests.

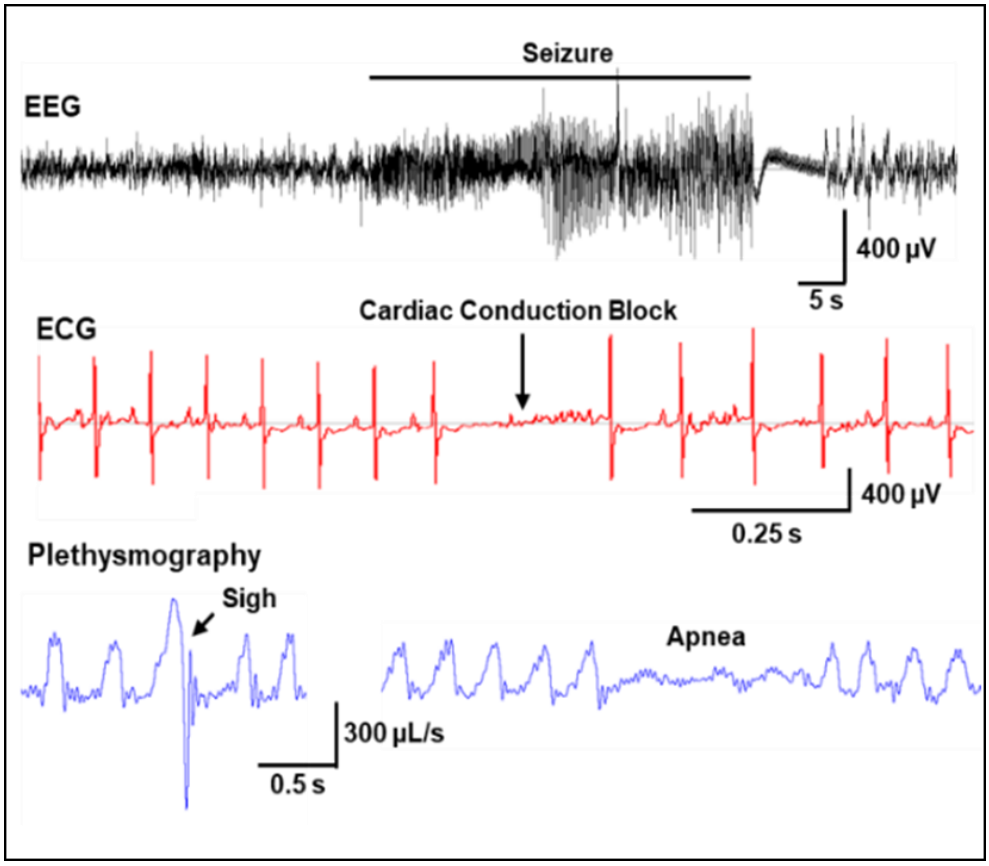

Figure 1.3. Sample waveforms from a corticolimbic cKO mouse.

Aim 2: To determine how Kv1.1 deficiency in the brainstem contributes to cardiorespiratory abnormalities and increased risk of seizure related death.

Rationale. The brainstem, comprised of the midbrain, medulla, and pons, contains neurons that act as the primary regulators of autonomic control of cardiorespiratory function. Within the brainstem are important regions such as the pre-Bötzinger complex, RTN, LC, DMNV, NA, and NTS which integrate sensory information to govern heart rate and respiratory patterns (Dubreuil et al., 2009; Fu et al., 2019; Menuet et al., 2020; Stornetta et al., 2006). Also associated with these regions is the vagus nerve which relays parasympathetic signals throughout the body, including the heart and lungs. Kv1.1 can be found in many cardiorespiratory nuclei throughout the brainstem and along the vagus nerve (Glasscock et al., 2010). *Kcna1* KO mice exhibit vagal hyperexcitability which is thought to contribute to cardiac and respiratory deficits in these mice (Glasscock et al., 2010). Therefore, we hypothesize that brainstem-specific *Kcna1* cKO will be sufficient to induce basal cardiorespiratory abnormalities and sudden death following a seizure-induced challenge. We do not anticipate seizures in these mice because *Kcna1* will be intact throughout the rest of the brain including the limbic region where the seizures are believed to originate.

Experimental Methods. To test this hypothesis, we have generated a brainstem-specific *Kcna1* cKO mouse model by crossing floxed *Kcna1* mice, which were developed in our lab, with Phox2b (paired like homeobox 2b)-Cre (JAX 016223) mice to generate cKOs (see crossing scheme in Fig 2). Phox2b-Cre drives expression primarily in hindbrain regions containing autonomic regulatory neurons including the RTN, LC, DMNV, NA, and NTS, but also expresses in the olfactory bulb (Dubreuil et al., 2008, 2009; Fu et al., 2019; Harper et al., 2015; M. M. Scott et al., 2011; Stornetta et al., 2006). The *PHOX2B* gene is associated with congenital central hypoventilation syndrome (CCHS), a lethal respiratory human disorder, and mice generated with a known human mutation

in *Phox2b* related to CCHS die soon after birth from respiratory failure (Dubreuil et al., 2008). *Phox2b*-Cre drives expression in most regions *Phox2b* is endogenously expressed, except in the peripheral ganglia and enteric nervous system (M. M. Scott et al., 2011). We will breed according to the same scheme as Aim 1, shown in Figure 2. The same WT, fl/-, and Cre genotypes will be used as controls. Cre-mediated deletion will be confirmed in cKO animals by PCR.

We will investigate the consequences of brainstem-specific *Kcna1* cKO in the context of the following subaims which are parallel to Aim 1: 1) lifespan (measurement of premature/sudden death phenotype); 2) video-EEG-ECG and video-EEG-ECG-Plethysmography (to record spontaneous neural, cardiac, and respiratory function). As these mice are not expected to spontaneously seize, we will also use a third subaim: 3) Flurothyl seizure susceptibility (to measure seizure threshold and survival following an inducible-seizure challenge). For all experiments, animals will be age- and sex-matched. For the *in vivo* and flurothyl recordings mice will be tested at approximately 30d old to make the measurements comparable with our previous studies in global KO and neuron-specific cKO mice which focused on this age since it corresponds to the median survival of global KO mice (Trosclair et al., 2020; Vanhoof-Villalba et al., 2018).

Subaim 2.1: We will generate Kaplan-Meier survival curves to measure whether brainstem-specific cKO of Kv1.1 is sufficient to cause premature death. We will measure lifespans up to 100 days for WT, Cre, and fl/- littermates as controls (5-15 per genotype).

Subaim 2.2: We will measure the contribution of brainstem-specific loss of Kv1.1 to neural and cardiorespiratory function by 24-h simultaneous video-EEG-ECG and 6-h video-EEG-ECG-Plethysmography in 4-6 week old freely moving, conscious mice (6-12 per genotype) as described in subaim 1.2.

Subaim 2.3: We will expose mice (~30-d old; 5-15 per genotype) to fluorothyl to examine how loss of Kv1.1 in the brainstem will impact latency to first clonic event, generalization time from clonic to tonic-clonic event, and survival as described previously. We will focus specifically on generalization time as this is where we anticipate the greatest difference between cKO and control animals as the generalization phase is directly related to brainstem activity.

Aim 3: To determine how Kv1.1 deficiency in the sinoatrial node contributes to intrinsic pacemaking and how Kv1.1 deficiency in the heart contributes to whole-animal cardiac function.

Rationale: Sinoatrial cells are the pacemaker cells of the heart which utilize unique electrical currents to drive the heartbeats which keep humans and mice alike alive. Part of the sinoatrial cell action potential involves potassium channel related repolarization, but to date Kv1.1 has not been classified as part of this process. Unpublished reports from our lab have shown that multielectrode array recordings of the right atria in the region of the sinoatrial node show slower firing rates in *Kcna1* global KO mice compared to wildtype mice suggesting intrinsic pacemaking deficits. It is not yet known how *Kcna1* contributes to sinoatrial cell physiology which would indicate its role in intrinsic pacemaking. Utilizing specialized cardiomyocyte dissociation techniques and electrophysiology, our lab is currently seeking to answer this question. While not directly handling the dissociation or patch clamp electrophysiology, my work in this project used immunocytochemistry in order to confirm the presence of Kv1.1 in WT cells, and its absence in the knockout cells. We hypothesize that not only is Kv1.1 present in the sinoatrial cells but is important in proper intrinsic cell firing.

Recent research has shown that *Kcna1* plays an underappreciated role in atrial and ventricular electrophysiology. Deletion of Kv1.1 from either region leads to impaired action

potential repolarization under patch clamp physiology. In unpublished reports from our lab, isolated hearts from *Kcna1* KO mice show bradycardia suggesting these single cell deficits may translate to whole organ dysfunction in intact *Kcna1* KO mice. However, studies into heart-specific *Kcna1* deficiency mice have not yet been done. Our lab has generated a novel heart-specific Kv1.1 conditional knockout mouse model and we hypothesize that this specific deficiency will result in overall basal cardiac dysfunction.

Experimental Methods: To test these hypotheses, we will use a combination of already established *Kcna1* global knockout mice, and novel cardiac-specific cKO mice using the *Myh6*-Cre driver. *Myh6* (*Myosin heavy chain 6*) drives expression throughout the heart. To generate this cKO strain, we will cross our floxed *Kcna1* mice to *Myh6*-Cre (Jax 011038) mice. Currently, all of the required strains are successfully breeding in our colony. We breed these animals according to the same breeding scheme as in aims 1 and 2. The same WT, fl/-, and Cre genotypes will be used as controls.

We measure the contribution of cardiac-specific loss of Kv1.1 to cardiac function in the following subaims.

Subaim 3.1: We will use immunocytochemistry to show the presence of Kv1.1 in the sinoatrial myocytes, and then further explore its function using patch clamp electrophysiology. To prove the presence of Kv1.1 in WT sinoatrial cells as well as their absence in the global knockout mice, immunocytochemistry will be performed. A lab colleague isolates the sinoatrial region from the mouse heart (either WT or KO) and uses specific dissociation protocols to obtain healthy, living, individual sinoatrial cells. These cells are plated into chambered slides to adhere, and then immunocytochemistry for Kv1.1 is performed (further described in the methods of Chapter 4).

Subaim 3.2: We will measure the contribution of cardiac-specific loss of Kv1.1 to cardiac function by 24-h simultaneous video-EEG-ECG in 4-6 week old freely moving, conscious mice (6-12 per genotype) as described in subaim 1.2.

CHAPTER 2:

EXCITATORY CORTICOLIMBIC NEURONS DRIVE SUDDEN UNEXPECTED DEATH IN EPILEPSY (SUDEP) IN THE *KCNA1* KNOCKOUT MODEL

2.1 Abstract

Sudden unexpected death in epilepsy (SUDEP) is the leading cause of epilepsy-related death, likely stemming from seizure activity disrupting vital brain centers controlling heart and breathing function. However, understanding of SUDEP's anatomical bases and mechanisms remains limited, hampering risk evaluation and prevention strategies. Prior studies using a neuron-specific *Kcna1* conditional knockout (cKO) mouse model of SUDEP identified the primary importance of brain-driven mechanisms contributing to sudden death and cardiorespiratory dysregulation, yet the underlying neurocircuits have not been identified. Here, using the Emx1-Cre driver, we generated a new cKO mouse model lacking *Kcna1* in excitatory neurons of the cortex, hippocampus, and amygdala to test whether the absence of Kv1.1 in forebrain corticolimbic circuits alone is sufficient to induce spontaneous seizures, premature mortality, and cardiorespiratory dysfunction. Performing survival studies and electroencephalography, electrocardiography, and plethysmography (EEG-ECG-Pleth) recordings, we demonstrate premature death and epilepsy in corticolimbic-specific cKO mice. During monitoring, we fortuitously captured one SUDEP event, which showed a generalized tonic-clonic seizure that initiated respiratory dysfunction culminating in cardiorespiratory failure. In addition, we observe that cardiorespiratory abnormalities are common during non-fatal seizures in cKO mice, but

mostly absent during interictal periods, implying ictal, not interictal, cardiorespiratory impairment as a more reliable indicator of SUDEP risk. These results pinpoint corticolimbic excitatory neurons as critical neural substrates in SUDEP and affirm seizure-related respiratory and cardiac failure as a likely cause of death.

2.2 Introduction

Sudden unexpected death in epilepsy (SUDEP) is the leading cause of epilepsy-related mortality with an incidence of approximately 1.2/1000 person-years (Hirtz et al., 2007; Thurman et al., 2014) and an overall public health burden that is second only to stroke among neurological diseases in years of potential life lost (Thurman et al., 2014). Besides having epilepsy, the affected individuals are otherwise healthy and have no accidental, pathological, or toxicological explanation for their death (Nashef et al., 2012). SUDEP is thought to be a predominantly seizure-related event affecting patients with poorly controlled epilepsy (Sveinsson et al., 2020). The current view of SUDEP is that seizures somehow trigger deleterious cardiac and respiratory dysfunction that culminates in death (Devinsky, 2011; Manolis et al., 2019). However, the exact details of how neural, cardiac, and respiratory dysfunctions contribute to this catastrophic outcome remain unresolved, in part because SUDEP cases are almost always unwitnessed.

Contemporary clinical understanding of SUDEP is based largely on the MORTEMUS study (MORTality in Epilepsy Monitoring Units Study), a description of 9 rare cases that were captured in epilepsy monitoring units (EMUs) by video-electroencephalography (EEG) and electrocardiography (ECG) and retrospectively analyzed for terminal seizure and cardiorespiratory patterns (Ryvlin et al., 2013). All of these SUDEP cases exhibited a pattern of generalized tonic-

clonic seizures (GTCS) followed by postictal (post-seizure) increases in respiratory and heart rates, which gave way to a lethal combination of central apnea (brain-mediated breathing cessation), bradycardia (heartrate slowing) and asystole (no heartbeat; i.e., flatline), coinciding with postictal generalized EEG suppression (PGES; absence of EEG brain activity) (Ryvlin et al., 2013). Terminal apnea always preceded cardiac arrest, suggesting the potential primacy of respiratory mechanisms (Ryvlin et al., 2013). However, it remains to be seen whether these limited observed human cases are representative of all SUDEP.

Because of the dearth of knowledge from human cases, much of what we know about potential SUDEP pathomechanisms and the underlying anatomy comes from work in animal models. One of the most widely-used models for identifying candidate mechanisms and biomarkers underlying SUDEP pathophysiology is the *Kcna1* global knockout (KO) mouse because it exhibits essential features and risk factors observed in humans. These characteristics include frequent generalized tonic-clonic seizures, seizure-related sudden death, and ictal cardiorespiratory dysfunction with aberrant breathing occurring before cardiac abnormalities. The *Kcna1* gene, which encodes pore-forming Kv1.1 voltage-gated potassium channel α-subunits, also has direct genetic relevance for human epilepsy and SUDEP. At least 21 different human *KCNA1* mutations have been identified that cause epilepsy, including four mutations in individuals with epileptic encephalopathy, an early-onset form of severe epilepsy with a high risk of SUDEP (Paulhus & Glasscock, 2023). Building upon findings in the *Kcna1* global KO mouse model, in a prior study we generated neuron-specific *Kcna1* conditional knockout (cKO) mice to test whether seizure-evoked cardiorespiratory dysfunction and SUDEP require the absence of Kv1.1 in both brain and heart or whether ablation in neurons is sufficient. We found that deletion of Kv1.1 in

neurons alone was sufficient to cause epilepsy, premature death, and cardiorespiratory dysregulation. However, the type and location of these neurons remain unknown.

To begin to map the brain regions contributing to SUDEP, here we generated cKO mice lacking Kv1.1 in forebrain corticolimbic circuits. We obtained these mice by crossing floxed *Kcna1* mice with Emx1-Cre mice, which selectively deletes *Kcna1* in excitatory neurons of the neocortex, hippocampus, and amygdala, areas where Kv1.1 is normally highly abundant. Using our rodent epilepsy monitoring unit (EMU), we simultaneously recorded brain (electroencephalogram; EEG), heart (electrocardiogram; ECG), and lung (plethysmography; pleth) activity to identify seizures and cardiorespiratory abnormalities in cKO mice. We find that deletion of *Kcna1* in excitatory corticolimbic neurons is sufficient to cause spontaneous seizures and premature mortality, as well as cardiorespiratory dysfunction during seizures but not during interictal periods. We also describe a rare captured SUDEP event, which revealed terminal cardiorespiratory patterns that resemble previous descriptions in humans. Our results pinpoint excitatory neurons within corticolimbic circuits as critical drivers of epilepsy and SUDEP due to cardiorespiratory failure. These findings provide the first identification of the brain regions underlying seizures and SUDEP in the widely-used *Kcna1* KO mouse model, as well as one of the only observations of a SUDEP event with cardiorespiratory data revealing the terminal sequence of events.

2.3 Materials and Methods

2.3.1. Animals

Corticolimbic-specific *Kcna1* conditional knockout (cKO) mice (i.e., *Emx1*-Cre$^{+/-}$; *Kcna1*$^{del/-}$) were generated by crossing heterozygous *Kcna1* floxed (fl) mice (*Kcna1*$^{fl/+}$) with heterozygous *Kcna1* global knockout mice (*Kcna1*$^{+/-}$) carrying one copy of the *Emx1* transgene (i.e., *Emx1*-Cre$^{+/-}$, *Kcna1*$^{+/-}$). *Emx1*-Cre$^{+/-}$, *Kcna1*$^{+/-}$ mice were generated by crossing hemizygous transgenic *Emx1*-Cre$^{+/-}$ mice with heterozygous *Kcna1*$^{+/-}$ mice. The *Emx1*-Cre$^{+/-}$ transgene causes Cre-mediated recombination of the *Kcna1*^{fl} allele to yield the conditionally deleted allele (i.e., *Kcna1*^{del}). This breeding paradigm, which has been utilized in previous studies (Trosclair et al., 2020), was selected because it prevents unwanted Cre-mediated germline recombination and promotes increased Cre-mediated recombination efficiency. The above breeding scheme also yields the following mice which were designated as control genotypes for experiments: *Kcna1*$^{+/+}$, *Emx1*$^{-/-}$ (WT), *Kcna1*$^{+/+}$, *Emx1*$^{+/-}$ (Cre), and *Kcna1*$^{fl/-}$, *Emx1*$^{+/+}$ (fl/-). *Emx1*-Cre mice were purchased from Jackson Labs (Bangor, MN) under the catalog name B6.129S2-*Emx1*$^{tm1(cre)Krj}$/J (JAX 005628). *Kcna1*$^{+/-}$ mice, which are maintained on a Tac:N:NIHS-BC genetic background, carry a KO allele of the *Kcna1* gene due to targeted deletion of the entire open reading frame (Smart et al., 1998). *Kcna1*$^{fl/+}$ mice, which are maintained on a C57BL/6J genetic background, were generated as described previously (Trosclair et al., 2020). Mice were housed at 22°C, fed *ad libitum*, and subjected to a 12-h day/night cycle. For lifespan analysis, both experimental and control mice were monitored for mortality until the age of 100 days. All experiments were performed in accordance with National Institutes of Health (NIH) guidelines with approval from the Institutional Animal Care and Use Committee of Southern Methodist University.

2.3.2. Genotyping

To identify experimental and control mice, genomic DNA was isolated by enzymatic digestion of tail clips using Direct-PCR Lysis Reagent (Viagen Biotech, Los Angeles, CA, USA). Genotypes were determined by performing PCR amplification of genomic DNA using allele-specific primers. For detection of the *Kcna1* global KO allele, the following primer sequences were used to yield amplicons of 337 bp for the wild-type (WT) allele and 475 bp for the KO allele: a WT-specific primer (5'-GCCTCTGACAGTGACCTCAGC-3'); a KO-specific primer (5'-CCTTCTATCGCCTTCTTGACG-3'); and a common primer (5'-GCTTCAGGTTCGCCACTCCCC-3'). For detection of the *Kcna1*^{fl} allele, the following primer sequences were used to yield amplicons of 197 bp for the WT allele and 260 bp for the floxed allele: a WT-specific primer (5'-GCTCCTCTACTATCAGCAAGTCTGAGTACATGG-3'); a floxed-specific primer (5'-ATCAAGTTGGACATCACCTCCCACAAC-3'); and a common primer (5'-AAGGGGTTTGTTTGGGGCTTTTGTT-3'). For detection of the deleted *Kcna1* floxed allele (i.e., *Kcna1*^{del}) resulting from Cre-mediated recombination, the following primers were used to yield an amplicon of 679 bp for the deleted allele: the common primer in the *Kcna1*^{fl} reaction above and 5'-CTCCAGTTTTACGAAGTTGTAAACAGATCGG-3′. For detection of the *Emx1*-Cre transgene, the following primer sequences were used to yield a product of 315 bp for the WT allele, and 195 bp for the Cre allele: a WT-specific primer (5'-CAAAGACAGAGACATGGAGAGC-3'); a *Emx1*-Cre specific primer (5'-TCGATAAGCCAGGGGTTC3'), and a common primer (5'-CAACGGGGAGGACATTGA-3').

2.3.3. Western blotting

To isolate and quantify protein levels of Kv1.1, age- and sex-matched mice (1-2 months old) were euthanized by isoflurane overdose, and their brains were quickly removed and dissected on ice to separate the cortex, hippocampus, and brainstem. Tissues were homogenized using a motorized mortar and pestle in ice-cold RIPA buffer (pH 7.4) containing EDTA and a cocktail of protease inhibitors (Thermo Scientific; Waltham, MA). Nuclei and cellular debris were separated from the homogenates by centrifuging at 12,000 revolutions per minute (RPM) for 15 minutes at 4°C. The samples were stored at -80°C until used. Biochroninic acid (BCA) assay (Thermo Scientific; Waltham, MA) was used to determine protein concentrations of the brain region homogenates and equal protein amounts were resolved on 8% SDS-polyacrylamide gels by electrophoresis. The resolved proteins were transferred onto nitrocellulose membranes by wet transfer at 4°C. The membranes were treated with blocking buffer made of tris buffered saline with Tween (TBST; 0.1% v/v) and milk protein (5% w/v) for 1 hour at room temperature (RT; ~22°C). The membranes were then incubated overnight with mild rocking at 4°C in primary antibody solution prepared in TBST with bovine serum albumin (BSA; 5% w/v). The primary antibodies used were mouse monoclonal anti-Kv1.1 (1:500; K20/78; Antibodies Incorporated; Davis, CA) and mouse monoclonal anti-β-actin (1:500, sc-47778, Santa Cruz Biotechnology; Dallas, TX). Following overnight incubation, the membranes were washed 3 times for 5 minutes with TBST, and then the membranes were treated for 1 hour at RT with goat anti-mouse IgG-HRP secondary antibody (1:5000; Cell Signaling Technology; Danvers, MA) in blocking buffer. After a final wash in TBST, immunoreactive bands were visualized using an enhanced chemiluminescence (ECL) detection kit (ImmunoCruz, Santa Cruz Biotechnology; Dallas, TX) and developed on a UVP ChemStudio imaging system (Analytik Jena; Upland, CA). Band intensity was quantified using

densitometry analysis on VisionWorks software (Analytik Jena; Upland, CA), normalized to β-actin levels, and reported as relative intensity.

2.3.4. Video-electroencephalography-electrocardiography-plethysmography (EEG-ECG-pleth) recordings

To record *in vivo* brain and heart activity, mice (4-6 weeks old) of both sexes were anesthetized using an anesthetic cocktail and surgically implanted with bilateral silver wire EEG and ECG electrodes (0.005-inch diameter) attached to a microminiature connector (Omnetics Connector Corporation, Minneapolis, MN) for recording in a tethered configuration. The anesthetic cocktail contained ketamine (100 mg/kg), xylazine (10 mg/kg), and acepromazine (2 mg/kg) and was administered by intraperitoneal (i.p.) injection. Following completion of the surgery, the reversal agent Antisedan (1 mg/kg) was administered by subcutaneous (s.c.) injection. Carprofen (5 mg/kg, s.c.) was given the day of surgery and 24 hours post-surgery for pain management. EEG wires were inserted into the subdural space through cranial burr holes overlying the parietotemporal cortex for the recording electrodes and above the frontal cortex for the ground and reference electrodes, as described previously (Mishra et al., 2018). Two ECG wires were tunneled subcutaneously on both sides of the thorax and sutured in place to record cardiac activity, as described previously (Mishra et al., 2018). Mice were allowed to recover for 48 hours before recording simultaneous EEG-ECG for 24 h continuously while the animals were housed in a plexiglass tank (40-cm length x 20-cm width x 23-cm height). Biosignals were band-pass filtered by applying 0.3 Hz high-pass and 75-Hz low pass filters for EEG and a 3.0-Hz high-pass filter for ECG. Sampling rates were set to 500 Hz for EEG and 2kHz for ECG.

For recording respiratory waveforms in tandem with EEG-ECG, mice were placed in an unrestrained whole-body plethysmography (pleth) chamber (Data Sciences International; St. Paul, MN, USA) with a lid that was modified to accommodate wires for recording EEG-ECG in a tethered configuration, as done previously (H. Dhaibar et al., 2019). Mice were provided a 45-min acclimatization period in the chamber before video and EEG-ECG-pleth were simultaneously recorded in 5-6 hour sessions during the light phase of the day (i.e. between 6:00 am and 6:00 pm) using Ponemah data acquisition and analysis software (Data Sciences International; St. Paul, MN, USA). Respiratory signals were acquired at a 500-Hz sampling rate. EEG-ECG-pleth recordings were always conducted immediately after completion of the 24-h EEG-ECG recordings.

2.3.5. Analysis of video-EEG, ECG, and pleth recordings

Seizures were identified by visual inspection of the EEG and defined as high-amplitude, rhythmic electrographic discharges lasting ≥ 5 s. The seizure duration was defined as the time from the onset of electrographic seizure until the cessation of spiking. Behavioral phenotypes during seizures were manually classified from video footage and quantified as the percentage of seizures manifesting the specific behavior.

The RR intervals of the ECG waveforms during the 24-h EEG-ECG recording period were used to estimate heart rate (HR) and heart rate variability (HRV). For each ECG recording, six separate RR interval series were derived by sampling 2-min ECG segments every 4 h to provide three day phase (6:00 AM to 6:00 PM) and three night phase (6:00 PM to 6:00 AM) measurements. RR interval series for each segment were automatically generated and manually confirmed using Ponemah software (Data Sciences International, St. Paul, MN). RR intervals were only sampled

during times when the mouse was stationary and when the ECG showed no abnormalities such as skipped or ectopic beats occurred. HRV was measured in the time domain using the standard deviation of the RR intervals (SDNN) and the root mean square of successive differences between the RR intervals (RMSSD). The HR and HRV values for each animal represent an average of the six total segments.

Respiratory rate (breaths per min; BPM) was measured using Ponemah analysis software (Data Sciences International, ST. Paul, MN). Average respiratory characteristics for each mouse were calculated by sampling 50 consecutive breaths every hour for 5 h for a total of 250 breaths, as done previously (H. Dhaibar et al., 2019). Measurements were only collected during periods when animals were stationary, as verified by video monitoring. Respiratory variability was calculated as the coefficient of variance (CV) using the formula: $CV = \sigma / \mu$, where σ is the standard deviation of breath intervals and μ is mean of breath intervals. Apneas were also manually quantified and were identified as cessations of plethysmographic signals for ≥ 2 respiratory cycles, or 0.8-s, as done previously (H. Dhaibar et al., 2019).

2.3.6. Analysis of ictal and peri-ictal respiratory and cardiac abnormalities

To identify cardiorespiratory dysfunction during seizures, respiratory and cardiac abnormalities were manually scored and quantified offline. The cardiac variables analyzed included tachycardia (increased heart rate), bradycardia (decreased heart rate), and cardiac conduction blocks (characterized by an RR interval 1.5x longer than the preceding RR interval). The respiratory variables analyzed included tachypnea (increased respiratory rate), bradypnea (abnormally slow respiratory rate), ataxic breathing (abnormal pattern of breathing characterized

by complete irregularity of breathing frequency and volume), hypopnea (abnormally shallow breathing), sigh (described above), apnea (described above), and gasp (breaths with a low inspiration-expiration ratio). For cardiac and respiratory measures related to rate, tachy- and brady-events were defined as rate changes of at least +20% or -20% respectively, relative to the 20-s pre-ictal period immediately before seizure onset. Pre- and post-ictal phenotypes were counted if they occurred in the 20-s before seizure onset or after its termination, respectively.

2.3.7. Statistical Analysis

Data are presented as mean ± SEM. Prism 10 for Windows (GraphPad Software Inc, La Jolla, CA, USA) was used for statistical analysis. Survival curves were evaluated using the Kaplan-Meier log rank (Mantel-Cox) test. For comparisons involving two or more groups, one-way analysis of variance (ANOVA) was used followed by Tukey post-hoc tests. Outliers were identified using the ROUT method with Q= 1% and excluded from analyses. Differences between groups were deemed statistically significant if $P< 0.05$.

2.4. Results

2.4.1. Molecular characterization of corticolimbic-specific Kcna1 cKO mice

We generated corticolimbic-specific *Kcna1* cKO mice (i.e., *Emx1*-Cre$^{+/-}$; *Kcna1*$^{del/-}$) using the breeding scheme outlined in the Materials and Methods. The Emx1-Cre driver is a commonly used transgene that selectively targets most excitatory neurons in the neocortex and hippocampus, olfactory bulb, and regions of the amygdala, including the basolateral, basomedial, lateral,

posterolateral cortical, and posteromedial amygdaloid nuclei (Briata et al., 1996; Gorski et al., 2002; Kohwi et al., 2007). To confirm the tissue-specific deletion of *Kcna1*, we performed PCR and immunoblots of brains from cKO and control mice. PCR amplification of regionally-dissected brain tissue revealed the presence of the $Kcna1^{del}$ allele in the neocortex, hippocampus, and olfactory bulb, but not in the brainstem (Fig. 1A). We next performed Western blots to measure Kv1.1 protein levels in the brains of cKO mice. Immunoblots showed the nearly complete absence of Kv1.1 in the neocortex and hippocampus corresponding to the reported expression pattern of the Emx1-Cre transgene (Fig 1B). Note that $Kcna1^{fl/-}$ mice exhibit a 50-75% reduction in Kv1.1 levels compared to WT because they carry one copy of the global KO allele.

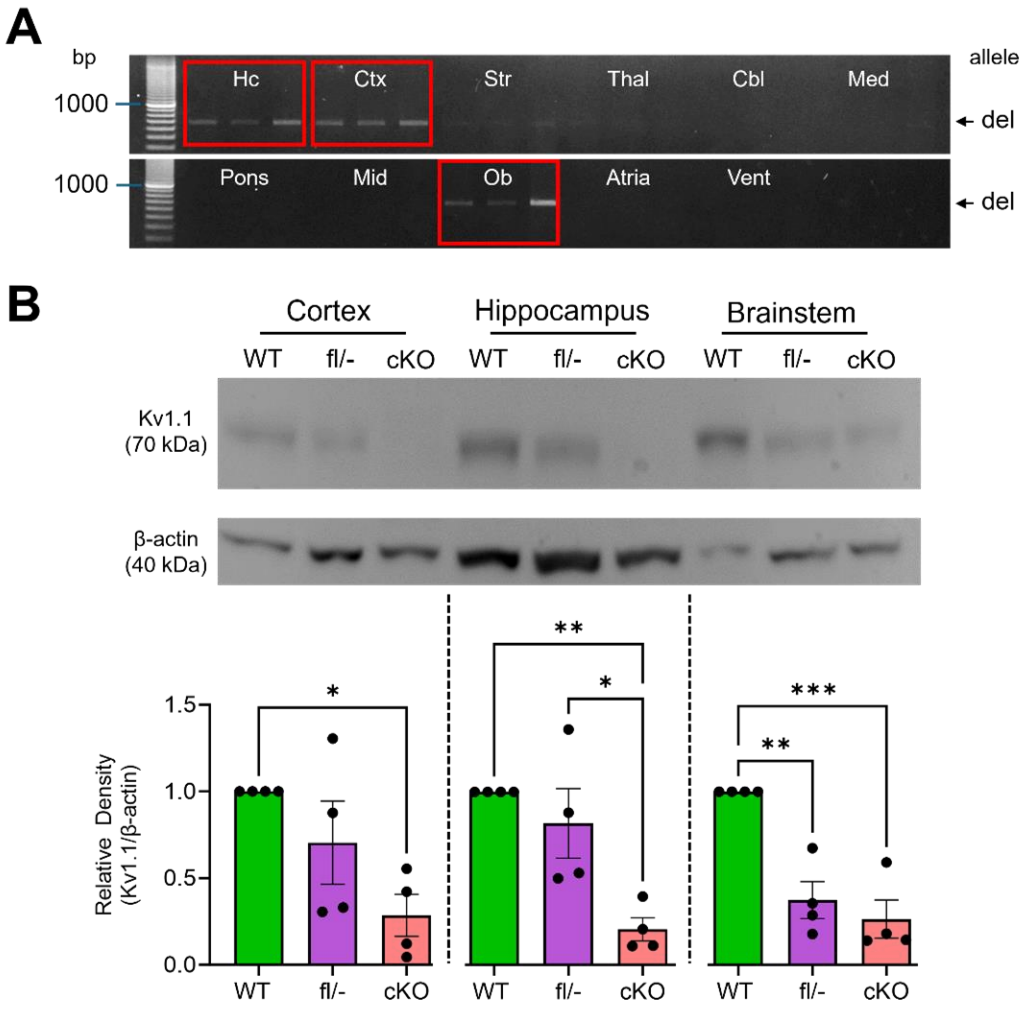

Figure 2.1. Molecular characterization of corticolimbic-specific Kcna1 cKO mice. (A) PCR detection of the *Kcna1* deletion (del; 679 bp) allele from genomic DNA isolated from hippocampus (Hc), cortex (Ctx), striatum (Str), thalamus (Thal), cerebellum (Cbl), medulla (Med), pons, midbrain (Mid), olfactory bulb (Ob), left atria (Atr), and left ventricle (Vent) for cKO mice. The three lanes for each region represent a different corticolimbic-specific cKO mouse (n=3 cKO mice per region). Red boxes indicate regions where the deletion band is observed at a high level. (B) Representative western blots for Kv1.1 and β-actin loading control from the cortex, hippocampus, and brainstem from wild type (WT), *Kcna1*$^{fl/-}$ (fl/-), and corticolimbic-specific *Kcna1* cKO mice (1-2 months old) with corresponding quantification of relative density for Kv1.1 protein levels (n=4/genotype). *P<0.05, **P<0.01, ***P<0.001; one-way ANOVA.

2.4.2. Corticolimbic-specific cKO mice die prematurely

To assess whether *Kcna1* deficiency in corticolimbic circuits contributes to premature mortality, we measured postnatal survival during the first 100 days of life. Corticolimbic-specific cKO mice showed significant premature mortality with 25% of animals dying between three to seven weeks of age (Fig 2A; $p<0.0001$, Log-Rank Test). Nearly all early deaths occurred between 3-4 weeks old, with the youngest age at death being 21 days old. In contrast, control mice all lived to 100-d old, showing no evidence of early lethality (Fig 2A). Thus, deletion of *Kcna1* in excitatory corticolimbic neurons induces premature sudden death.

2.4.3. Corticolimbic-specific cKO mice exhibit spontaneous seizures

To test for the occurrence of spontaneous seizures, we performed video-EEG-ECG recordings for 24 h continuously. EEG analysis revealed the presence of spontaneous seizures in four of eight (50%) cKO mice during the recording period but none in control mice (Fig 2B-C). The EEG patterns typically consisted of runs of polyspike activity with progressively increasing amplitude followed by postictal flattening (Fig 2B). Immediately following seizure termination, about 80% of seizures exhibited postictal EEG suppression characterized by prolonged flattening of EEG activity lasting for several seconds. For the cKO mice that exhibited seizures, the average seizure frequency was 0.5 ± 0.1/h with an average seizure duration of 39.9 ± 13.9s (Fig 2C). Of the 52 individual seizures recorded in cKO mice, 5.77% (3/52) lasted > 60 s.

Using the corresponding video recordings, we also analyzed the behaviors associated with the EEG seizures (Fig 2D). Most seizures (75%) exhibited milder behavioral manifestations, such as head nodding and forelimb clonus. However, we also observed more severe convulsive

behaviors, such as running and bouncing, rearing, and loss of posture, but those behaviors occurred less frequently in about 15-30% of seizures. Thus, selective Kv1.1 deficiency in corticolimbic circuits is sufficient to cause spontaneous generalized tonic-clonic seizures in mice.

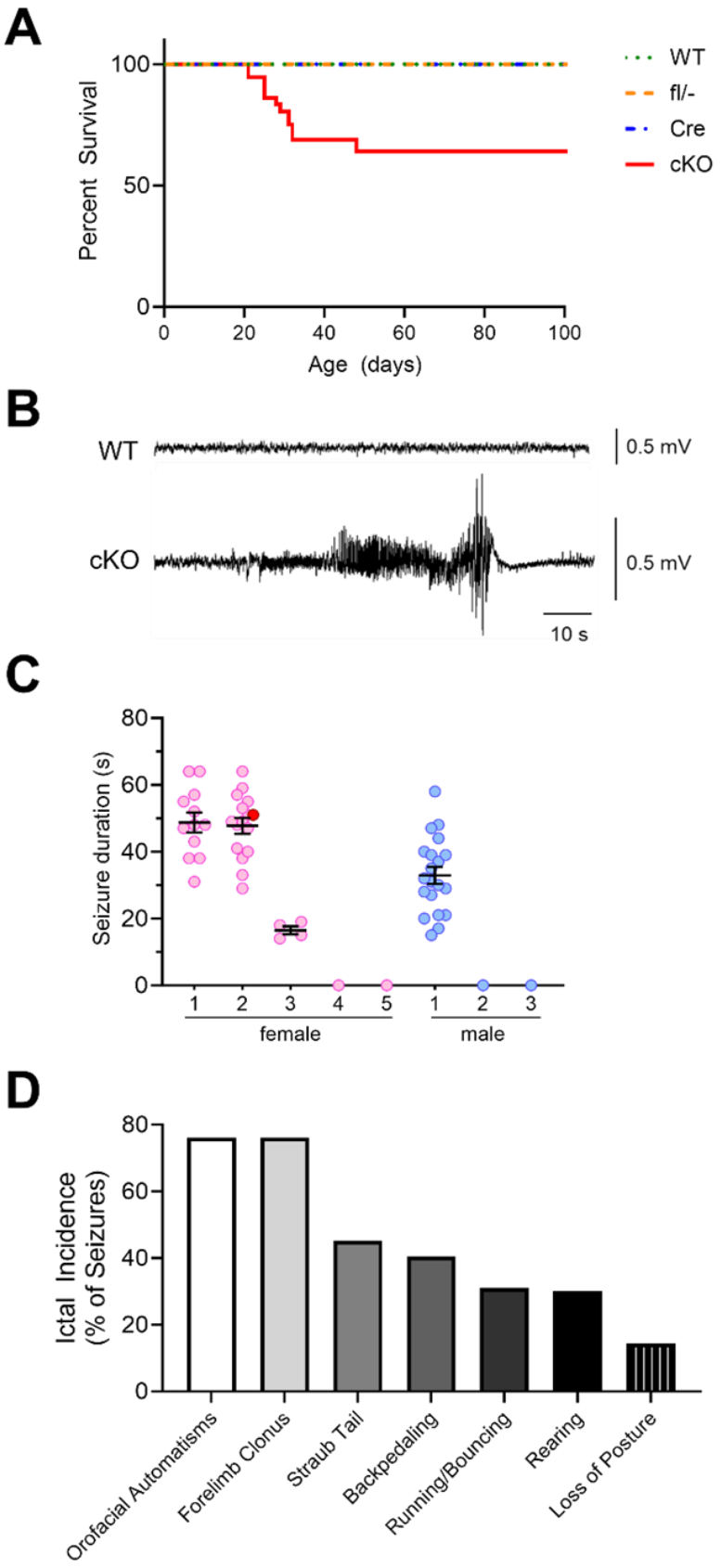
A
Percent Survival
100
50
0
0
20
40
60
80
100
Age (days)
WT
fl/-
Cre
cKO
B
WT
cKO
0.5 mV
0.5 mV
10 s
C
Seizure duration (s)
80
60
40
20
0
1
2
3
4
5
1
2
3
female
male
D
Ictal Incidence
(% of Seizures)
80
60
40
20
0
Orofacial Automatisms
Forelimb Clonus
Straub Tail
Backpedaling
Running/Bouncing
Rearing
Loss of Posture

Figure 2.2. Corticolimbic-specific *Kcna1* cKO mice exhibit premature death and spontaneous seizures. (A) Kaplan-Meier survival curves showing lifespan for WT (n=20), hemizygous *Emx1*-Cre (Cre; n=41), compound heterozygous *Kcna1*$^{fl/-}$ (fl/-; n=72), and corticolimbic-specific cKO (n=36) mice. In cKO mice, survival was significantly decreased compared to Cre, fl/-, and WT controls ($P<0.0001$, Log-rank test). (B) Representative EEG traces from a WT and cKO mouse showing normal and seizure activity, respectively. (C) Plot of individual seizure durations for every seizure recorded in each cKO animal in the study. Female mice are denoted by pink circles and the males are represented by blue circles. Female mouse number two died from SUDEP during the recording, and the terminal seizure is indicated by the dark red circle. (D) Frequency of various seizure-associated behaviors in cKO mice, quantified as the percentage of total seizures in which they occurred.

2.4.4. Corticolimbic-specific cKO mice exhibit seizure-related cardiac dysfunction

To determine whether cKO mice exhibit ictal or post-ictal cardiac dysfunction, ECG recordings were analyzed during and immediately after seizures. We found that seizures evoked a variety of cardiac abnormalities ranging from cardiac conduction blocks to rhythm disturbances. Cardiac conduction blocks were the most common cardiac abnormality observed during seizures, occurring in 27% of seizures (Fig. 3A,B). The second most common cardiac phenotype was bradycardia which was present in 23% of seizures (Fig 3A,C). We also observed ictal tachycardia, but it was rarer occurring in less than 10% of seizures (Fig 3A). During post-ictal periods, cardiac dysfunction was relatively infrequent with cardiac conduction blocks, bradycardia, and tachycardia occurring after 4-10% of seizures (Fig 3A). Thus, *Kcna1* deficiency in corticolimbic circuits is sufficient to cause ictal and peri-ictal cardiac dysfunction.

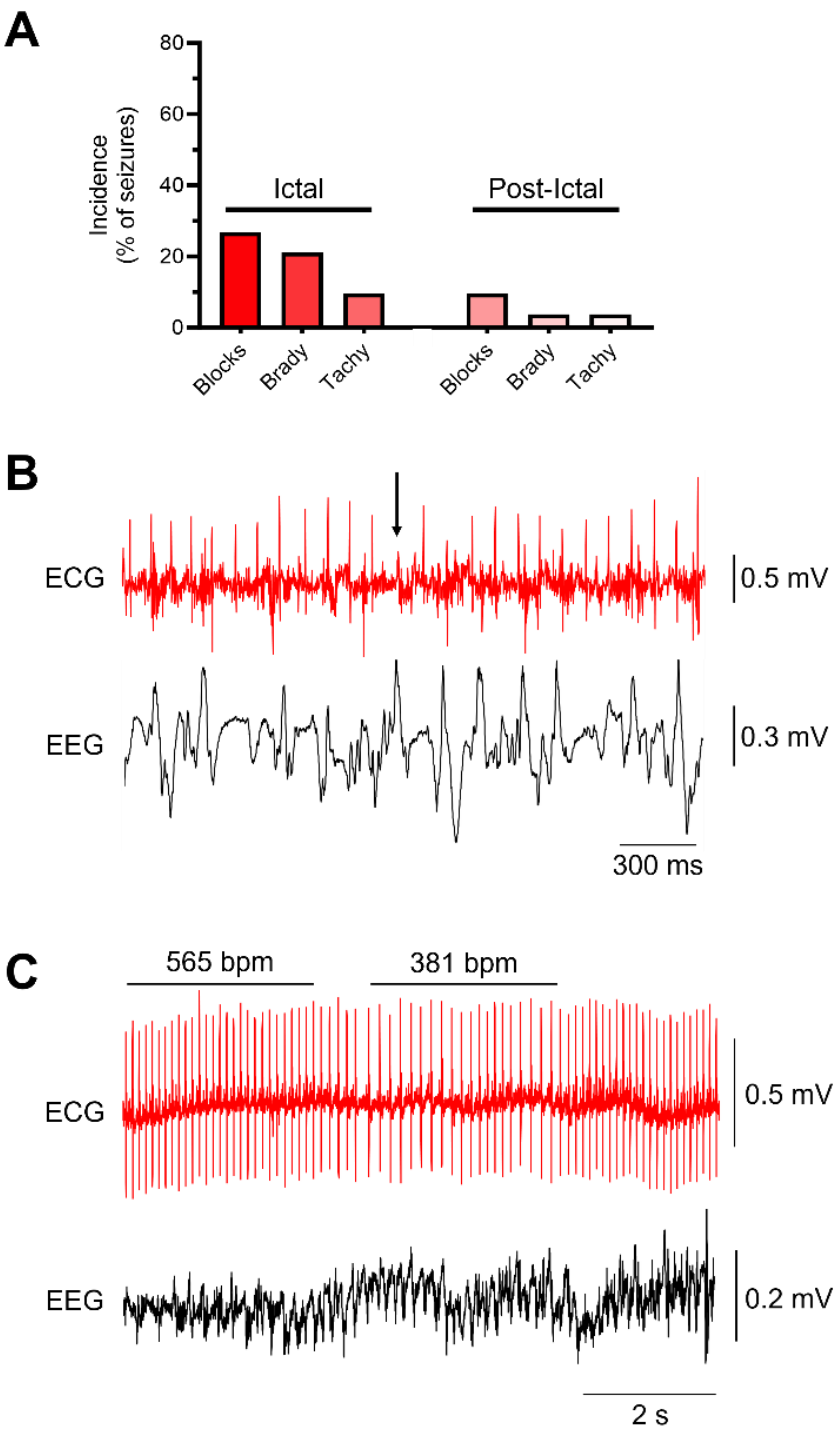
A
80
60
40
20
0
Incidence
(% of seizures)
Ictal
Post-Ictal
Blocks
Brady
Tachy
Blocks
Brady
Tachy
B
ECG
0.5 mV
EEG
0.3 mV
300 ms
C
565 bpm
381 bpm
ECG
0.5 mV
EEG
0.2 mV
2 s

Figure 2.3. Corticolimbic-specific *Kcna1* cKO mice exhibit ictal cardiac dysfunction. (A) Quantification of the incidence of various cardiac abnormalities during seizures (ictal) and post-ictal periods, represented as the percentage of total seizures in which they occurred. Blocks = cardiac conduction blocks; Brady = bradycardia; Tachy = tachycardia. (B) Representative ECG trace of an ictal cardiac conduction block (arrow) with corresponding EEG seizure activity. (C) Representative ECG trace showing ictal bradycardia with corresponding EEG seizure activity. The heart rates before (left) and during (right) the bradycardia event are indicated by bars above the corresponding ECG segments with the rates labeled in beats per minute (bpm).

2.4.5. Corticolimbic-specific cKO mice display seizure-related respiratory dysfunction

To examine whether corticolimbic-specific *Kcna1* deficiency is associated with respiratory dysregulation during seizures, we performed whole-body plethysmography (pleth) recordings in combination with video-EEG-ECG recordings. During seizures, respiratory dysfunction occurred more often than cardiac dysfunction. The most common ictal respiratory phenotypes were tachypnea and ataxic breathing, which occurred in 70% and 60% of seizures, respectively (Fig 4A-C). Of note, when respiratory and cardiac dysfunction were both present during seizures, respiratory dysfunction always appeared to occur first. Interestingly, while global KO and neuron-specific cKO mice consistently displayed hyperventilation/tachycardia coinciding with seizure onset, the corticolimbic-cKO mice did not reliably present with this increase in respiration at the start of a seizure. These findings suggest that the absence of Kv1.1 in corticolimbic circuits is sufficient to cause seizures that impair breathing, which may lead to cardiac dysfunction and an increased risk of SUDEP.

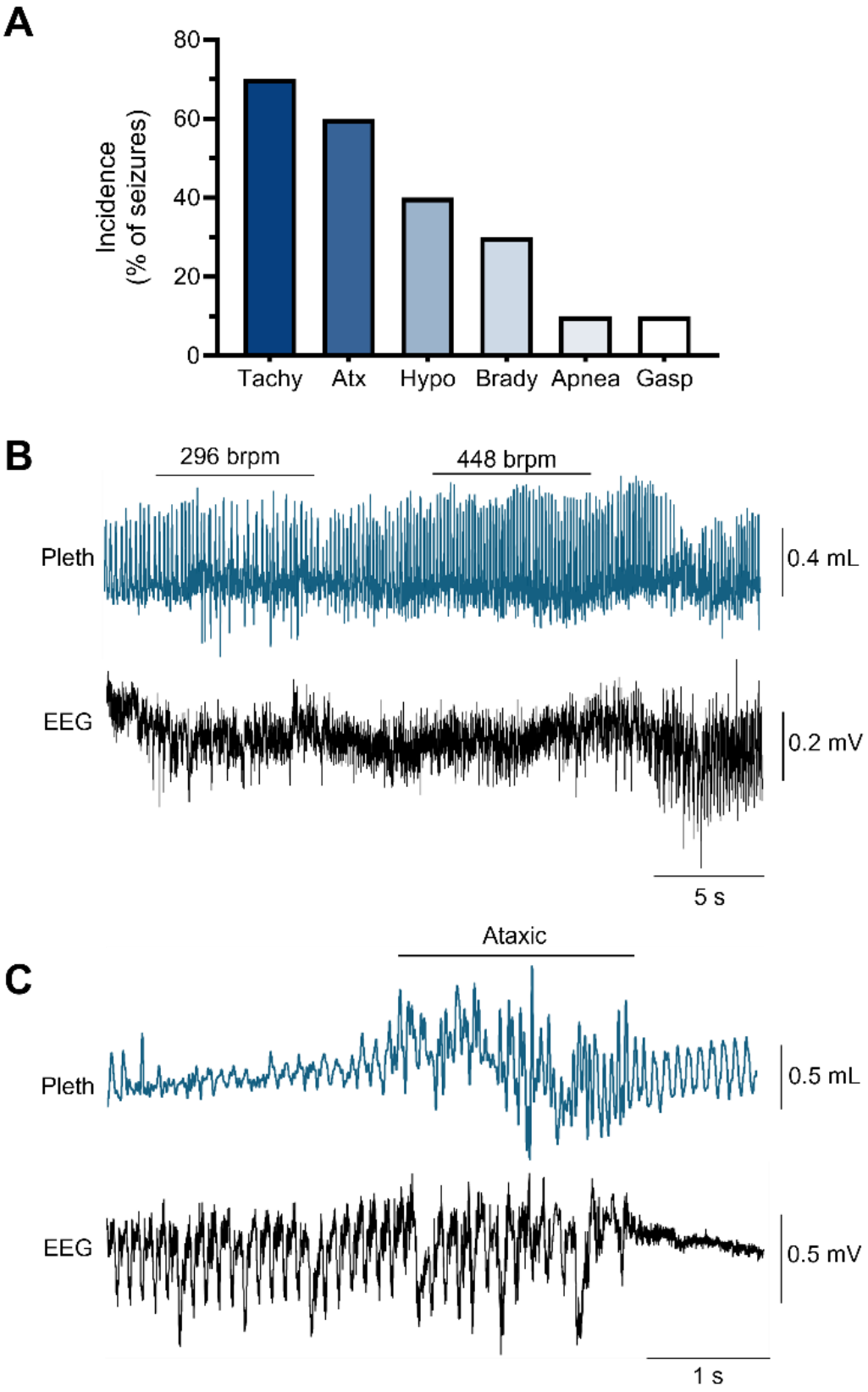
A
80
60
40
20
0
Incidence
(% of seizures)
Tachy
Atx
Hypo
Brady
Apnea
Gasp
B
296 brpm
448 brpm
Pleth
0.4 mL
EEG
0.2 mV
5 s
C
Ataxic
Pleth
0.5 mL
EEG
0.5 mV
1 s

Figure 2.4. Corticolimbic-specific *Kcna1* cKO mice exhibit ictal respiratory dysfunction. (A) Quantification of the incidence of various respiratory abnormalities during seizures, represented as the percentage of total seizures in which they occurred. Tachy = tachypnea; Atx = ataxic breathing; Hypo = hypopnea; Brady = bradypnea; Gasp = gasping. (B) Representative plethysmography (Pleth) trace of ictal tachypnea with corresponding EEG seizure activity. The breathing rates before (left) and during (right) the tachypnea event are indicated by bars above the corresponding Pleth segments with the rates labeled in breaths per minute (brpm). (C) Representative Pleth trace showing ictal ataxic breathing (indicated by the labeled bar) with corresponding EEG seizure activity.

2.4.6. Corticolimbic-specific cKO mice exhibit SUDEP due to seizure-evoked cardiorespiratory dysfunction

During EEG-ECG-pleth monitoring, we fortuitously captured a SUDEP event in a 30-d old female cKO mouse (labeled cKO #2 in Fig 2C), providing critical insight into the circumstances leading up to and during the terminal seizure. In the 24 hours preceding the terminal seizure, the mouse exhibited 15 seizures, the second most seizures of any cKO mouse (Fig 2C). Furthermore, the seizures had averaged 47.4 ± 9.4 s in duration, the second longest averages of any cKO (Fig 2C), suggesting the animal's seizure disorder was particularly severe.

When the SUDEP event occurred, the mouse had a generalized seizure lasting slightly longer than average, about 51-s (denoted by the red dot in Fig 2C). This seizure triggered abnormal breathing and cardiac patterns, followed by post-ictal generalized EEG suppression (PGES), ultimately resulting in death. Behaviorally, the seizure started with a Straub tail, circling, and forelimb myoclonus, then escalated to running and bouncing before culminating in tonic hindlimb extension and death.

As the seizure intensified with running and bouncing, respiration became irregular indicating ataxic breathing. About 5 seconds after ataxic breathing began, the heart rate slowed,

becoming bradycardic. As the seizure ended with tonic hindlimb extension, breathing abruptly stopped and post-ictal apnea ensued, coinciding with PGES (Fig 5A). After PGES onset, both breathing and brain activity did not resume. Moreover, the bradycardia observed during the seizure worsened postictally, with the RR intervals getting progressively longer and interspersed with non-conducted P waves indicative of cardiac conduction blocks (Fig 5B). Finally, about 8.2 min after the seizure ended, all cardiac activity ceased. These findings suggest that SUDEP in this case was triggered by a generalized tonic-clonic seizure that evoked primary respiratory failure leading to subsequent cardiac arrest.

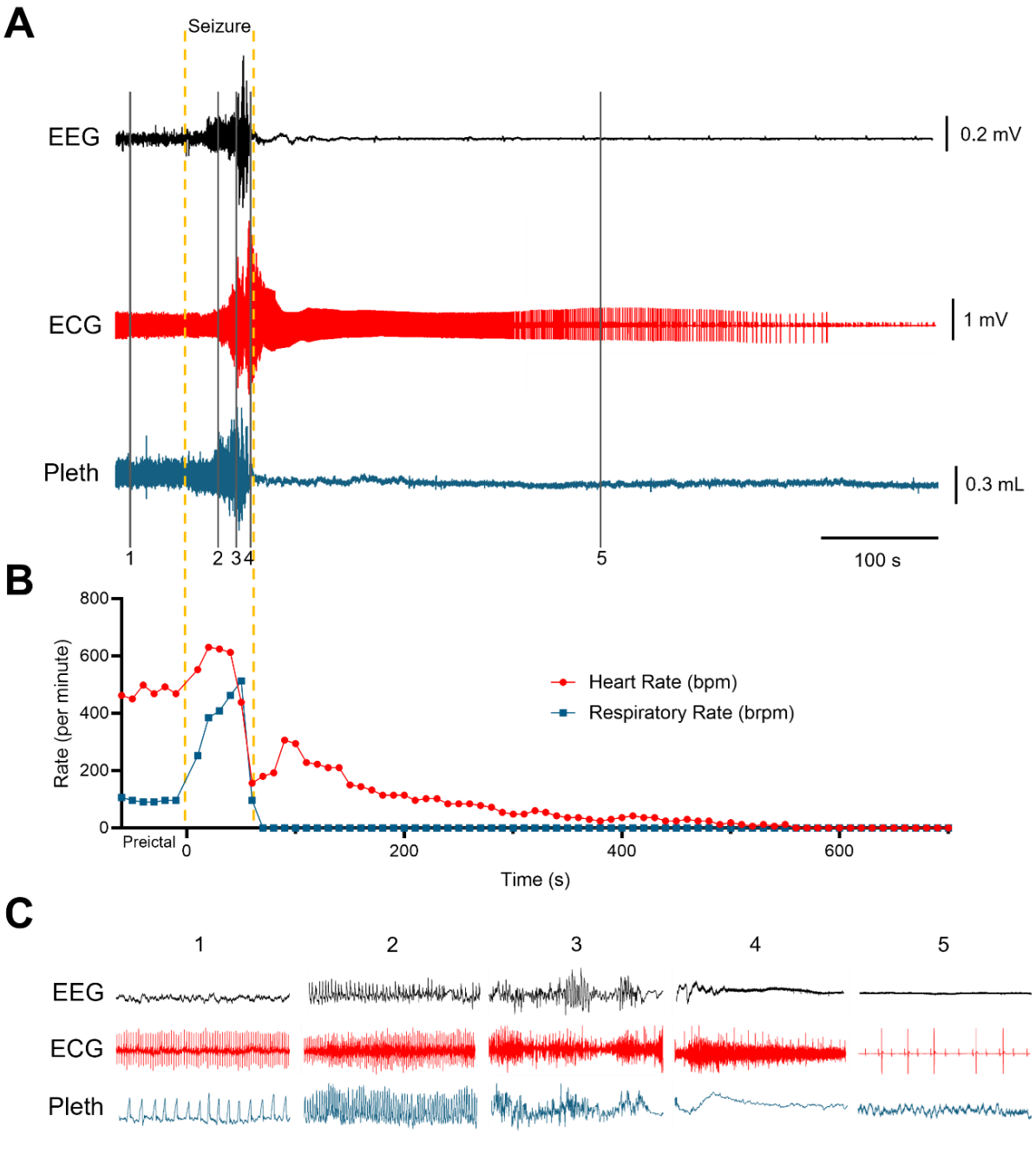
A
Seizure
EEG
0.2 mV
ECG
1 mV
Pleth
0.3 mL
1
2
3
4
5
100 s
B
800
600
400
200
0
Rate (per minute)
Heart Rate (bpm)
Respiratory Rate (brpm)
Preictal
0
200
400
600
Time (s)
C
1
2
3
4
5
EEG
ECG
Pleth

Figure 2.5. A SUDEP event in a corticolimbic-specific *Kcna1* cKO mouse. (A) Recording of simultaneous EEG-ECG-Pleth activity during a spontaneous seizure in a 30-day old female cKO mouse. The top black trace indicates the neural EEG signal, the middle red trace represents the cardiac ECG signal, and the bottom blue trace shows the respiratory Pleth signal. Onset and termination of the seizure are indicated by the dotted orange lines. EEG = electroencephalography; ECG = electrocardiography; Pleth = plethysmography. (B) Respiratory (brpm) and heart rates per minute (bpm) corresponding to the recording in (A). Each dot in the plot represents a 10-s mean value. Time 0 represents seizure onset, and the pre-ictal segment shows the 60-s immediately preceding seizure onset. Some movement artifacts are present in the Pleth and ECG signals; therefore, scoring of breaths and heartbeats was done manually as needed. (C) Expanded 10-s traces of EEG, ECG, and Pleth at the times indicated by the solid grey lines numbered 1-5 in (A). The numbers mark the following events: 1, pre-ictal phase; 2, tachypnea with slightly increased heart rate shortly after seizure onset; 3, ataxic breathing and mild bradycardia shortly before seizure termination; 4, post-ictal generalized EEG suppression with terminal apnea and severe bradycardia; 5, extreme post-ictal bradycardia approximately. The high frequency activity in the ECG during portions of the seizure reflects skeletal muscle activity.

2.4.7 Interictal cardiorespiratory function appears normal in corticolimbic-specific cKO mice

Corticolimbic circuits play important roles in the autonomic regulation of heart and lung function, so we examined ECG and plethysmography recordings for evidence of cardiorespiratory dysfunction during interictal periods that could be indicative of increased SUDEP risk. In ECG recordings, we found no obvious differences in interictal cardiac parameters. Both heart rate and heart rate variability appeared similar between cKO mice and controls (Fig 6A-C). In plethysmography recordings, cKO mice also showed no significant differences in interictal respiration. In cKO mice, breathing rate, respiratory variability, and apnea frequency appeared indistinguishable from control mice (Fig 6D-F). Thus, cardiorespiratory measurements did not reveal any obvious interictal abnormalities that could indicate heightened risk of SUDEP.

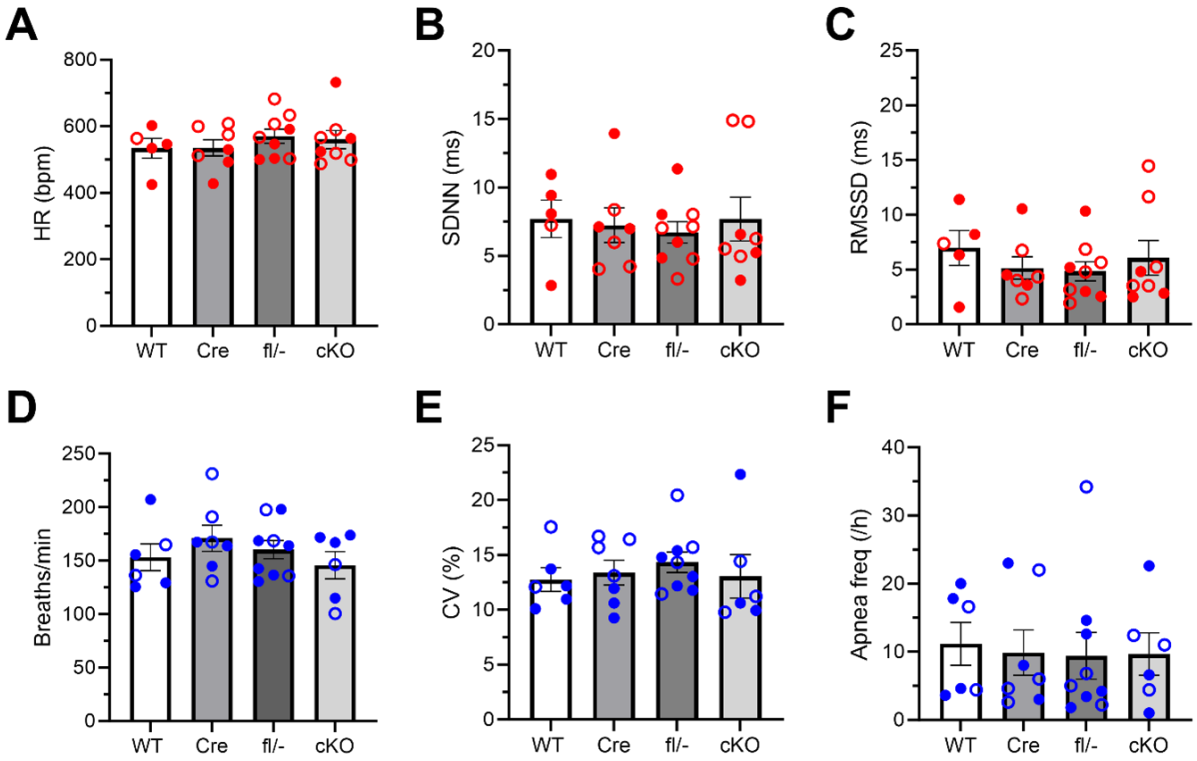

Figure 2.6. Corticolimbic-specific cKO mice do not display obvious interictal cardiorespiratory dysfunction. Quantification of interictal cardiac measures for HR (A), SDNN as an estimate of total autonomic activity (B), and RMSSD as an estimate of parasympathetic activity for WT (n=5), Cre (n=7), fl/- (n=9), and cKO (n=7) mice. HR = heart rate; SDNN = standard deviation of beat-to-beat intervals; RMSSD = root mean square of successive beat-to-beat differences. Quantification of interictal respiratory measures for respiratory rate (D), CV as an estimate of respiratory variability (E), and total apnea frequency (F) for WT (n=6), Cre (n=7), fl/- (n=9), and cKO (n=5) mice. Total apnea frequency included post-sigh and spontaneous apneas. CV = coefficient of variance.

2.5. Conclusions

This study is the first to identify excitatory neurons of the neocortex and limbic system as critical neural substrates driving seizures and SUDEP in the *Kcna1* KO mouse model. In addition, our findings reveal that the absence of Kv1.1 in forebrain corticolimbic circuits alone is sufficient to cause deleterious ictal cardiorespiratory dysfunction. Notably, we recorded a SUDEP event in a corticolimbic-specific cKO mouse, offering valuable insights into the terminal sequence of events leading to death. During the SUDEP episode, the mouse exhibited a pattern of seizure-

induced cardiorespiratory failure resembling clinical cases reported in humans. Our documentation of a SUDEP event, complete with cardiorespiratory data, is significant because such recordings have only been achieved in four other rodent models with spontaneous seizures, and never before in a K^+ channel model of SUDEP. Surprisingly, we did not observe any obvious interictal cardiorespiratory deficits that could signal susceptibility to SUDEP. Thus, this work narrows the brain circuitry underlying SUDEP in the *Kcna1* KO mouse model to excitatory corticolimbic neurons while also providing support for seizure-related respiratory impairment as a key mechanism in the pathophysiology of SUDEP.

Our recorded SUDEP event offers a rare glimpse into the terminal sequence of events in a preclinical model. Additionally, it represents the first report of a SUDEP event in a K^+ channel model with comprehensive cardiorespiratory monitoring. Capturing SUDEP events with corresponding cardiorespiratory data in mouse models with spontaneous seizures is challenging due to the low incidence and unpredictable nature of SUDEP, along with technical challenges in simultaneous biosignal collection (Smith et al., 2024). To our knowledge, recorded SUDEP events with peri-ictal brain, heart, and breathing data have only been reported for four other genetic mouse models of chronic epilepsy: *Depdc5* cKO mice deleting the gene in forebrain regions under the *Rbp4*-Cre driver; *Scn1a*$^{R1407X/+}$ mice; *Scn8a*$^{R1872W/+}$ mice; and *Scn8a*$^{R1872W/+}$ mice with the mutation in *Emx1*-Cre targeted forebrain excitatory neurons (Kao et al., 2023; Y. Kim et al., 2018; Wenker et al., 2021). These models exhibit a common SUDEP pattern of a generalized tonic-clonic seizure followed by tonic hindlimb extension and postictal generalized electroencephalographic suppression (PGES). Furthermore, during fatal seizures each model displays ictal apnea followed by cardiac slowing. Postictally, breathing never resumes and heart rate gradually decreases before terminal cardiac arrest.

The SUDEP event we describe here follows a similar pattern, with a generalized tonic-clonic seizure ending in tonic hindlimb extension and exhibiting ictal cardiorespiratory irregularities, where respiratory dysfunction precedes cardiac dysfunction. However, unlike previous reports in other mouse models, terminal apnea in our model began postictally when EEG seizure activity ceased and PGES was evident. Compared to the *Depdc5* cKO and Na^+ channel models, this pattern aligns more closely with observations from the human MORTEMUS study, where cardiorespiratory collapse consistently occurred postictally, with terminal apnea preceding asystole. *Kcna1* mouse models have seizures typical of temporal lobe epilepsy, while the other four SUDEP mouse models have seizures characteristic of other types of epilepsy (developmental epileptic encephalopathy, familial focal epilepsy, etc.) (Gautier & Glasscock, 2015; Glasscock et al., 2010; Kao et al., 2023; Y. Kim et al., 2018; Wenker et al., 2021). The patients in the MORTEMUS study all had temporal lobe epilepsy like the *Kcna1* mouse models which could help explain why the SUDEP captured in this corticolimbic cKO more closely represents what was captured in clinical cases (Ryvlin et al., 2013). Collectively, mouse models and human cases show a common theme of breathing dysfunction preceding cardiac abnormalities, suggesting respiratory factors may drive fatal cardiorespiratory collapse. However, this remains to be conclusively demonstrated. An alternative explanation could be that seizures independently initiate respiratory and cardiac dysfunction, with differing time courses favoring the appearance of apnea first. Determining the relative importance of respiratory and cardiac mechanisms in mediating death will be imperative for developing proper risk diagnostic and preventative strategies.

The presence of seizure-induced cardiorespiratory dysfunction in corticolimbic-specific cKO mice highlights the importance of forebrain corticolimbic structures in the autonomic regulation of cardiac and respiratory function. Although the brainstem is generally thought of as

the primary locus of autonomic cardiorespiratory control, corticolimbic regions such as the cortex, hippocampus, and amygdala also exert significant influence on heart and lung function through direct communication with brainstem nuclei. In people with epilepsy, the spread of seizures to or direct electrical stimulation of the amygdala and/or hippocampus can induce apnea, often without air hunger perception, potentially increasing susceptibility to SUDEP (Dlouhy et al., 2015; Harmata et al., 2023; Lacuey et al., 2017; Nobis et al., 2019; Rhone et al., 2020). From a cardiac standpoint, epileptic discharges in or electrical stimulation of the amygdala and hippocampus can produce tachy- or bradycardia, indicating forebrain influence over cardiac autonomic control (Healy & Peck, 1997; Inman et al., 2020; Mazzola et al., 2023). Thus, seizures can hijack the normal autonomic regulatory roles of corticolimbic circuits resulting in cardiorespiratory dysfunction and potentially increasing the risk of SUDEP.

Our discovery that the specific absence of Kv1.1 in corticolimbic circuits alone is capable of inducing epilepsy brings together previous findings that hinted at the crucial role of these structures in facilitating seizures resulting from Kv1.1 deficiency. Protein studies have shown that Kv1.1 is abundant throughout corticolimbic brain regions, including the hippocampus (CA3, hilus, and dentate gyrus) (H. Wang et al., 1994; Wenzel et al., 2007), amygdala (including the basolateral amygdala (H. A. Dhaibar et al., 2021), and neocortical pyramidal cells (Guan et al., 2006; Lorincz & Nusser, 2008; H. Wang et al., 1994). In the absence of Kv1.1 in these structures, brain slice recordings have revealed neuronal hyperexcitability and epileptiform-like activity, indicating a low threshold for epileptic activity (Glasscock et al., 2007; Lopantsev et al., 2003; T. A. Simeone et al., 2013; Smart et al., 1998; Thouta et al., 2021). Moreover, spontaneous seizures in *Kcna1* KO mice exhibit behaviors characteristic of limbic seizures induced by kainate or kindling, such as facial twitching, head nodding, rearing and falling, and forelimb and hindlimb clonus (Rho et al.,

1999; Smart et al., 1998; Wenzel et al., 2007). EEG recordings using depth electrodes show that seizures in *Kcna1* KO mice sometimes originate in the hippocampus before spreading to the cortex (Wenzel et al., 2007). Furthermore, spontaneous seizures in *Kcna1* KO mice significantly activate Fos, a protein marker of intense neuronal activity, in the dentate hilus and basolateral amygdala, indicating ictal recruitment of these brain regions (Gautier & Glasscock, 2015). Additionally, the hippocampus and amygdala of *Kcna1* KO mice exhibit extensive gliosis, suggesting potential brain injury due to repeated seizures (H. A. Dhaibar et al., 2021; Wenzel et al., 2007). Magnetic resonance imaging of *Kcna1* KO brains reveals significant enlargement of the hippocampus and ventral cortex, including the amygdala, suggesting brain volume increases associated with seizures (Persson et al., 2007). Thus, our study demonstrates for the first time that selective Kv1.1 deficiency in corticolimbic circuits is sufficient to cause seizures in *Kcna1* KO mice, consolidating multiple lines of evidence from previous studies.

Restricting Kv1.1 deficiency to corticolimbic circuits resulted in premature death, seizures, and cardiorespiratory phenotypes that were generally less severe than those observed in neuron-specific *Kcna1* cKO and global *Kcna1* KO mice. Corticolimbic-specific cKO mice exhibited lower SUDEP rates, with approximately 75% of animals surviving to 100 days old compared to only 45% and 23% of neuron-specific cKO and global KO mice, respectively (H. Dhaibar et al., 2019; Trosclair et al., 2020). The onset of SUDEP in corticolimbic-specific and neuron-specific cKO mice occurred at approximately the same age, around 3-4 weeks old, which was about a week later than SUDEP onset in global KOs. Although average seizure frequencies and durations appeared similar across the different *Kcna1* models, long-duration seizures (>60 s) were rare in corticolimbic-specific cKO mice (about 6% of the time) compared to 17% and 35% in neuron-specific cKO and global KO mice, respectively (H. Dhaibar et al., 2019; Trosclair et al., 2020).

During seizures, all *Kcna1* models exhibited varying degrees of ictal cardiorespiratory abnormalities, with respiratory dysfunction being more prevalent and consistently preceding cardiac dysfunction (H. Dhaibar et al., 2019; Trosclair et al., 2020). While cardiac conduction blocks and bradycardia were relatively rare in neuron-specific cKO mice (occurring in less than 10% of seizures), they were more prevalent in corticolimbic-specific cKO mice, present in about 20-30% of seizures. However, the most significant difference between corticolimbic-specific cKO mice and the other *Kcna1* models was the absence of interictal cardiorespiratory dysfunction. Unlike neuron-specific cKO and global KO mice, which showed increased heart rate variability and a nearly complete lack of apneas between seizures (H. Dhaibar et al., 2019; Trosclair et al., 2020), corticolimbic-specific cKO mice exhibited no obvious cardiorespiratory abnormalities during interictal periods. This suggests that Kv1.1 may not be necessary in corticolimbic circuits for proper baseline cardiorespiratory function. Thus, corticolimbic-specific cKO mice displayed seizure characteristics generally similar to neuron-specific cKO and global KO mice, but with lower mortality rates, and the most marked difference lies in their relative lack of interictal cardiorespiratory dysfunction.

In summary, our findings identify excitatory forebrain neurons as sufficient to drive epilepsy and SUDEP in the *Kcna1* mouse model. The similarity of our recorded SUDEP event to observations in humans underscores the significance of corticolimbic-specific cKO mice as valuable tools for understanding the pathophysiological mechanisms underlying SUDEP. A critical objective of future research will be to capture cardiorespiratory data surrounding additional SUDEP events across various models to ascertain whether the observed terminal pattern of seizure-induced fatal apnea preceding cardiac dysfunction is a consistent feature of SUDEP cases or if multiple mechanisms can lead to the same outcome. Furthermore, it will be essential to investigate

the potential contributions of other neuronal subpopulations, such as those in the brainstem, to seizures, cardiorespiratory dysfunction, and SUDEP in the *Kcna1* model and other preclinical models.

CHAPTER 3

UNDERSTANDING THE UNIQUE CONTRIBUTION OF BRAINSTEM-SPECIFIC *KCNA1* TO CARDIORESPIRATORY FUNCTION AND SEIZURE RELATED MORTALITY AS IT RELATES TO SUDEP MECHANISMS

3.1 Abstract

Sudden unexpected death in epilepsy (SUDEP) stands as a primary cause of death among individuals with epilepsy, yet the critical anatomical substrates and pathological mechanisms remain elusive. While research hints at seizure-related cardiorespiratory collapse as a potential mechanism, definitive proof remains lacking. The preclinical *Kcna1* deficiency mouse model has yielded valuable insights into potential SUDEP mechanisms and risk factors. However, it falls short of addressing inquiries regarding anatomical substrates. As the primary regulator of the heart and lungs is the autonomic nervous system, we limited *Kcna1* deletion to the brainstem to determine the effects on cardiorespiratory function and seizure-related death. Brainstem-specific *Kcna1* deficiency was not sufficient to cause detectable cardiac deficits but was potentially linked to elevated levels of hypoxia at rest. Furthermore, brainstem-specific *Kcna1* deficiency did not significantly alter mortality following induced seizures, although there was a trend in the data towards augmented seizure generalization from the forebrain to brainstem. Thus, in Kv1.1-deficient mice, the brainstem may contribute to SUDEP pathomechanisms by providing an important anatomical substrate for proper chemosensation and seizure spread.

3.2 Introduction

The most common cause of epilepsy-related death is sudden unexpected death in epilepsy (SUDEP), and it occurs when an otherwise healthy person with epilepsy dies suddenly with no cause of death revealed following post-mortem autopsy. SUDEP research has uncovered important risk factors and risk genes, but ultimately the anatomical substrates and mechanisms behind SUDEP remain largely elusive. Cardiorespiratory dysfunction is a widely observed phenomenon in both clinical cases and animal models of SUDEP suggesting neurocircuits which regulate heart and lung function may be important players contributing to these phenotypes. The autonomic nervous system (ANS) is comprised of such neural circuits as it is best known for being the primary regulator of the heart and lungs.

The primary role of the ANS is to regulate involuntary processes such as heart rate and respiratory rate in response to changes in the internal and external environment. The two main branches of the ANS are the sympathetic and parasympathetic arms which work in cooperation with one another to regulate physiological processes in the body. The brainstem is regarded as the classical autonomic brain region and is responsible for multiple cardiorespiratory functions. The retrotrapezoid nucleus (RTN) is the primary pCO_2 sensor, but it also receives input from the carotid bodies regarding blood oxygen levels which can result in respiratory changes to restore blood gas balance (Guyenet et al., 2019). The nucleus of the solitary tract (NTS) is the central brainstem nuclei receiving afferent sensory stimuli and communicates with multiple different brainstem nuclei including the nucleus ambiguus (NA), dorsal motor nucleus of the vagus (DMNX), and the locus coeruleus to elicit the proper efferent signals (Dubreuil et al., 2009; Fu et al., 2019; Menuet et al., 2020; Stornetta et al., 2006) . Specifically, cardiopulmonary sensors communicate with the NA which then signals the NTS to control heart rate. While the classic autonomic circuitry resides

in the brainstem, forebrain circuits including corticolimbic regions such as the hippocampus and amygdala also make direct connections with the brainstem helping to fine tune the efferent response to afferent sensory stimuli.

The brainstem has known regulatory influences over the heart and lungs and has previously been suggested as an important driver of SUDEP mechanisms. The 2016 MORTEMUS study showed that clinical cases of SUDEP involve cardiorespiratory collapse which has been recapitulated in animal models of SUDEP. Imaging studies of temporal lobe epilepsy patients show specific loss of brainstem volume in those with SUDEP (Mueller et al., 2014). Importantly, another imaging study of those who died from SUDEP showed that the degree of brainstem volume loss and damage correlates with closeness to SUDEP (Mueller et al., 2018). These brainstem volume alterations correlate with functional consequences in epilepsy patients since brainstem volume reductions were linked to reduced HRV, a proposed SUDEP risk factor (Mueller et al., 2018). Ultimately, this combined evidence suggests the brainstem may be an important region which could drive cardiorespiratory aspects of SUDEP pathology.

The preclinical *Kcna1* deficiency model is useful for studying SUDEP mechanisms as it displays measurable cardiorespiratory dysfunction that resembles the observations in the MORTEMUS study. Global *Kcna1* KO mice display both ictal and interictal cardiorespiratory dysfunction. Interictally, KO mice display elevated HRV (RMSSD: root mean square of successive beat to beat differences), cardiac conduction blocks, respiratory rate, and respiratory variability while also showing a significant decrease in all types of apneas (H. Dhaibar et al., 2019; Glasscock et al., 2010; Mishra et al., 2017). During spontaneous seizures, the global KO mice display a greater overall abundance of respiratory abnormalities (hyperventilation, tachypnea, ataxic breathing, etc.) compared to cardiac dysfunction (tachycardia, bradycardia, conduction

blocks, etc.), which occurs less often (H. Dhaibar et al., 2019). Significantly, restricting *Kcna1* deletion to only the neurons of the brain (i.e., neuron-specific cKO mice) recapitulated many of these cardiorespiratory deficits. Interictal heart rate variability was still significantly elevated in these mice, most apparently in the daytime suggesting diurnal dysregulation of HRV (Trosclair et al., 2020). Furthermore, the near absence of apneas was still apparent in neuron-specific cKO mice which suggests the brain as the primary cause (Trosclair et al., 2020). During spontaneous seizures in the cKO mice, cardiac and respiratory dysfunctions were still present with respiratory abnormalities appearing the most prominent (Trosclair et al., 2020). Unfortunately, the specific anatomical regions contributing to these phenotypes are not yet known.

The objective of this study was to test how the brainstem uniquely contributes to SUDEP-related phenotypes. To answer this question, we generated a novel brainstem-specific *Kcna1* cKO which we monitored using our epilepsy monitoring unit (EMU) to simultaneously record brain (electroencephalogram; EEG), heart (electrocardiogram; ECG), and lung (plethysmography; pleth) activity. We also utilized non-invasive ECG (ECGenie) and pulse oximetry (MouseOx) to look at ECG waveform characteristics and blood gas stability, respectively. Lastly, we induced seizures using the chemical convulsant flurothyl to understand how brainstem-specific Kv1.1 deficiency may contribute to seizure susceptibility and generalization and seizure-related survival. We found that brainstem-specific cKO mice did not display any obvious cardiac dysfunction but showed potential, but not yet significant, increases in hypoxia when at rest. The inducible seizure challenge revealed a trend for augmented seizure generalization, but this was not significant, nor was there significantly altered mortality. Ultimately, this work suggests the brainstem alone may be an important anatomical substrate for maintaining proper blood oxygen levels and dampening seizure generalization which, when disrupted, could lead to an increased risk of SUDEP.

3.3 Materials and Methods

3.3.1 Animals

Brainstem-specific conditional knockout (cKO) mice (i.e., *Phox2b*-Cre$^{+/-}$; *Kcna1*$^{flox/-}$) were generated by crossing heterozygous *Kcna1* floxed (fl) mice (*Kcna1*$^{fl/+}$) with heterozygous ^{Kcna1} global knockout mice (*Kcna1*$^{+/-}$) carrying one copy of the *Phox2b* transgene (i.e., *Phox2b*-Cre$^{+/-}$; *Kcna1*$^{+/-}$). *Phox2b*$^{+/-}$; *Kcna1*$^{+/-}$ mice were generated by crossing hemizygous transgenic *Phox2b*-Cre$^{+/-}$ mice with heterozygous *Kcna1*$^{+/-}$ mice. Control mice include *Kcna1*$^{+/+}$; *Phox2b*-Cre$^{-/-}$ (WT), *Kcna1*$^{+/+}$; *Phox2b*-Cre $^{+/-}$ (Cre), and *Kcna1*$^{fl/-}$; *Phox2b*$^{+/+}$ (fl/-). *Phox2b*-Cre mice were purchased from Jackson Labs (Bangor, MN) under the catalog name B6(Cg)-Tg(Phox2b-cre)3Jke/J (JAX 016223). *Kcna1*$^{+/-}$ mice which are maintained on a Tac:N:NIHS-BC genetic background, carry a KO allele of the *Kcna1* gene due to targeted deletion of the entire open reading frame (Smart et al 1998). *Kcna1*$^{fl/+}$ mice, which are maintained on a C57BL/6J background, were generated and described previously (Trosclair et al., 2020). Mice were housed at 22°C, fed *ad libitum*, and subjected to a 12-h day/night cycle. Throughout the study, both experimental and control mice were monitored until they reached their natural mortality or until 100 days elapsed, whichever occurred first. This monitoring was conducted for the purpose of lifespan curve analysis. All experiments were performed in accordance with National Institutes of Health (NIH) guidelines with approval from the Institutional Animal Care and Use Committee of Southern Methodist University.

3.3.2 Genotyping

To identify experimental and control mice, genomic DNA was isolated by enzymatic digestion of tail clips using Direct-PCR Lysis Reagent (Viagen Biotech, Los Angeles, CA, USA). Genotypes were determined by performing PCR amplification of genomic DNA using allele-specific primers. For detection of the *Kcna1* global KO allele, the following primer sequences were used to yield amplicons of 337 bp for the wild-type (WT) allele and 475 bp for the KO allele: a WT specific primer (5'-GCCTCTGACAGTGACCTCAGC-3'); a KO-specific primer (5'-CCTTCTATCGCCTTCTTGACG-3'); and a common primer (5'-GCTTCAGGTTCGCCACTCCCC-3'). For detection of the $Kcna1^{fl}$ allele, the following primer sequences were used to yield amplicons of 197 bp for the WT allele and 260 bp for the floxed allele: a WT-specific primer (5'-GCTCCTCTACTATCAGCAAGTCTGAGTACATGG-3'); a floxed-specific primer (5'-ATCAAGTTGGACATCACCTCCCACAAC-3'); and a common primer (5'-AAGGGGTTTGTTTGGGGCTTTTGTT-3'). For detection of the *Phox2b*-Cre transgene, the following primer sequences were used to yield a product of 300 bp for the WT allele, and 700 bp for the Cre allele: a WT specific primer (5'-GTACGGACTGCTCTGGTGGT-3'); a *Phox2b*-Cre specific primer (5'-ATTCTCCCACCGTCAGTACG-3'), and a common primer (5'-CCGTCTCCACATCCATCTTT-3'). For detection of the deleted *Kcna1* floxed allele (i.e., $Kcna1^{del}$) resulting from Cre-mediated recombination, the following primers were used to yield an amplicon of 679 bp for the deleted allele: the common primer in the *Kcna1* floxed reaction above and 5'-CTCCAGTTTTACGAAGTTGTAAACAGATCGG-3'.

3.3.3 Video-electroencephalography-electrocardiography-plethysmography (EEG-ECG-pleth) recordings

To measure *in vivo* brain and heart activity, mice (4-6 weeks old) of both sexes were anesthetized using an anesthetic cocktail and surgically implanted with bilateral silver wire EEG and ECG electrodes (0.005-inch diameter) attached to a microminiature connector (Omnetics Connector Corporation, Minneapolis, MN) for tethered configuration recording. The anesthetic cocktail contained ketamine (100 mg/kg), xylazine (10 mg/kg), and acepromazine (2 mg/kg) and was administered by intraperitoneal (i.p.) injection. Following completion of the surgery, the reversal agent Antisedan (1 mg/kg) was administered by subcutaneous (s.c.) injection. Carprofen (5 mg/kg, s.c.) was given the day of surgery and 24 hours post-surgery for pain management. EEG wires were inserted into the subdural space through cranial burr holes overlying the parietotemporal cortex for the recording electrodes and above the frontal cortex for the ground and reference electrodes, as described previously (Mishra et al., 2018). Two ECG wires were tunneled subcutaneously on both sides of the thorax and sutured in place to record cardiac activity, as described previously (Mishra et al., 2018). Mice were allowed to recover for 48 hours before recording simultaneous EEG-ECG for ≥ 24h continuously while the animals were housed in a plexiglass tank (40-cm length x 20-cm width x 23-cm height). Biosignals were band-pass filtered by applying 0.3 Hz high-pass and 75-Hz low pass filters for EEG and a 3.0-Hz high-pass filter for ECG. Sampling rates were set to 500 Hz for EEG and 2kHz for ECG.

For recording respiratory waveforms in tandem with EEG-ECG, mice that completed the 24 hour EEG-ECG recording were placed in an unrestrained whole-body plethysmography (pleth) chamber (Data Sciences International, St. Paul, MN, USA) with a lid that was modified to

accommodate wires for recording EEG-ECG in a tethered configuration, as done previously (H. Dhaibar et al., 2019). Mice were provided a 45-min acclimatization period in the chamber before video and EEG-ECG-pleth were simultaneously recorded in 5-6 hour sessions during the day (i.e. between 6:00 am and 6:00 pm) using Ponemah data acquisition and analysis software (Data Sciences International, St. Paul, MN, USA). Respiratory signals were acquired at a 500-Hz sampling rate.

3.3.4 Analysis of video-EEG, ECG, and pleth recordings

Visual inspection of the EEG was used to look for the presence of seizures which were defined as high-amplitude, rhythmic electrographic discharges lasting ≥ 5 s. Collected EEG data was also converted from the time domain to the frequency domain to analyze 24-hr power spectrum for five different frequencies: alpha (8-13 Hz), beta (13-30 Hz), delta (1-4 Hz), gamma (30-80 Hz), and theta (4-8 Hz). The frequency range for each band was derived from the 2017 International League Against Epilepsy (ILAE) Guidelines (Kadam et al., 2017). Individual EEG recordings were analyzed with NeuroScore™ software (Data Sciences International, New Brighton, MN), and an initial 0.3-55 Hz band pass filter was applied to the data. For both the T3 and T4 EEG signals, periodogram power bands were calculated with an epoch duration of 10 s and a Fast Fourier transformation order 10 for each of the power bands (alpha, beta, delta, gamma, and theta) defined as the frequency ranges described above. The data was then exported to Excel (Microsoft Corporation, Redmond, WA) and manually trimmed to include exactly 24 hours. The 10-s epochs for each frequency band were averaged between T3 and T4 and then averaged overall to yield a single average value for each of the five frequency bands. For consistency, the "COUNT" function

on Excel was used to determine the number of data points for each 24-h recording to ensure they were the same. Values are expressed as relative power compared to the other bands.

The RR intervals of the ECG waveforms were used to estimate heart rate (HR) and heart rate variability (HRV) for the first 24-h recording period overall as a whole, and for the 24-h day- (6:00 AM to 6:00 PM) and 12-h night phase (6:00 PM to 6:00 AM) portions. For each ECG recording, six separate RR interval series were derived by sampling 2-min ECG segments every four hours to provide three-day (6:00 AM to 6:00 PM) and three night (6:00 PM to 6:00 AM) measurements. RR interval series for each segment were automatically generated and manually confirmed using Ponemah software (Data Sciences International, St. Paul, MN). RR intervals were only sampled during times when the mouse was stationary and no physiological artifacts such as skipped or ectopic beats occurred. HRV was measured in the time domain using the standard deviation of the RR intervals (SDNN); the coefficient of variance (CV; defined as $SDNN/RR_{mean}$ x100); the root mean square of successive differences between the RR intervals (RMSSD); and the percentage of consecutive RR intervals differing my >6 ms (pNN6). The HR and HRV values for each animal represent an average of the six total segments or an average of the three daytime or three nighttime segments, as indicated in the text.

Respiratory rate (breaths per min; BPM) was measured using Ponemah analysis software (Data Sciences International, ST. Paul, MN). Average respiratory characteristics for each mouse were calculated by sampling 50 consecutive breaths every hour for 5 h for a total of 250 breaths, as done previously (H. Dhaibar et al., 2019). Measurements were only collected during periods when

animals were stationary, as verified by video monitoring. Respiratory variability was calculated as the coefficient of variance (CV) using the formula: $CV = \sigma / \mu$, where σ is the standard deviation of breath intervals and μ is mean of breath intervals. Sighs and apneas were also manually quantified and were identified as deep augmented breaths with ≥25% higher amplitude and ≥125% higher tidal volume compared to the preceding 10 s (sighs), and cessations of plethysmographic signals for ≥ 2 respiratory cycles, or 0.8-s (apneas), as done previously (H. Dhaibar et al., 2019).

3.3.5 Non-invasive electrocardiography

To non-invasively assess ECG waveform characteristics, age- and sex-matched mice (4-6 weeks old) were placed inside an ECGenie recording tower (Mouse Specifics Inc., Framingham, MA, USA) for at least ten minutes to acclimate to the new environment. Subsequently, ECG waveforms were recorded to obtain segments of at least 25 consecutive noise-free cardiac waveforms. This process was repeated until at least 10 clean segments per mouse were collected. EzCG analysis software (Mouse Specifics Inc., Framingham, MA, USA) trimmed down each of the 10 recordings such that there were 21 valid beats for a total of 210 beats. The software then calculated the values for each phase of the cardiac waveform which was averaged across all beats.

3.3.6 Pulse oximetry

Blood gas stability was assessed using noninvasive MouseOx Plus infrared pulse oximetry (Starr Life Sciences Corp, Oakmont, PA, USA) in age and sex matched mice (4-6 weeks). Dark fur on mice disrupts the oximetry sensor, so mice were gently shaved using an animal-safe electric razor at the two points on the neck where the sensor makes contact. Subsequently, the CollarClip Sensor (Starr Life Sciences Corp) was placed on the neck of the mouse, and the mouse was placed in a

plastic recording chamber to acclimate for at least 10 minutes. After acclimation, mice were recorded for ≥ 60 minutes to capture pulse distension, arterial oxygen saturation, pulse rate, respiratory rate, and activity level, which were acquired at 5 Hz. Only measurements which were error free for all parameters were included in the analysis, and only recordings which contained more than 5000 usable points and an average heart rate above 499 bpm were used. The percentage of hypoxic events was calculated as the percentage of total error free data points in a recording where the arterial oxygen saturation was < 90%.

3.3.7 Statistical Analysis

Data are presented as mean ± SEM. Prism 10 for Windows (GraphPad Software Inc, La Jolla, CA, USA) was used for statistical analysis. Survival curves were evaluated using the Kaplan-Meier log rank (Mantel-Cox) test. For comparisons involving two or more groups, one-way analysis of variance (ANOVA) was used followed by Tukey post-hoc tests. Outliers were identified using the ROUT method with Q = 1% and excluded from analyses. Results were significant if $P < 0.05$. Sex for each data point is indicated as open circles for females and closed circles for males.

3.4 Results

3.4.1 Confirmed cre-mediated deletion of Kcna1 in the brainstem

We generated brainstem-specific *Kcna1* cKO mice (i.e., *Phox2b*-Cre$^{+/-}$;*Kcna1*$^{del/-}$) using the breeding scheme outlined in the Materials and Methods. The Phox2b-Cre driver is a commonly used transgene that primarily targets hindbrain regions containing autonomic regulatory neurons including the RTN, LC, DMNV, NA, and NTS, but also expresses in the olfactory bulb (Dubreuil

et al., 2008, 2009; Fu et al., 2019; M. M. Scott et al., 2011; Stornetta et al., 2006). To confirm tissue-specific deletion of *Kcna1*, we performed PCR of brains from cKO mice. PCR amplification of regionally-dissected brain tissue revealed the presence of the *Kcna1*^{del} allele in the brainstem (medulla, pons, midbrain), and olfactory bulb, but not in the neocortex, or hippocampus (Fig. 1A).

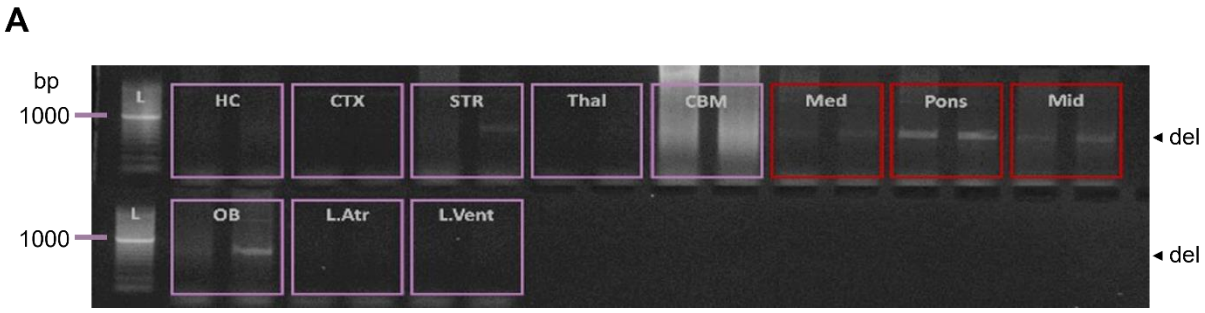

Figure 3.1. Molecular characterization of brainstem-specific *Kcna1* cKO mice. **A**, PCR detection of the *Kcna1* deletion (del; 679 bp) allele from the genomic DNA isolated from hippocampus (HC), cortex (CTX), striatum (STR), thalamus (Thal), cerebellum (CBM), medulla (Med), pons, midbrain (Mid), olfactory bulb (OB), left atria (L.Atr), and left ventricle (L.Vent) for the cKO mice.

3.4.2 Brainstem-cKO mice do not display spontaneous seizures or premature mortality, but do have altered brain dynamics

We monitored mice with *in vivo* video-EEG to determine how brainstem-specific deletion of *Kcna1* contributes to spontaneous seizures. Neither brainstem-specific cKO mice nor control mice exhibited any obvious seizure activity (Fig. 2 A,C). This result was not surprising, as other research has suggested the epileptogenic zone for *Kcna1* deficiency mouse models resides in the forebrain regions (H. Dhaibar et al., 2019; Gautier & Glasscock, 2015; Trosclair et al., 2020). The absence of seizures coincided with a lack of premature mortality in the mice (Fig. 2B). To assess whether brainstem-specific *Kcna1* deletion impacted overall brain dynamics, we performed power spectrum analysis to determine the relative power of delta, theta, alpha, beta, and gamma waves

during the 24-h recordings. Brain-stem-specific cKO mice exhibited significantly elevated theta power compared to the WT group (Fig. 2D), indicating they have abnormal EEG rhythms despite their lack of seizures.

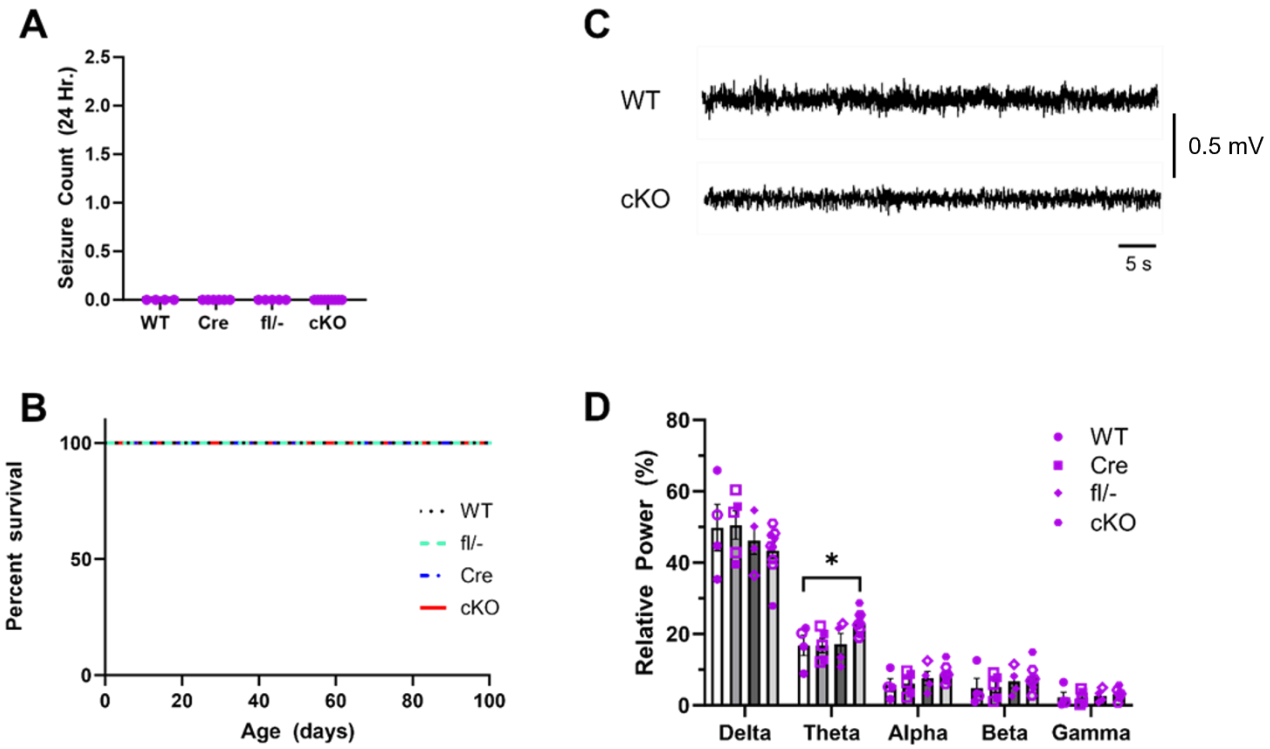

Figure 3.2. A, Quantification of seizures over 24 hours for WT (n=4), cre (n=6), fl/- (n=5), and cKO (n=9) mice. No electrographic seizures were captured for any of the groups. **B**, Kaplan-Meier survival curves for WT (n=17), Cre (n=22), fl/- (n=51), and cKO (n=39) mice. No premature mortality was observed for any of the groups. **C**, Representative EEG traces from a WT (top) and cKO (bottom) mouse. **D**, Quantification of relative EEG power for WT (n=4), Cre (n=5), fl/- (n=4), and cKO (n=9) mice. The designated wavelengths for each frequency band are as follows: delta (1-4 Hz), theta (4-8 Hz), alpha (8-13 Hz), beta (13-30 Hz), gamma (30-80 Hz). One-way ANOVA reveals significantly elevated theta power in brainstem cKO mice compared to WT ($P < 0.05$).

3.4.3 Inducing seizures in brainstem-cKO mice does not significantly increase mortality

Because brainstem-specific cKO mice did not show evidence of spontaneous seizures, we next assessed their susceptibility to seizures and seizure-induced mortality when exposed to the volatile chemical convulsant flurothyl, as previously described (Vanhoof-Villalba et al., 2018).

Upon inhalation of flurothyl, mice routinely develop a stereotypical seizure pattern characterized by: 1) an initial brief myoclonic jerk (event 1) followed by a 2) post-ictal return to normal behavior and then a 3) secondary generalized tonic-clonic seizure (event 2), which leads to a 4) post-ictal phase that often involves tonic hindlimb extension leading to death (Ferland, 2017). The myoclonic event one is associated with forebrain activation, and the generalized tonic-clonic event two occurs after neural activation spreads to the brainstem (Ferland, 2017; Kadiyala & Ferland, 2017). Immediately before testing, we verified that there were no significant differences in the average body weights between the groups of mice which could impact the effects of flurothyl (Fig. 3A). In response to flurothyl administration, brainstem-specific cKO mice showed a time latency to the first seizure event that was similar to controls (Fig. 3B); however, they exhibited a tendency towards a faster latency for manifestation of the second seizure event (Fig. 3C). This trend is more easily identifiable when looking at the generalization time (calculated as: time to event 2 minus time to event 1), which shows a nonsignificant but apparent decrease between brainstem-specific cKO mice and controls (Fig. 3D). Mortality was not significantly impacted though, as the cKO and fl/- mice had identical mortality percentages, suggesting the risk of seizure related mortality is the same in heterozygous *Kcna1* KO mice and brainstem-specific *Kcna1* cKO mice (Fig. 3E).

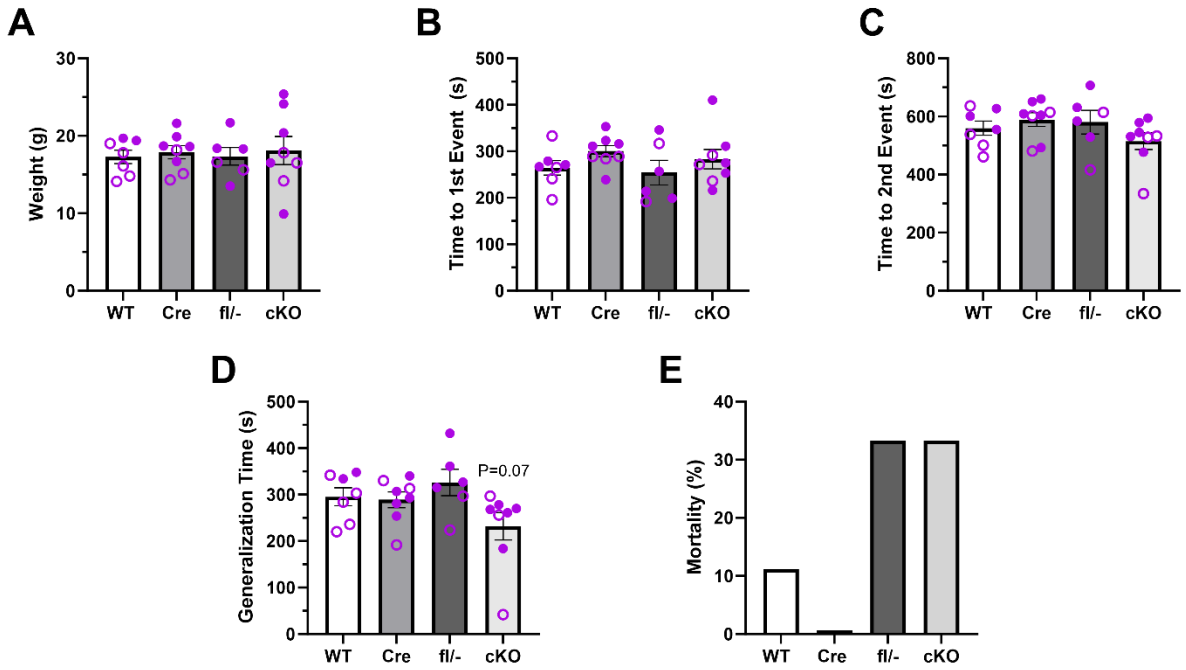

Figure 3.3. Quantification of the (**A**) animal weights at the time of convulsant exposure, (**B**) time latency to the first clonic event, (**C**) second generalized tonic-clonic event, (**D**) generalization time between event 1 and 2, (**E**) and mortality in WT (n=9), Cre (n=9), fl/- (n=6), and cKO (n=9) mice. The brainstem-specific cKO mice showed a trend towards faster seizure generalization and higher mortality, but one-way ANOVA revealed no significant differences between any of the groups. Open circles represent female data points, and male data points are indicated by closed circles.

3.4.4 Brainstem-cKO mice do not display overt cardiac dysfunction

The brainstem acts as one of the primary regulators of cardiac activity, so we monitored mice using *in vivo* ECG in order to determine how *Kcna1* deletion in this region impacts overall heart function. A short WT ECG trace in Fig. 4A shows the different components of the heartbeat used to calculate cardiac function. Brainstem-specific cKO mice exhibited heart rates that were similar to control mice (Fig. 4B). They also displayed no significant differences in autonomic cardiac measures (Fig.4C-4F). The root mean square of successive beat to beat differences (RMSSD), a metric of parasympathetic tone, showed no differences in overall, daytime, or

nighttime measurements (Fig. 4C). The standard deviation of beat to beat differences (SDNN), a measure of overall autonomic tone, also showed similar values between cKO and control mice, as did the coefficient of variance ($SDNN/RR_{mean}$) which normalizes SDNN to heart rate (Fig. 4D-E). Lastly, we measured the percentage of beat-to-beat intervals which differed by more than 6 ms (pNN6), another indicator of parasympathetic tone. This measurement showed the most inter-animal variability of all the cardiac metrics, but we still found no significant differences (Fig. 4F). We next quantified the frequency of cardiac conduction blocks (i.e., skipped heart beats). The fl/- control mice exhibited more variability in the frequency of conduction blocks compared to the other genotypes, but none of the groups showed a significant difference (Fig. 4G). Because we identified no major changes that could indicate cardiac autonomic dysregulation, we next used non-invasive ECG to examine the ECG waveform properties in more detail. The PQ interval, which represents the time it takes for cardiac conduction to travel from the sinoatrial node (SA node) and through the atrioventricular node (AV node) to the ventricles, was the first parameter examined. This value was not significantly different between groups (Fig. 4H). Another similar way to look at this measure is through the PR interval, which represents the time between atrial depolarization and ventricular depolarization, an indicator of electrical conduction through the AV node. This measure was also not significantly different between groups (Fig. 4I). The duration of the QRS complex, a measure of ventricular depolarization, also exhibited no significant differences (Fig. 4J). The QT interval, an indicator of the time it takes for the heart to contract and refill with blood before the next cardiac cycle begins (i.e., repolarization), also appeared normal in cKO mice (Fig. 4K). The ST segment, which measures the time between ventricular depolarization and repolarization (i.e., the time needed to reset for the next beat), showed no

differences between groups (Fig. 4L). Collectively, this data shows that overall cardiac function is apparently not significantly impacted by brainstem-specific *Kcna1* deletion.

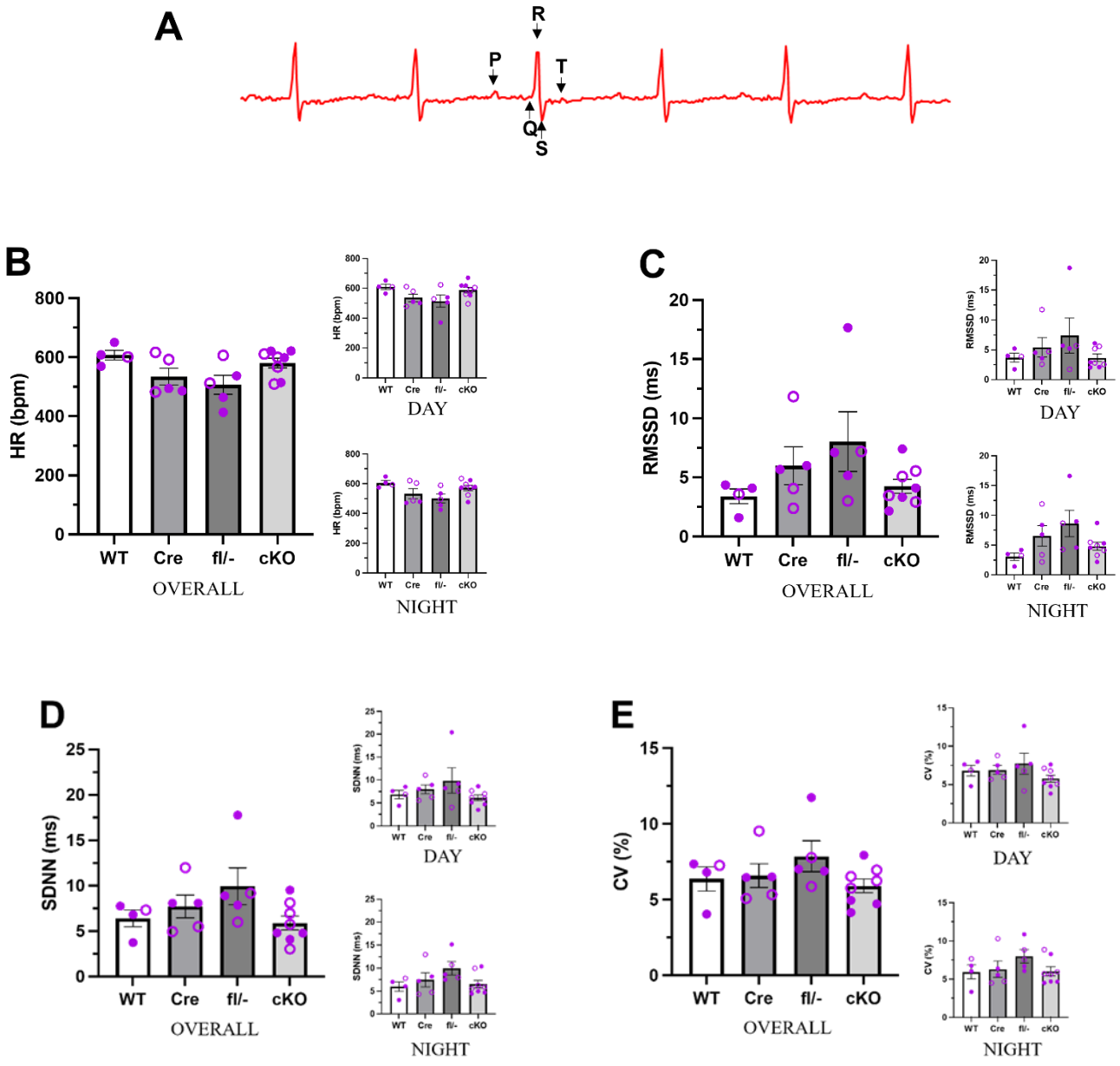

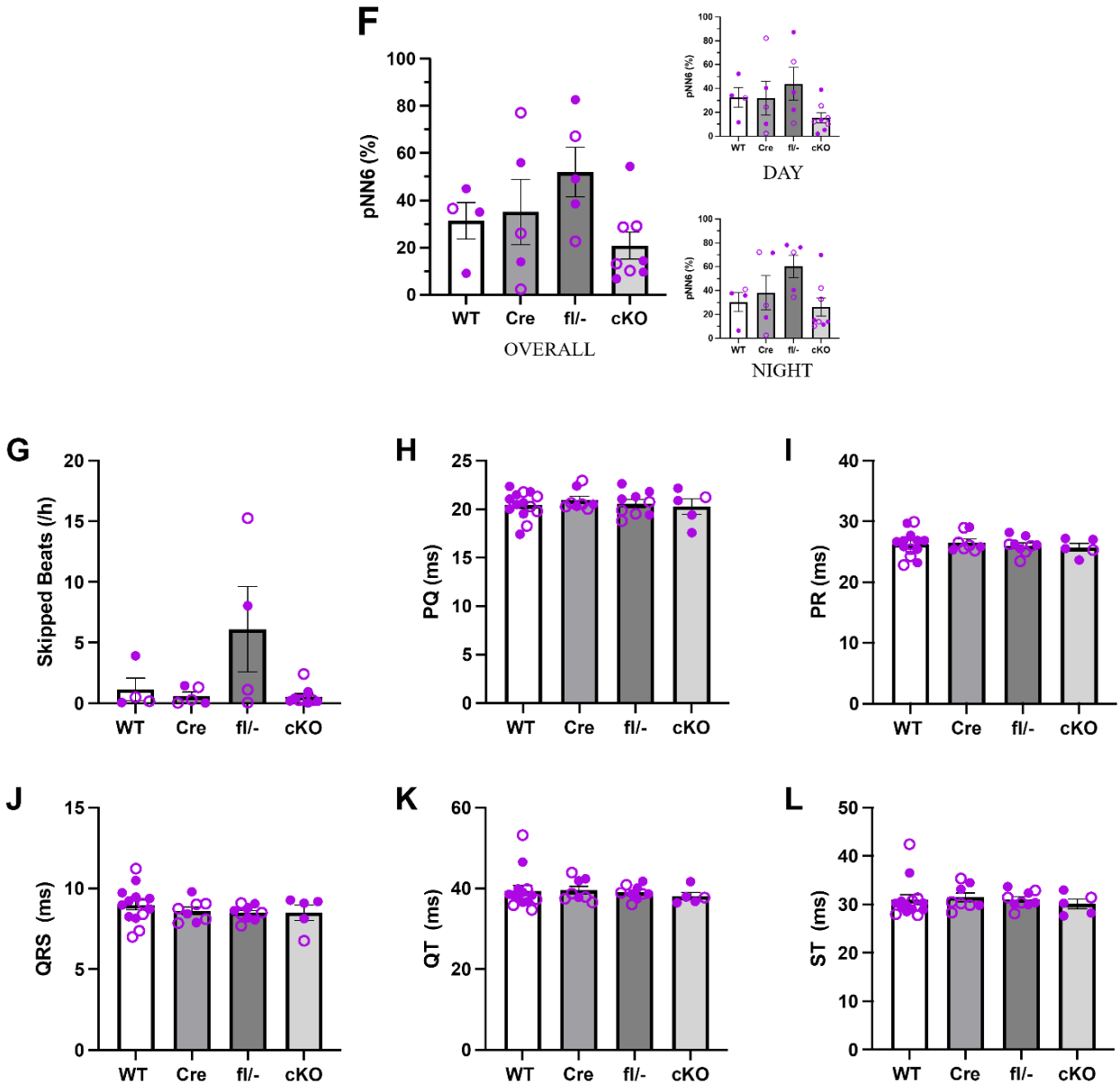

Figure 3.4. A, Sample ECG trace from a WT animal showing the location of P, Q, R, S, and T elements in a heartbeat. Quantification of (**B**) heart rate, (**C**) RMSSD, (**D**) SDNN, (**E**) CV, (**F**) pNN6, and (**G**) cardiac conduction blocks (skipped beats) from 24-h *in vivo* ECG recordings in WT (n=4), Cre (n=5), fl/- (n=5), and cKO (n=8) mice. Each box for panels B-F contain the overall, day, and night quantifications for each respective measure. RMSSD, root mean square of successive beat to beat differences; SDNN, standard deviation of beat to beat intervals; CV, coefficient of variance; skipped beats, cardiac conduction blocks. Quantification of (**H**) PQ interval, (**I**) PR interval, (**J**) QRS interval, (**K**) QT interval, and (**L**) ST interval from ECGenie cardiac waveform analysis in WT (n=14), Cre (n=8), fl/- (n=9), and cKO (n=5) mice. One-way ANOVA revealed no statistically significant differences across all parameters. Open circles represent female data points, and closed circles indicate male data points.

3.4.5 Basal respiratory parameters are not altered in brainstem-cKO mice

The brainstem is known for its regulatory role in respiration, so we used *in vivo* plethysmography to assess basal respiratory characteristics in the brainstem-specific cKO mice. Brainstem-specific cKO mice did not exhibit significantly different rates of respiration (Fig. 5A) or respiratory variability (Fig. 5B) compared to control mice. The brainstem is important for regulating chemosensory behaviors as well, so plethysmography waveforms were analyzed to determine if there were any differences in the presence of different types of apneas. Previous studies have shown that global and neuron-specific *Kcna1* knockout mice have significant reductions in all types of apneas signifying potential chemosensation deficits. Neither post-sigh, spontaneous, nor overall total (combined post-sigh and spontaneous) apneas were significantly different between groups (Fig. 5C). Compared to WT mice, brainstem-specific cKO mice exhibited a slight trend towards decreased apnea frequency, but the differences were not statistically significant (Fig. 5C). We also found no significant differences in the duration of apneas (Fig. 5D), or the frequency of sighs (which evoke post-sigh apneas) (Fig 5E). Lastly, when post-sigh apnea frequency was normalized to the frequency of sighs, there remained no significant differences between any of the groups (Fig. 5F). Thus, brainstem-specific *Kcna1* deficiency alone is not sufficient to cause basal respiratory dysfunction.

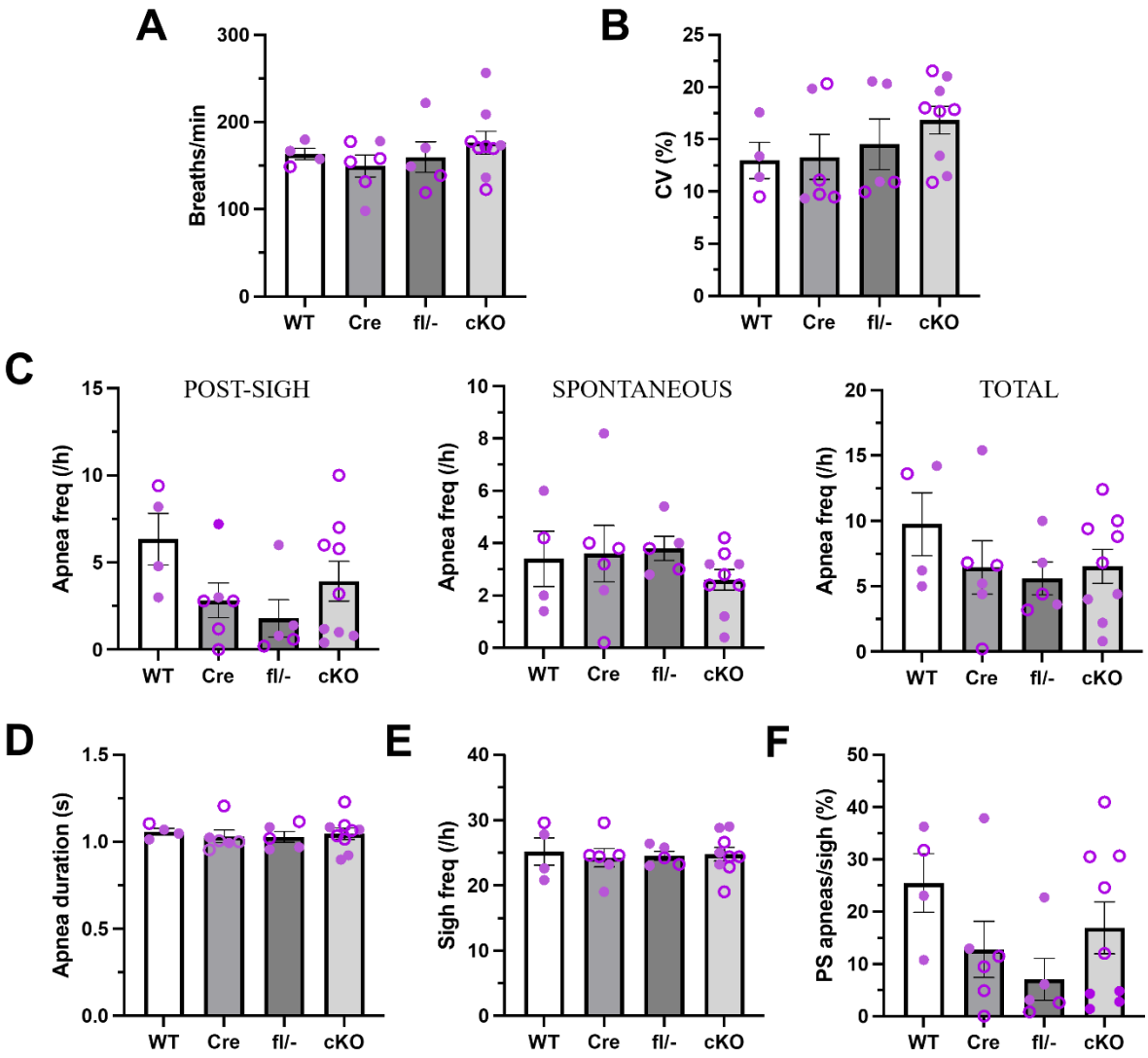

Figure 3.5. Quantification of (**A**) respiratory rate, (**B**) respiratory variability, (**C**) apnea frequency, (**D**) apnea duration, (**E**) sigh frequency, and (**F**) post-sigh apneas per sigh from 5-hour plethysmography in WT (n=4), cre (n=6), fl/- (n=5), and cKO (n=9) mice. The boxed panel **C** displays post-sigh, spontaneous, and total apnea frequency from left to right, respectively. One-way ANOVA revealed no statistically significant differences among any of the measured parameters. The open circles indicate female data points, and the closed circles represent male data points.

3.4.6 Brainstem cKO mice display a trend towards increased basal hypoxia levels

The brainstem houses the central chemosensory nuclei, so we used mouse pulse oximetry to assess how lacking Kv1.1 may impact blood oxygen levels. The pulse oximetry readings yielded respiratory rates (Fig. 6A) similar to those measured via plethysmography (Fig. 5A), but no significant differences were observed between the groups. Furthermore, average basal arterial oxygen saturation values also appeared comparable between the groups (Fig. 6B). Interestingly, we found that the percentage of hypoxic events appears to be potentially increased in the brainstem-specific cKO mice compared to controls (Fig. 6C). Unfortunately, at this early stage in the data collection, inter-animal variability hinders drawing final conclusions so additional work is ongoing to expand the sample sizes to determine if a significant difference exists.

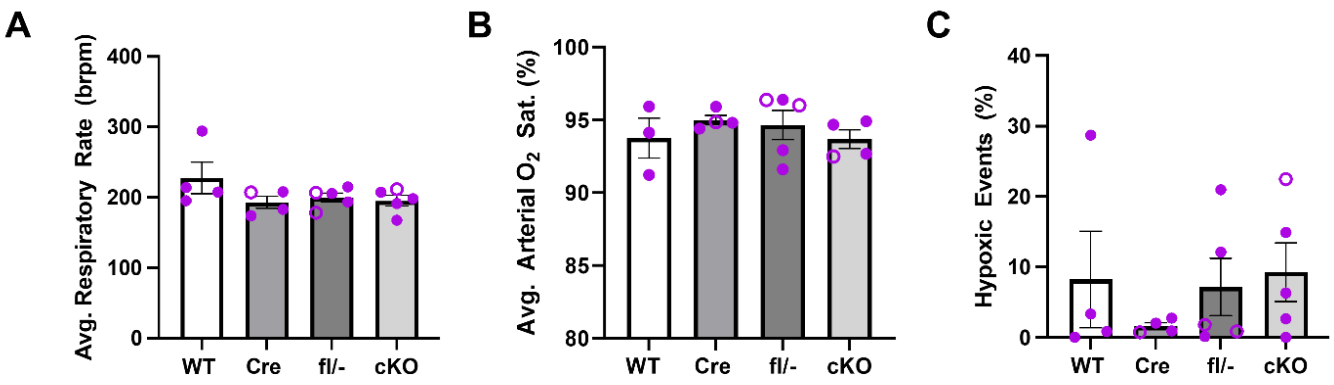

Figure 3.6. Quantification of (**A**) average respiratory rate, (**B**) average arterial oxygen saturation, and (**C**) hypoxic events from mouse pulse oximetry in WT (n=4), cre (n=4), fl/- (n=5), and cKO (n=5) mice. Hypoxic events are defined as the percentage of total data points where blood oxygen levels drop below 90%. One-way ANOVA reveals no statistically significant differences in any parameters, but there is a trend towards greater hypoxic event percentage in cKO mice compared to controls. The open circles indicate female data points, and the closed circles represent male data points.

3.5 Conclusions

This study is the first to characterize the neuro-cardiorespiratory consequences of *Kcna1* deletion specifically in the brainstem. Prior studies using pre-clinical *Kcna1* deficiency mouse models have outlined the phenotypes associated with global and neuron-specific deletion of *Kcna1*. However, this study, along with our work on forebrain-specific *Kcna1* deletion presented in Chapter 2, represent the first investigations into how specific neurocircuits contribute to potential SUDEP pathomechanisms and risk in the widely used *Kcna1* deficiency mouse model. SUDEP research often emphasizes cardiorespiratory collapse as a critical event in the terminal cascade, implicating the autonomic nervous system, which regulates heart and lung function. The brainstem houses traditional autonomic circuitry, and for this reason it was explored as a potential anatomical contributor to SUDEP mechanisms.

The brainstem-specific cKO mice did not share any obvious phenotypes with previously characterized *Kcna1* deficiency mouse models. The global *Kcna1* deficiency model resulted in mice that displayed spontaneous seizures, premature morality, and both ictal and interictal cardiac dysfunction (H. Dhaibar et al., 2019; Glasscock et al., 2010; Mishra et al., 2017). Restricting *Kcna1* deletion to neurons of the brain showed that the global KO phenotypes are largely brain-derived, as the neuron-specific cKO mice shared similar, albeit attenuated, phenotypes compared to the global KO mice (Trosclair et al., 2020). Unpublished work from the lab (presented in Chapter 2) has also characterized a novel *Kcna1* deficiency model where deletion of the gene is limited to excitatory neurons of the forebrain. This model displayed spontaneous seizures and premature mortality similar to the neuron-specific cKO, however there were significant differences in their cardiorespiratory phenotypes as compared to the global and neuron-specific models. Forebrain-specific cKO mice retained the ictal cardiorespiratory dysfunction phenotypes but their interictal

cardiorespiratory phenotypes resembled WT mice. The brainstem-specific cKO mice did not have spontaneous seizures (Fig. 2A), nor did they have any premature mortality (Fig. 2B). Previous research with the *Kcna1* deficiency models has shown that seizures result in increased neural activity in limbic regions, including the hippocampus and amygdala, suggesting the epileptogenic onset zone for these mice is in forebrain. Therefore, seizures were not predicted in the brainstem model in which the forebrain retains normal levels of *Kcna1* (Gautier & Glasscock, 2015). As *Kcna1* deficiency mice are a model of SUDEP, the lack of spontaneous seizures is a likely explanation for the lack of premature mortality. Because the brainstem-specific cKO mice do not have spontaneous seizures, we challenged them with the chemical convulsant flurothyl to examine seizure-related mortality. The brainstem-specific cKO mice showed a non-significant enhancement in the time required for seizure generalization to the brainstem, but this did not translate to any significant differences in mortality (Fig 3). We observed no instances of interictal cardiac (Fig. 3) or respiratory (Fig. 5) dysfunction in brainstem-specific cKO mice, suggesting Kv1.1 deficiency in this circuit alone is not sufficient to alter the basal function of the heart and lungs.

Because the brainstem is a primary regulator of the heart and lungs, finding no effects of brainstem-specific *Kcna1* deletion on cardiorespiratory function was surprising. One explanation for this result could be that the *Phox2b*-Cre driver did not target *Kcna1* deletion in the key nuclei driving the cardiorespiratory dysfunction phenotype. Previous work shows that *Phox2b* is not endogenously expressed in the respiratory rhythm generators (Bötzinger and pre-Bötzinger nuclei) which convey heavy influence over respiratory rate and variability (Blanchi et al., 2003). However, *Phox2b* is expressed in the retrotrapezoid nucleus, nucleus ambiguus, and nucleus of the solitary tract which all play important roles in cardiorespiration (Dubreuil et al., 2008, 2009; Fu et

al., 2019; M. M. Scott et al., 2011; Stornetta et al., 2006). In fact, the RTN does not develop properly in *Phox2b* null mice, causing them to die hours after birth from respiratory failure, thereby demonstrating the importance of this region for respiration and survival (Gallego & Dauger, 2008; Goridis et al., 2010). Furthermore, experimental manipulation of Phox2b-containing neurons activates pre-Bötzinger neurons suggesting the two are directly linked (Fu et al., 2019; N. Liu et al., 2021). Therefore, a more likely explanation for the absence of cardiorespiratory dysfunction in brainstem-specific *Kcna1* cKO mice is that the interplay and communication between the brainstem and forebrain autonomic circuits could be masking the phenotypes. In the brainstem-specific cKO mice, the forebrain has WT levels of *Kcna1*, so the forebrain may be able to neutralize the impact of the excitation-prone brainstem to mask potential cardiorespiratory deficits. Lastly, important contributions to cardiorespiratory dysfunction may reside outside of the traditional circuitry that governs autonomic brain control. One such region is the cerebellum. The neuron-specific cKO model does not target the cerebellum, and these mice show normal basal respiratory rate/variability, along with attenuated cardiac dysfunction compared to global KO mice. The Cre lines used to generate the forebrain- and brainstem-specific cKO mice also fail to target *Kcna1* deletion to the cerebellum, and both of these cKO models exhibit normal interictal cardiorespiratory function (Trosclair et al., 2020). Thus, the cerebellum may have an underappreciated influence on cardiorespiratory activity, and working with a cerebellum-specific *Kcna1* deficiency model could elucidate this region's potential role in SUDEP pathomechanisms.

The brainstem appears to have a potentially important role in blood gas stability, as the cKO mice had a trend towards more hypoxic events basally. Importantly, it has been shown that *Kcna1* mRNA is not present in the lungs, so deficits in the respiratory parameters are likely coming from neural influences (K. A. Simeone et al., 2018). This result would be in line with research on

global *Kcna1* KO mice showing that they experience a significantly increased number of hypoxic events regardless of their activity status, and hypoxic KO mice showed an increase in respiration as a response which was greater than in control mice (Kline et al., 2005; K. A. Simeone et al., 2018). *Kcna1* KO mice show a greater level of spontaneous and miniature EPSCs in the NTS than control mice, suggesting hyperexcitability defects which could functionally impair blood oxygen regulation (Kline et al., 2005). *Kcna1* KO mice with intermittent hypoxia exhibit improved oxygen saturation after treatment with a dual orexin (hypothalamic neuropeptide involved in arousal) antagonist (Iyer et al., 2020). An interesting future study would be to see if the dual orexin antagonist could attenuate the hypoxia deficits in brainstem-specific cKO mice (if they are ultimately found to be statistically significant) because it would suggest that the brainstem is critical in regulating the oxygen saturation chemoreflex. Interestingly, when heterozygous *Kcna1* KO mice are exposed to hypoxia at postnatal day 6, they show increased susceptibility to flurothyl-induced seizures at postnatal day 50 (Leonard et al., 2013). Furthermore, a subset of the heterozygous mice exposed to hypoxia developed spontaneous seizures, suggesting poor blood oxygen saturation in development can have large neurological consequences during the aging process (Leonard et al., 2013). The flurothyl experiments performed here were done at postnatal day 30 to correspond to studies in other *Kcna1* deficiency models, but these hypoxia exposure studies suggest that testing the mice at older ages could potentially uncover susceptibility to flurothyl-induced seizures in brainstem-specific cKO mice.

To summarize, our findings show that brainstem-specific deletion of *Kcna1* may cause chemoreflex deficits in the absence of other basal cardiac and respiratory abnormalities. Neurologically, EEG power spectrum analysis reveals that brainstem-specific cKO mice possess a significant increase in relative resting-state theta power, which has been shown to be increased

in human epilepsy syndromes (Clemens et al., 2021, 2023). Of note, the EEGs performed in this study only had parietotemporal subdural leads meaning that the brainstem-specific *Kcna1* deletion was able to produce cortically measured differences in EEG relative power. Though no seizures were captured, there may yet be more neurological deficits that were not measured in this study such as brainstem hyperexcitability. One of the most prominent findings in brainstem-specific cKO mice was the apparent trend in increased prevalence of hypoxic events in the resting state compared to WT mice (Fig 6C). Together with other *Kcna1* deficiency models, the results here implicate brainstem Kv1.1 as potentially important in basal blood gas chemoreception. Chemosensory dysregulation could contribute to SUDEP mechanisms as patients have been found in the prone position at night and they do not always recognize air hunger signals from the brain, suggesting deficits in proper chemoreflex and arousal mechanisms may increase overall SUDEP risk (Harmata et al., 2023). Therefore, we propose the brainstem as one of many key anatomical regions which, when dysfunctional, could contribute to SUDEP risk and pathomechanisms.

CHAPTER 4:

IDENTIFICATION OF THE REGIONAL DISTRIBUTION OF KV1.1 IN THE HEART AND HOW IT CONTRIBUTES TO CARDIAC PHYSIOLOGY

4.1 Abstract

Voltage-gated potassium channels are recognized for their significant roles in cardiac function. However, only recently has Kv1.1 been acknowledged as both present and functionally active in both the atria and ventricles, particularly in the repolarization of action potentials. Atrial and ventricular cardiomyocytes lacking *Kcna1* show prolonged action potentials which could be a risk factor for arrhythmia. Importantly, the presence and functional significance of Kv1.1 in sinoatrial node intrinsic pacemaking activity has not yet been described. Furthermore, knowledge of how Kv1.1 function in the heart contributes to *in vivo* cardiac function remains incomplete. The work in this chapter represents collaborative pieces of larger research papers that I have contributed to experimentally in an attempt to address these gaps in knowledge. First, I used immunocytochemistry to show that Kv1.1 is present in sinoatrial cells in very low abundance but using immunolabeling amplification allowed for detection and quantification. Furthermore, I used *in vivo* ECG to assess cardiac function in cardiac-specific *Kcna1* cKO mice which revealed no overt cardiac abnormalities. Therefore, cardiomyocyte-specific deletion of *Kcna1* is not sufficient to evoke significant *in vivo* cardiac deficits at the level of ECG. Ultimately, we find that *Kcna1* is present in the major regions of the heart where it contributes significantly to cardiomyocyte repolarization, but these deficits are not necessarily severe enough to impair overall heart function.

4.2 Introduction

The heart is a complex organ which, through fine-tuned electrical signaling, beats consistently day in and day out to sustain life. The electrical activity initiates in the sinoatrial node where pacemaker cells propagate their signals through the atria and to the atrioventricular node (Nerbonne & Kass, 2005). This signal then spreads downward to the apex of the heart and into the ventricles completing one cycle (Nerbonne & Kass, 2005). Specifically, the cardiac action potential is shaped through a combination of inward Na^+ and Ca^{2+} currents which depolarize the cell, and outward K^+ currents which repolarize the cell (Nerbonne & Kass, 2005). Importantly, there are many potassium channels which are active during different parts of the repolarization process depending on their voltage dependence, gating, and kinetics, which suggests that research into understanding each of these contributing currents is essential to understanding and effectively providing clinical therapeutics for arrhythmias (Nerbonne, 2016).

The voltage-gated potassium channel alpha subunit Kv1.1 (encoded by the *Kcna1* gene) is one such channel that has a long-established role in neuronal action potentials but has only recently been confirmed as present and active in the heart. Kv1.1 was the first potassium channel gene to be cloned and linked to human disease (namely episodic ataxia type 1) in the late 1900s making the gap in knowledge of its role in cardiac function surprising (Glasscock, 2019). One factor which contributed to this was a set of studies done in the 1990s and early 2000s which were either unsuccessful in their attempts to show Kv1.1 expression in the heart, or the results were difficult to interpret and often attributed to neural influences leaving researchers at the time under a consensus that Kv1.1 was not present in the heart (Brahmajothi et al., 1997; Dixon & McKinnon, 1994; Glasscock, 2019; London et al., 2001; Roberds & Tamkun, 1991). Advancement of experimental detection techniques allowed for more confident confirmation of *Kcna1* mRNA in

the heart including the sinoatrial node (Harrell et al., 2007; Leoni et al., 2006a; Marionneau et al., 2005), but the functional expression of the protein had yet to be confirmed. Western blot and immunohistochemistry performed in the Glasscock lab showed Kv1.1 protein expression in the atrial and ventricular cells of both mice and humans (Glasscock et al., 2010, 2015; Trosclair et al., 2021) This long and arduous path to identifying cardiac Kv1.1 expression confirmed its presence in the heart, but work needed to be done to confirm what, if any, functional role it is playing.

Subsequent studies demonstrated that Kv1.1 functionally contributes to atrial and ventricular action potential repolarization. In a study using isolated human atrial cardiomyocytes, application of the Kv1.1 specific blocker dendrotoxin-K (DTX-K) reduced both peak and late outward K^+ currents which was the first piece of evidence that Kv1.1 is functionally active in cardiac repolarization (Glasscock et al., 2015). Furthermore, patch clamp recordings showed that atrial cardiomyocytes isolated from *Kcna1* KO mice have impaired repolarization and altered action potential shape which was also recapitulated in WT atrial cells treated with DTX-K, further solidifying that Kv1.1 is functionally active in the heart (Si et al., 2019). In the ventricles, whole-cell patch clamp recordings demonstrated that ventricular cardiomyocytes from *Kcna1* KO mice also show prolonged action potentials, further indicating repolarization deficits (Trosclair et al., 2021). Despite the abundance of evidence for both the presence and function of Kv1.1 in atrial and ventricular cardiomyocytes, there remains a gap in knowledge regarding the potential role of Kv1.1 in the sinoatrial node.

Genetic manipulation of *Kcna1* has revealed important roles for the gene in regulating *in vivo* cardiac physiology. *Kcna1* global KO mice are commonly used as a model for sudden unexpected death in epilepsy (SUDEP) because they have spontaneous seizures, premature mortality, and cardiorespiratory dysfunction (H. Dhaibar et al., 2019; Glasscock et al., 2010; Iyer

et al., 2020; Smart et al., 1998). Recordings of global KO mice using simultaneous electroencephalography (EEG)- electrocardiography (ECG) showed multiple types of cardiac abnormalities during seizures including cardiac conduction blocks, bradycardia, and asystole (Glasscock et al., 2010). Echocardiography of *Kcna1* KO mice also revealed decreased ejection fraction and fractional shortening indicative of contractile dysfunction (Trosclair et al., 2021). Furthermore, restricting *Kcna1* deletion to either the neurons of the brain or more specifically to neurons of the corticolimbic circuit (Chapter 2) causes ictal cardiac dysfunction similar to global KO mice (Trosclair et al., 2020, Paulhus et al, unpublished). EEG-ECG recordings in both global *Kcna1* KO and corticolimbic-specific *Kcna1* cKO mice have captured SUDEP events which present with progressively worsening bradycardia leading to death, emphasizing the role of the heart in SUDEP pathomechanisms (Glasscock et al., 2010; Moore et al., 2014, Paulhus et al, unpublished). Global KO and neuron-specific cKO mice also show interictal cardiac deficits including increased cardiac conduction blocks (global KO only) and increased parasympathetic tone as detected by the root mean square of successive beat-to-beat differences (RMSSD), a heart rate variability (HRV) measure (Glasscock et al., 2010; Mishra et al., 2017; Trosclair et al., 2020; Vanhoof-Villalba et al., 2018). This evidence shows that Kv1.1 plays an important role in cardiac function by regulating either heart-intrinsic processes or brain-derived autonomic mechanisms Kv1.1. However, the contribution of cardiac-specific of Kv1.1 to intrinsic cardiac function at the level of the whole animal has not been directly tested.

This chapter is comprised of collaborative contributions made by the dissertation author towards larger publications seeking to fill two primary gaps in the knowledge of Kv1.1 in the heart. The first is whether Kv1.1 is present in the sinoatrial node, a step towards identifying how Kv1.1 functionally contributes to pacemaking. The second is to identify how heart-specific *Kcna1*

contributes to overall cardiac function measured by *in vivo* experiments. These studies suggest that *Kcna1* is present in the sinoatrial node. Furthermore, a post-doctoral researcher in the lab (Dr. Man Si) has confirmed the functional importance of Kv1.1 in sinoatrial cells by performing a series of patch clamp electrophysiology experiments. However, ECG recordings in heart-specific *Kcna1* mice did not reveal evidence of *in vivo* cardiac dysfunction. Ultimately these results suggest that the cardiac dysfunction identified in *Kcna1* deficiency models is likely predominantly brain-derived, but Kv1.1 is present in the heart where it makes a significant contribution towards action potential repolarization in atrial, ventricular, and sinoatrial cells, providing a potentially vulnerable substrate for seizures to act upon.

4.3 Materials and Methods

4.3.1 Animals

Heart-specific conditional knockout (cKO) mice (i.e., *Myh6*-Cre$^{+/-}$;*Kcna1*$^{fl/-}$) were generated by crossing heterozygous *Kcna1* floxed (fl) mice (*Kcna1*$^{fl/+}$) with heterozygous *Kcna1* global knockout mice (*Kcna1*$^{+/-}$) carrying one copy of the *Myh6* transgene (i.e., *Myh6*-Cre$^{+/-}$, *Kcna1*$^{+/-}$). *Myh6*-Cre$^{+/-}$, *Kcna1*$^{+/-}$ mice were generated by crossing hemizygous transgenic *Myh6*-Cre$^{+/-}$ mice with heterozygous *Kcna1*$^{+/-}$ mice. Control mice include *Kcna1*$^{+/+}$,*Myh6*$^{-/-}$ (WT), *Kcna1*$^{+/+}$, *Myh6*$^{+/-}$ (Cre), and *Kcna1*$^{fl/-}$,*Myh6*$^{+/+}$ (fl/-). *Myh6*-Cre mice were purchased from Jackson Labs (Bangor, MN) under the catalog name B6.FVB-Tg(Myh6-cre)2182Mds/J (JAX 011038). *Kcna1*$^{+/-}$ mice which are maintained on a Tac:N:NIHS-BC genetic background, carry a KO allele of the *Kcna1* gene due to targeted deletion of the entire open reading frame (Smart et al., 1998). *Kcna1*$^{fl/+}$ mice, which are maintained on a C57BL/6J, were generated and described previously (Trosclair et al.,

2020). Mice were housed at 22°C, fed *ad libitum*, and subjected to a 12-h day/night cycle. All experiments were performed in accordance with National Institutes of Health (NIH) guidelines with approval from the Institutional Animal Care and Use Committee of Southern Methodist University.

4.3.2 Genotyping

To identify experimental and control mice, genomic DNA was isolated by enzymatic digestion of tail clips using Direct-PCR Lysis Reagent (Viagen Biotech, Los Angeles, CA, USA). Genotypes were determined by performing PCR amplification of genomic DNA using allele-specific primers. For detection of the *Kcna1* global KO allele, the following primer sequences were used to yield amplicons of 337 bp for the wild-type (WT) allele and 475 bp for the KO allele: a WT specific primer (5'-GCCTCTGACAGTGACCTCAGC-3'); a KO-specific primer (5'-CCTTCTATCGCCTTCTTGACG-3'); and a common primer (5'-GCTTCAGGTTCGCCACTCCCC-3'). For detection of the $Kcna1^{fl}$ allele, the following primer sequences were used to yield amplicons of 197 bp for the WT allele and 260 bp for the floxed allele: a WT-specific primer (5'-GCTCCTCTACTATCAGCAAGTCTGAGTACATGG-3'); a floxed-specific primer (5'-ATCAAGTTGGACATCACCTCCCACAAC-3'); and a common primer (5'-AAGGGGTTTGTTTGGGGCTTTTGTT-3'). For detection of the *Myh6*-Cre transgene, the following primer sequences were used to yield a product of 300 bp for the Cre allele: a *Myh6*-Cre specific forward primer (5'-ATGACAGACAGATCCCTCCTATCTCC-3'), and a *Myh6*-Cre reverse primer (5'-CTCATCACTCGTTGCATCATCGAC-3').

4.3.3 Video-electroencephalography-electrocardiography (EEG-ECG) recordings

To measure *in vivo* brain and heart activity, mice (4-6 weeks old) of both sexes were anesthetized using an anesthetic cocktail and surgically implanted with bilateral silver wire EEG and ECG electrodes (0.005-inch diameter) attached to a microminiature connector (Omnetics Connector Corporation, Minneapolis, MN) for tethered configuration recording. The anesthetic cocktail contained ketamine (100 mg/kg), xylazine (10 mg/kg), and acepromazine (2 mg/kg) and was administered by intraperitoneal (i.p.) injection. Following completion of the surgery, the reversal agent Antisedan (1 mg/kg) was administered by subcutaneous (s.c.) injection. Carprofen (5 mg/kg, s.c.) was given the day of surgery and 24 hours post-surgery for pain management. EEG wires were inserted into the subdural space through cranial burr holes overlying the parietotemporal cortex for the recording electrodes and above the frontal cortex for the ground and reference electrodes, as described previously (Mishra et al., 2018). Two ECG wires were tunneled subcutaneously on both sides of the thorax and sutured in place to record cardiac activity, as described previously (Mishra et al., 2018). Mice were allowed to recover for 48 hours before recording simultaneous EEG-ECG for ≥ 24 h continuously while the animals were housed in a plexiglass tank (40-cm length x 20-cm width x 23-cm height). Biosignals were band-pass filtered by applying 0.3 Hz high-pass and 75-Hz low pass filters for EEG and a 3.0-Hz high-pass filter for ECG. Sampling rates were set to 500 Hz for EEG and 2 kHz for ECG.

4.3.4 Analysis of video-EEG-ECG recordings

The RR intervals of the ECG waveforms were used to estimate heart rate (HR) and heart rate variability (HRV) for the first 24-h recording period overall as a whole, and for the 24-h day- (6:00

AM to 6:00 PM) and 12-h night phase (6:00 PM to 6:00 AM) portions. For each ECG recording, six separate RR interval series were derived by sampling 2-min ECG segments every four hours to provide three day (6:00 AM to 6:00 PM) and three night (6:00 PM to 6:00 AM) measurements. RR interval series for each segment were automatically generated and manually confirmed using Ponemah software (Data Sciences International, St. Paul, MN). RR intervals were only sampled during times when the mouse was stationary and no physiological artifacts such as skipped or ectopic beats occurred. HRV was measured in the time domain using the standard deviation of the RR intervals (SDNN); the coefficient of variance (CV; defined as $SDNN/RR_{mean}$ x100); the root mean square of successive differences between the RR intervals (RMSSD); and the percentage of consecutive RR intervals differing my >6 ms (pNN6). The HR and HRV values for each animal represent an average of the six total segments or an average of the three daytime or three nighttime segments, as indicated in the text.

4.3.5 Immunocytochemistry

Isolated SAN cells were allowed to settle on laminin-coated chambered slides for at least 2 h followed by fixation with 3.2% paraformaldehyde for 10 min. Cells were permeabilized using 0.1% Triton in phosphate-buffered saline (PBS) and blocked in 10% goat serum for 1 h at room temperature (RT; ~22°C). Cells were incubated overnight at RT with 1:200 dilution of rabbit polyclonal anti-Hcn4 antibody (APC-052, Alomone) and 1:500 dilution of mouse monoclonal anti-Kv1.1 antibody (K20/78, NeuroMab). Hcn4 and Kv1.1 immunoreactivities were visualized with 1:1000 Alexa Fluor 594 and 488 secondary antibodies (Invitrogen), respectively. After three

washes with PBS, a coverslip was mounted onto the slides using ProLong Glass Antifade Mountant with NucBlue (Invitrogen).

Tyramide signal amplification (kit B40941, Invitrogen) was used to boost the Kv1.1 immunoreactivity signal according to the manufacturer's recommended protocol using a 1:500 dilution of mouse anti-Kv1.1 (NeuroMab) and a 1:1000 tyramide-labeled Alexa Fluor 488 antibody. Anti-Hcn4 immunoreactivity was performed the same as described above without tyramide amplification. After three washes with PBS, a coverslip was mounted onto the slides using ProLong Glass Antifade Mountant with NucBlue (Invitrogen).

Images were collected at 40-times magnification using an automated microscope (LionHeart FX, BioTek). SAN cell identity was confirmed by Hcn4 labeling. Negative control experiments were performed by incubating cells with secondary antibodies only which yielded no detectable signal. Images were always acquired using the same optimized settings for each fluorophore. Brightness and contrast were minimally adjusted to improve visualization of acquired images, but these settings were applied equally to each fluorophore for all images. Merged images were not further adjusted. Analysis was performed for 10 cells/animal for WT (n=4) and KO (n=4) using ImageJ software. Equal sexes were used for each genotype (2 males and 2 females). Corrected total cell fluorescence (CTCF) was calculated for individual cells from the following equation: CTCF = Integrated Density - (selected cell area X mean fluorescence of background reading).

4.3.6 Statistical Analysis

Data are presented as mean ± SEM. Prism 10 for Windows (GraphPad Software Inc, La Jolla, CA, USA) was used for statistical analysis. For comparisons involving two or more groups, one-way analysis of variance (ANOVA) was used followed by Tukey post-hoc tests. For comparisons of corrected total cell fluorescence, the data was not normally distributed, so it was first log transformed and then a non-parametric Mann-Whitney test was performed on the log-transformed data. Outliers were identified using the ROUT method with Q= 1% and excluded from analyses. Results were significant if $P < 0.05$. Gender for each ECG data point is indicated as open circles for females and closed circles for males.

4.4 Results

4.4.1 Kcna1 is present in low abundance in sinoatrial myocytes

To complement previous work that has demonstrated *Kcna1* transcripts in the sinoatrial node, we performed immunocytochemistry to investigate the corresponding Kv1.1 protein levels (Glasscock et al., 2010; Leoni et al., 2006b; Marionneau et al., 2005). Kv1.1 immunocytochemistry was performed alongside HCN4 immunodetection to specifically label sinoatrial myocytes. Traditional immunocytochemistry resulted in very weak Kv1.1 staining in WT cells, so tyramide signal amplification (TSA) was used to increase the Kv1.1 sensitivity. This strategy has been leveraged previously for low abundance ion channels in sinoatrial cells (Lai et al., 2014). TSA Kv1.1 immunocytochemistry showed Kv1.1 protein in WT cells which was largely diffuse intracellularly (Fig. 1A). Corrected total cell fluorescence (CTCF) was used to quantify the Kv1.1

signal which showed a significant reduction in knockout cells compared to WT (Fig. 1B). Overall, this work demonstrated that Kv1.1 protein is detectable in sinoatrial myocytes, but at a low level.

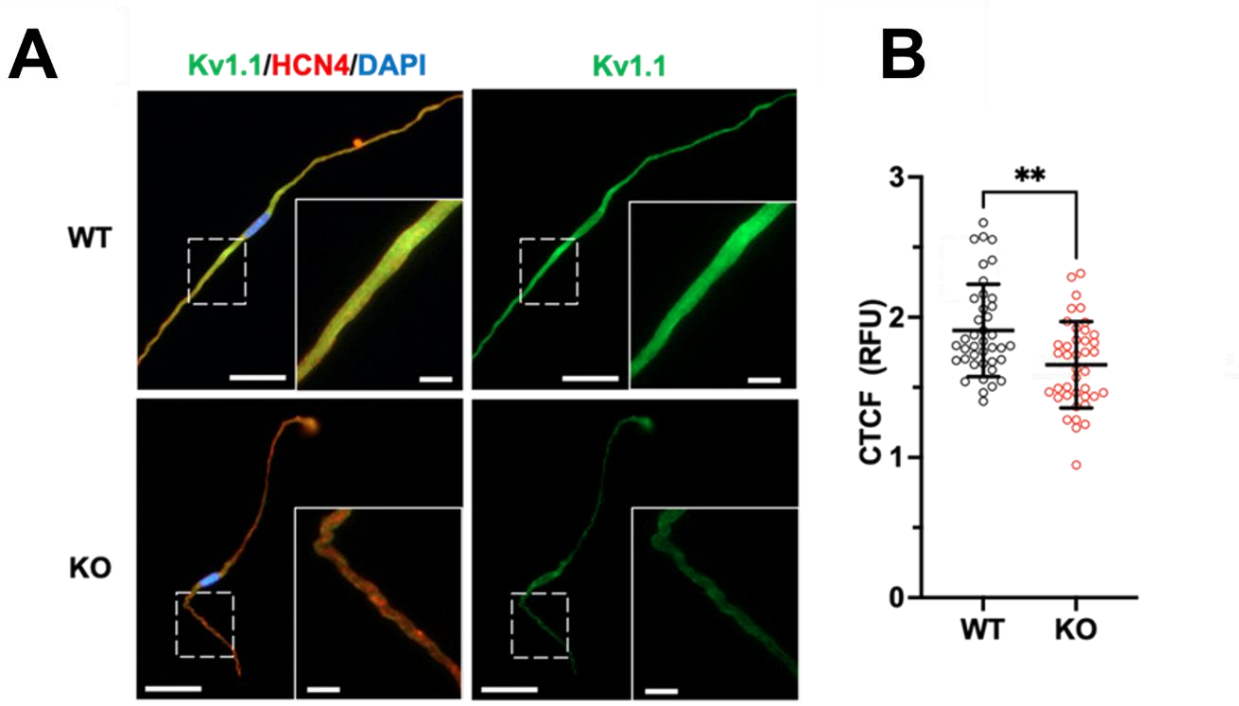

Figure 4.1. Immunocytochemistry shows Kv1.1 immunoreactivity present at low levels in WT SAN myocytes. (**A**) Representative images of WT (top row) and KO (bottom row) sinoatrial myocytes after labeling with tyramide signal amplification of the KV1.1 signal. Left panels: representative merges images showing co-labeling for Kv1.1, the SAN-specific marker HCN4, and the nuclear marker nuc blue. Right panels: immunoreactivity for Kv1.1 in the same cells. Inset images correspond to the dashed box. Scale bars: 25 µm for the primary image and 5 µm for the inset. (**B**) WT cells showed significantly increased levels of Kv1.1 corrected total cell fluorescence (CTCF) compared to KO cells. For both groups, 4 animals were used, and 10 cells/animal were imaged and quantified for a total of 40 cells/genotype. RFU, relative fluorescence units. **, P = 0.0029 (Mann Whitney U test of log-transformed values).

4.4.2 Cardiac-specific Kcna1 deletion does not incite ECG recorded cardiac dysfunction

With the presence and functional activity of Kv1.1 shown throughout the brain, it was important to analyze the cardiac consequences of *Kcna1* deletion specifically in the heart. Previous

work genetically manipulating *Kcna1* looked at either isolated hearts, isolated cardiomyocytes, or global and brain-specific *Kcna1* deletion in mice, but none of these studies has investigated the contribution of heart-specific *Kcna1* to normal mouse cardiology. Analysis of ECG recordings from heart-specific *Kcna1* cKO mice showed that their heart rates were not significantly different from controls (Fig. 2A). This result is in line with other *Kcna1* deficiency models which also do not show heart rate differences in ECG recordings (H. Dhaibar et al., 2019; Mishra et al., 2017; Trosclair et al., 2020, Paulhus et al, unpublished). Next, measures of HRV were assessed beginning with RMSSD as a measure of parasympathetic tone. We found no significant differences in overall, daytime, or nighttime RMSSD values between groups (Fig. 2B). The measures of sympathetic tone, SDNN and CV (coefficient of variance = SDNN/ RR_{mean}), were also statistically similar across all groups (Fig. 2C-2D). Analysis of individual heart beats showed that the percent of consecutive beats differing by more than 6 ms (pNN6) and the prevalence of cardiac conduction blocks (i.e., conduction blocks) were not statistically different between groups (Fig. 2E-2F). Ultimately, this work shows that heart-specific Kv1.1 deficiency is not sufficient for detectable cardiac dysfunction at the level of the ECG.

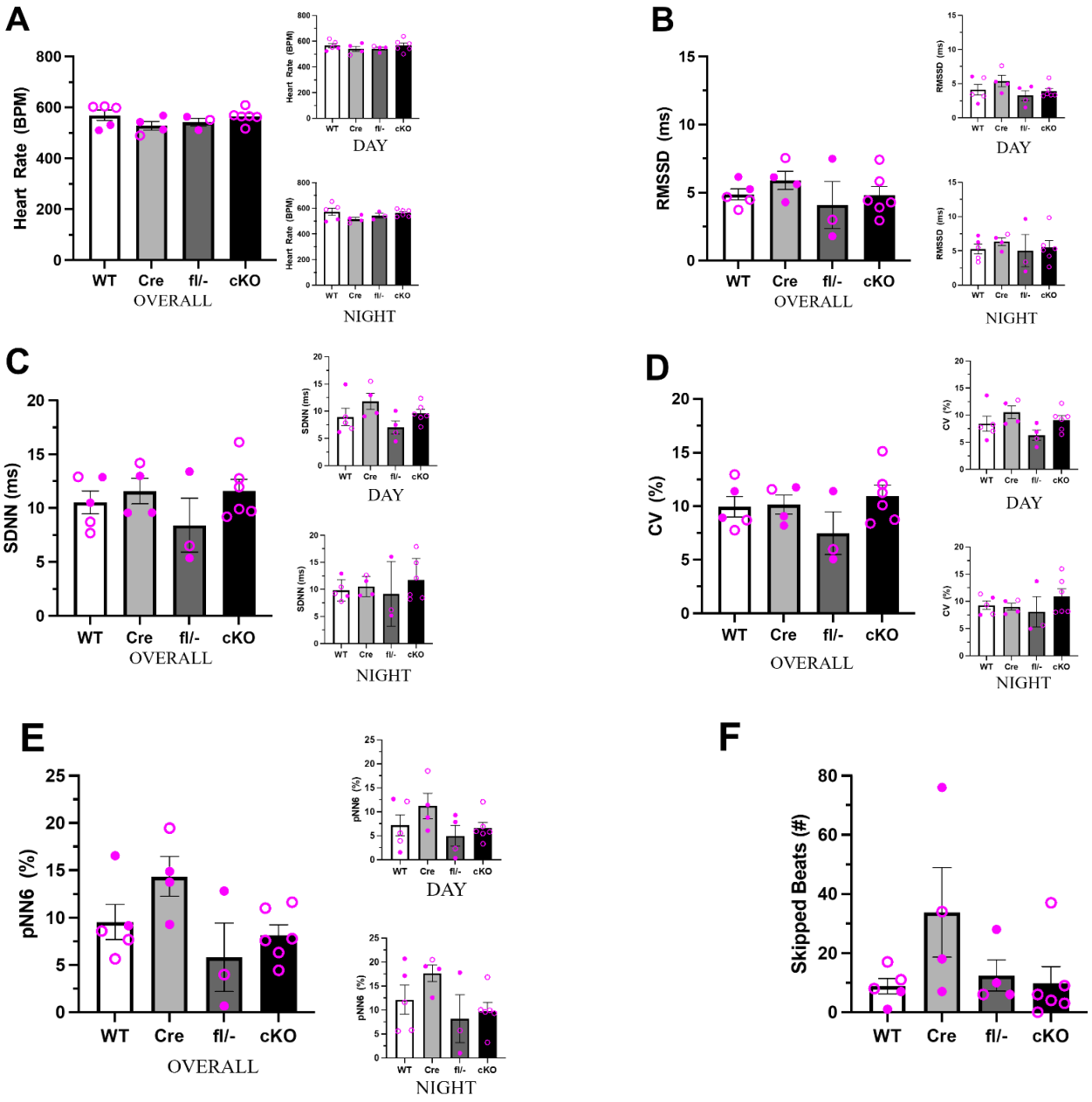

Figure 4.2. Quantification of (**A**) heart rate, (**B**) RMSSD, (**C**) SDNN, (**D**) CV, (**E**) pNN6, and (**F**) skipped beats from 24 hour *in vivo* ECG recordings in WT (n=5), cre (n=4), fl/- (n=3), and cKO (n=6) mice. RMSSD, root mean square of successive beat to beat differences; SDNN, standard deviation of beat to beat intervals; CV, coefficient of variance; skipped beats, cardiac conduction blocks. One-way ANOVA revealed no statistical differences in any of the measured parameters.

4.5 Conclusions

The first experiment presented (Fig. 1) shows that Kv1.1 is expressed in mouse sinoatrial myocytes, but at low levels. Previous research has shown that Kv1.1 is present and functionally active in both atrial and ventricular cells, and this current experiment confirms that Kv1.1 is also present in the sinoatrial node (Si et al., 2019; Trosclair et al., 2021). Importantly, unpublished experiments from the lab have also shown that Kv1.1 is functionally required for normal sinoatrial myocyte firing rate and cardiac pacemaking in mice (Si et al, unpublished). This extends our knowledge of cardiac Kv1.1 by showing its presence and functional activity in three of the major anatomical regions of the heart: the atria, ventricles, and sinoatrial node. The immunological detection of Kv1.1 revealed that the protein was only present at low levels yet electrophysiology shows that it still makes significant functional contributions in sinoatrial myocyte (Si et al; unpublished; Fig 1). This current (now deemed $I_{Kv1.1}$) should be considered in clinical cases of sinus node dysfunction and could potentially be targeted in cases of cardiac arrhythmia (Si et al unpublished).

The second set of experiments (Fig. 2) revealed that limiting *Kcna1* deficiency to only the heart is not sufficient for ECG-measured cardiac dysfunction. Previous studies using *Kcna1* deficiency models have shown both ictal and interictal ECG abnormalities; however, these models were either global gene knockouts, or they restricted *Kcna1* deletion to the brain (H. Dhaibar et al., 2019; Glasscock et al., 2010; Mishra et al., 2017; Trosclair et al., 2020, Paulhus, unpublished). The absence of measurable cardiac dysfunction in the heart-specific deficiency model was surprising given the electrophysiological evidence that Kv1.1 is present and functioning in the atria, ventricles, and sinoatrial node, but there could be explanations outside the heart that account for this (Si et al., 2019; Trosclair et al., 2021; Si et al., unpublished). The brain houses the

autonomic nervous system nuclei which directly communicate with the heart to regulate the balance of autonomic tone. Therefore, it is possible that these autonomic influences can mask intrinsic cardiac deficits. The neuron-specific cKO mice exhibit interictal cardiac dysfunction despite not deleting *Kcna1* in the heart. This suggests that the brain itself can drive cardiac dysfunction even with an otherwise healthy heart (Trosclair et al., 2020). There could also be neuro-humoral influences, remodeling, or other actions at play which compensate for intrinsic cardiac dysfunction (Al Kury et al., 2022; MacDonald et al., 2020). Overall, however, the results show cardiac-specific *Kcna1* deletion does not impair cardiac function *in vivo* at the level of the ECG.

In summary, Kv1.1, a previously underappreciated channel in the heart, is present and functional in the major regions of the heart where it contributes to action potential repolarization. Even in the case of the sinoatrial node, where Kv1.1 is present at low levels in sinoatrial myocytes, the channel still has major contributions to intrinsic firing rate. These findings illustrate the important principle that even low levels of ion channel proteins can play big roles in cardiac function. Furthermore, restricting *Kcna1* deletion specifically to the heart does not result in significant cardiac dysfunction as measured by ECG. Importantly, cardiac dysfunction is a common phenotype in SUDEP cases, so understanding the anatomical substrates for this dysfunction is critical for designing appropriate therapeutics and managing risk stratification in the epilepsy community. It appears that, in the case of the *Kcna1* deficiency mouse models, the primary driver of cardiac dysfunction is aberrant signaling from the brain. However, because *Kcna1* plays an important role in overall cardiomyocyte electrophysiology, it is important to consider that mutations in *KCNA1* in clinical cases may render the heart more vulnerable to the repeated stress of electrical activity propagating to the heart from seizures. Ultimately, Kv1.1

appears to be clinically relevant for both sinus node dysfunction, as well as for potentially rendering an epileptic heart vulnerable to potentially dangerous arrhythmias which could increase the risk of death.

CHAPTER 5:

FINAL CONCLUSIONS

5.1 Summary

Sudden unexpected death in epilepsy (SUDEP) is a complex biological phenomenon with mechanisms and anatomical substrates that have yet to be fully elucidated. Many efforts have focused on developing a better understanding of SUDEP, but at this stage researchers only have working hypotheses. A subset of the research suggests seizures communicate pathological signals to the heart and brain which leads to mortality through cardiorespiratory collapse, but the specific mechanisms are not known. Furthering this hypothesis, the MORTEMUS study showed that the cascade of events leading to SUDEP appeared to be the terminal seizure and subsequent apnea followed by asystole emphasizing both the heart and lungs in the process.

One barrier to understanding SUDEP more comprehensively is finding a good model to use that captures relevant phenotypes that have been identified in clinical cases. The preclinical Kv1.1 deficiency mouse model is one such model. *Kcna1* encodes Kv1.1 alpha subunits which assemble with other voltage-gated potassium channel alpha subunits and the corresponding beta subunits to form a fully functional channel. Kv1.1 channels are critically important in action potential repolarization and maintaining normal electrical activity. When the gene is globally deleted, the resulting KO mouse model displays spontaneous seizures, cardiorespiratory dysfunction, and premature mortality. These phenotypes are a reasonable approximation of what

was described in the MORTEMUS study and thus, this model is at the core of the SUDEP research performed in the lab.

Utilizing Kv1.1 deficiency mouse models has helped guide knowledge on potential SUDEP mechanisms. As stated above, the global KO mice have spontaneous, unprovoked, seizures which typically present with both ictal cardiac and respiratory dysfunction. The most common of these include hyperventilation, tachypnea, and ataxic breathing for respiratory phenotypes, and tachycardia, bradycardia, and cardiac conduction blocks for cardiac events (H. Dhaibar et al., 2019). These mice also displayed cardiorespiratory dysfunction interictally including elevated respiratory rate and variability, an abnormal decrease in apneas, and increased heart rate variability (RMSSD; parasympathetic tone measure) (H. Dhaibar et al., 2019; Mishra et al., 2017). A near SUDEP event was also captured in the global KO mice which showed a 14-s apnea at the end of the seizure and into the postictal period with cardiac dysfunction beginning secondary to respiratory deficits. Cardiac dysfunction included agonal QRS and ST depression which are often associated with comorbid oxygen saturation deficits which also suggests cardiorespiratory failure as a critical step in the SUDEP pathological cascade. This model has laid important groundwork for understanding potentially important SUDEP mechanisms, but anatomical substrates cannot be gleaned because the gene is globally knocked out.

To further this work, a neuron-specific *Kcna1* cKO was generated to determine if the phenotypes previously seen in global KO mice were brain-derived. Limiting Kv1.1 deficiency to neurons helped to identify the regions that are active for SUDEP-related phenotypes observed clinically and in mouse models. Neuron-specific cKO mice also showed spontaneous seizures, cardiorespiratory abnormalities, and premature mortality, but the phenotypes observed were slightly attenuated from what was observed in global KO mice. During seizures, tachypnea,

hyperventilation, and ataxic breathing still were observed as common respiratory phenotypes, and bradycardia was commonly observed as a cardiac phenotype (Trosclair et al., 2020). Interictally, the absence of apneas and an increase in heart rate variability (RMSSD; parasympathetic tone) were observed, similar to the global KO mice. Collectively, the neuron-specific cKO mouse model showed that the SUDEP-relevant phenotypes observed in Kv1.1 deficiency mouse models appear to be largely brain-driven. However, the lesser severity of the phenotypes in the neuron-specific cKO mouse suggested that other regions outside the brain might contribute to SUDEP phenotypes. Furthermore, the neuron-specific cKO was a brain-wide deletion that encompassed a multitude of complex neural circuits, hindering the identification of the individual contributions of discrete neuronal subpopulations to SUDEP. For this reason, this dissertation examined the contribution of two specific neural circuits (the corticolimbic circuit and the brainstem), as well as the heart to better understand the anatomical underpinnings of SUDEP pathology.

Chapters 2 and 3 of this dissertation utilized novel corticolimbic- and brainstem-specific *Kcna1* cKO mice to measure how the primary autonomic circuits influence the phenotypes that were relevant to both the global and neuron-specific cKO mice. In chapter 2, it was shown that *Kcna1* deletion in corticolimbic circuits is sufficient for spontaneous seizures, premature mortality, ictal cardiorespiratory dysfunction, and even SUDEP (Ch. 2, Fig. 2A-C). In fact, the average seizure duration of ~40s in corticolimbic-specific cKO mice was similar to both the global KO and neuron-specific cKO mice (Ch 2., Fig. 2C). Previous work has shown elevated FOS activation in the corticolimbic circuit following spontaneous seizures in the global KO mice which suggested this region may be the epileptogenic zone for *Kcna1* deficiency mouse models (Gautier & Glasscock, 2015). Supporting this, deleting *Kcna1* in only the brainstem did not cause spontaneous seizures, and furthermore, it did not lead to any detectable premature mortality (Ch. 3, Fig. 2A-C).

The corticolimbic-specific cKO mice exhibited premature mortality which was attenuated relative to the neuron-specific cKO mice. Only approximately 25% of corticolimbic-specific cKO mice showed early lethality, but the other models both reached 50% or more mortality (by 1 month old for global KO mice and by 3 months old for neuron-specific cKO mice). One factor that could be contributing to this is the milder seizure phenotypes typically seen in the corticolimbic-specific cKO mice. Their generalized tonic-clonic seizure behaviors, including running and bouncing, rearing, and falling, were seen in less than 40% of all seizures recorded (Ch. 2, Fig. 2D). Furthermore, the differences in mortality imply regions not impacted by the corticolimbic *Emx1*-Cre driver may be important contributors to overall premature death. Thus, the corticolimbic circuit is a critical anatomical substrate for the initiation of spontaneous seizures, premature mortality, and SUDEP.

Ictal cardiorespiratory dysfunction has been a consistent phenotype in previous *Kcna1* deficiency models and was measured in the corticolimbic-specific cKO mice as well. Tachypnea and ataxic breathing were the two most common respiratory phenotypes measured in the corticolimbic cKO mice, which aligns with the other models which also showed a prevalence of the same phenotypes (Ch. 2, Fig. 4A). Similarly, in corticolimbic-specific cKO mice, cardiac conduction blocks, bradycardia, and tachycardia were the most frequent ictal cardiac dysfunction phenotypes, which were also seen in previous *Kcna1* mouse models (Ch. 2, Fig. 3A). Of note, all three models report respiratory dysfunction preceding cardiac dysfunction which suggests that seizures are activating the same networks to elicit consistent phenotypes. This work shows that the ictal cardiorespiratory dysfunction can be driven by the corticolimbic circuit, and that further exploring this circuit may help to uncover more specific anatomical substrates that could be leveraged for potential therapeutics.

Not only has the corticolimbic *Kcna1* deficiency model recapitulated important phenotypes seen in previous *Kcna1* mouse models, but a SUDEP case was also captured during tethered a video EEG-ECG-pleth recording in one corticolimbic-specific cKO animal (Ch. 2, Fig. 5). We compared this recording to SUDEP or near SUDEP events that were previously captured in global KO mice, but those recordings were captured during video EEG-ECG only so respiration data was not available for them. Regardless, all three cases shared striking similarities, including similar terminal seizure durations, behavioral severity, and ictal and postictal cardiac phenotypes. Importantly, global KO mice commonly display ataxic breathing prior to the beginning of cardiac dysfunction in non-fatal seizures. This series of events was observed in the corticolimbic-specific cKO SUDEP case, suggesting respiratory phenotypes could be similar between all three SUDEP cases. Thus, the corticolimbic circuit is not only anatomically critical for seizures, ictal cardiorespiratory dysfunction, and premature mortality, but also appears to be sufficient to mediate a SUDEP event as well.

Both the corticolimbic- and brainstem-specific cKO mice lacked interictal cardiorespiratory dysfunction which was surprising given both the autonomic regulation provided by these circuits as well as the consistent capturing of these phenotypes in previous *Kcna1* deficiency models. One explanation for this difference could be that the forebrain and brainstem autonomic regions can compensate for one another in the case of neural dysfunction. For example, in the corticolimbic-specific cKO, the forebrain circuitry may be sending aberrant autonomic signals, but the brainstem has normal Kv1.1 levels and can neutralize or appropriately compensate for those signals to maintain normal cardiorespiratory function. In this case, it is possible that both the forebrain and brainstem regions are needed to elicit basal cardiorespiratory dysfunction. There is extensive research showing that both regions have direct contacts with one another and can

activate or influence efferent autonomic signals (Feinstein et al., 2022; Huang et al., 2019; Mueller et al., 2014; Nieuwenhuys et al., n.d.; Ritz et al., 2020; Schimitel et al., 2012; Yang et al., 2020) .

In addition to speculation that the forebrain and brainstem must coordinate to evoke cardiorespiratory dysfunction, it remains possible that another part of the brain may be responsible for influencing these phenotypes. One such region could be the cerebellum which was not targeted in the neuron-, corticolimbic-, or brainstem-specific cKO mice. The neuron-specific cKO mice display interictal cardiac dysfunction and the absence of apneas, but respiratory rate and variability were similar to WT levels. The cerebellum has more recently been described as having important roles in the brain respiratory control network and could be responsible for helping to maintain normal eupneic respiratory behavior (Krohn et al., 2023; Y. Liu et al., 2020). Aside from the cerebellum, there may be important corticolimbic or brainstem regions that were not impacted by the Cre-mediated deletion which could account for the basal cardiorespiratory differences. In corticolimbic-specific cKO mice, *Kcna1* should not be deleted in the central amygdala which can control cardiovascular function through connections with the NTS and RVLM in the brainstem, communicate with the periaqueductal gray and pre-Bötzinger to regulate ventilation, and regulate the surrounding amygdalar subnuclei (Feinstein et al., 2022; Keifer et al., 2015; Saha, 2005). Furthermore, in the brainstem-specific cKO mice, *Kcna1* is not deleted in the respiratory rhythm generators (Bötzinger and pre-Bötzinger) which could influence the basal respiratory phenotypes. More work needs to be done to determine which anatomical substrates regulate the interictal or basal cardiorespiratory functions.

The heart was also examined in Chapter 4 as a potentially important anatomical substrate for SUDEP. Previous research has shown that Kv1.1 is both present and functionally active in the atria and ventricles, but its presence in the sinoatrial node had never been explored.

Immunohistochemistry performed on isolated sinoatrial cardiomyocytes showed that Kv1.1 is present at low but detectable levels (Ch. 4, Fig. 1A). Unpublished work by a colleague shows that sinoatrial Kv1.1 makes significant contributions to action potential repolarization. This result is novel in that it shows that $I_{Kv1.1}$ is important to pacemaking in mice. With Kv1.1 present and functionally significant in the major regions of the heart, the next experiment sought to understand how heart-specific *Kcna1* deletion contributes to basal cardiac dysfunction. Interestingly, all measured ECG parameters including heart rate, heart rate variability measures, and cardiac conduction blocks were not significantly different in the cKO mice (Ch. 4, Fig. 2A-F). This work collectively showed that Kv1.1 is of significant importance in cardiomyocyte action potentials, but at the whole-animal level these deficits are masked. However, one explanation for this could be that repeated stress on the heart from seizures unmasks these deficits and renders the heart vulnerable, but this has not been proven yet.

5.2 Limitations

There were limitations to this set of studies, the first of which being the Cre lines used. *Emx1*-Cre is expressed in almost 90% of excitable cells in the neocortex, hippocampus, olfactory bulb, and select regions of the amygdala (Briata et al., 1996; Gorski et al., 2002; Kohwi et al scott., 2007). This means that select regions of the amygdala, as well as the inhibitory cells of the same regions, are not impacted. *Phox2b*-Cre is expressed in some, but not all, brainstem nuclei including the retrotrapezoid nucleus, locus coeruleus, dorsal nucleus of the vagus, nucleus ambiguus, and nucleus of the solitary tract (Dubreuil et al., 2008, 2009; Fu et al., 2019; M. M. Scott et al., 2011; Stornetta et al., 2006). The respiratory rhythm generators (bötzinger and pre-bötzinger) are not targeted by this Cre line, and there are certainly other nuclei that are not directly impacted. This is

to be expected as there is no perfect Cre line, but an important consideration for the interpretation of experimental results. Thus, the cKO mice may not show certain phenotypes because the region of the brain or specific cell type responsible is not being targeted by the Cre line.

There was also a limitation in generating the corticolimbic-specific cKO mice. After observing a non-Mendelian ratio of genotypes in mouse litters, a deep literature dive revealed that both *Emx1* and *Kcna1* are close together on the same chromosome. During the breeding process, when our Cre mice (*Emx1*-Cre$^{+/-}$; *Kcna1*$^{+/+}$) are crossed to heterozygous *Kcna1* mice (*Kcna1*$^{+/-}$), recombination between the two alleles was rare which implies that they reside nearby to one another on the chromosome. During the second generation cross used to make the cKO animals needed for experiments (Fig. 1), we normally need parental mice carrying both Cre^{+}, and *Kcna1*$^{-}$ alleles which we can then cross with a *Kcna1* floxed mouse to generate a cKO mouse (*Emx1*-Cre$^{+/-}$; *Kcna1*$^{fl/-}$). Instead, the crosses yield a disproportionately large number of *Kcna1*$^{fl/-}$and *Emx1*-Cre$^{+/-}$ mice and only rarely cKO animals. The combination of difficulty obtaining cKO mice and premature mortality in cKO made significantly hindered obtain adequate sample sizes for experiments. For example, for thoroughness we ideally wanted to verify Kv1.1 loss in the cells targeted by *Emx1*-Cre using immunohistochemistry but were unable to obtain enough animals for those experiments. Any cKO mice born during the study were almost immediately used for *in vivo* recordings which rendered them censored in the lifespan curve. Ultimately, these experiments took longer than expected, and the number of cKO mice used is smaller than what would normally have been desirable.

5.3 Future Directions

The studies in this dissertation prompt many future directions. Firstly, it would be extremely interesting to delete *Kcna1* in both the corticolimbic circuit and brainstem circuits simultaneously. These regions are the two main components of brain autonomic circuitry, and the results suggest that, while the corticolimbic circuit is sufficient for spontaneous seizures and premature mortality, both regions may need to synergize to result in basal cardiorespiratory dysfunction. Both regions have bidirectional influence and communication with each other which could mask potentially deleterious signals to the heart and lungs. In both the neuron-specific cKO and global KO mice, the corticolimbic circuit and brainstem are both simultaneously impacted which could be an explanation for their interictal dysfunction. Unfortunately, generating double cKO mice with *Kcna1* deletion targeted to both corticolimbic and brainstem regions would be incredibly breeding intensive and potentially not feasible as this cross has not been attempted.

The excitatory neurons in the corticolimbic circuit have proven sufficient for spontaneous seizures, ictal cardiorespiratory abnormalities, premature mortality, and even SUDEP, but this circuit comprises many different regions and nuclei. Another future direction would be to further dissect the corticolimbic circuit to identify which specific phenotypes are being driven by which anatomical substrates in the circuit. In a previous study, both the hippocampus and amygdala showed immediate early gene activation following seizures in the global KO mice, but region-specific *Kcna1* deletion could help in understanding the seizure origin and propagation pathways (Gautier & Glasscock, 2015). From a respiratory forward perspective, clinical literature suggests stimulation of the amygdala can promote apnea generation with an absence of air hunger; hippocampal stimulation can also generate apneas (Harmata et al., 2023; Lacuey et al., 2017; Rhone et al., 2020). Specifically deleting *Kcna1* in the amygdala or hippocampus could help reveal

which is responsible for apneas in this model, providing a more fine-tuned delineation of the neuronal subpopulations involved compared to what was possible with the Cre lines described in this work. These region-specific deletions could be done through stereotaxic lesioning, adenoviral or lentiviral injection, or a yet unknown strategy. Perhaps a lesion encompassing the entire amygdala could reproduce the lack of interictal apneas observed in global *Kcna1* deficiency mice. Ultimately, the more specific we can be in our anatomical understanding of SUDEP, the better we can design therapeutics and risk management strategies.

The heart needs Kv1.1 for proper cardiomyocyte repolarization in the atria, ventricles, and sinoatrial node however lacking Kv1.1 uniformly in the heart does not result in detectable whole-animal ECG abnormalities. Future studies of heart-specific cKO mice that examine the effects of stress on the heart from repeated seizures could reveal an increased risk of seizure-related death. Seizures are known to affect both heart rate and rhythm, and repeated stress of seizures can cause anatomical abnormalities including cardiac fibrosis (Nei, 2009). This fibrosis could further put the heart at risk of arrhythmia with the stress from subsequent seizures (Nei, 2009). Utilizing inducible seizure strategies such as flurothyl, kainic acid, or pentylenetetrazol to expose heart-specific cKO mice to repeated seizures would be a logical way to explore this question.

The ultimate goal of SUDEP research is to understand the critical neuronal subpopulations and pathomechanisms which underlie this phenomenon for targeted therapeutics, but we are simply not at this stage yet. However, the current body of SUDEP research is substantial and can be translated into big picture strategies which could potentially help attenuate risk. Given the primacy of respiratory failure in both the MORTEMUS study and animal models of SUDEP, strategies which closely monitor respiratory function could help alert patients or caregivers to vulnerable periods of time where enhanced vigilance could be lifesaving. Wearables which

monitor both respiratory rate and blood oxygen levels would be an excellent starting point. Should the respiratory rate or blood oxygen level fall below a healthy range, alerts could be sent to the patient and designated caregivers who can step in and help. This strategy relies on the brain still being alive however, and if the onset of terminal respiratory patterns coincides with irreversible loss of brain function, then intervention would be ineffective. Future research will help to fully elucidate SUDEP mechanisms and neuronal substrates which will more accurately guide therapeutics and intervention strategies.

5.4 Conclusions

The collective works in this dissertation show that specific autonomic circuits in the brain make significant contributions to SUDEP-related phenotypes. Furthermore, Kv1.1 is an important ion channel in the heart that makes contributions to intrinsic pacemaking. Understanding the anatomical substrates underlying SUDEP is invaluable because currently no clinical test exists that can accurately predict who is most at risk or how to prevent it. Clinical imaging studies have shown brain volume and connectivity differences in both limbic and brainstem regions, but which of these regions is functionally most important for SUDEP phenotypes and mechanisms is not known. Continuing to dissect these circuits to reveal the phenotypic contributions of their component nuclei will ultimately shed light on the critical brain regions that should be the focus of future diagnostic and therapeutic measures. These types of more detailed structure-function studies will aid further identification of the critical anatomical regions contributing to phenotypes in the *Kcna1* deficiency model. In the *Scn1a* mouse model of SUDEP, advances have been made in identifying the specific cellular populations driving seizures and SUDEP, enabling this model to serve as a preclinical platform for therapeutic discovery. Gaining additional knowledge about the

mechanistic underpinnings of *Kcna1* deficiency models will enable comparisons across SUDEP models to identify shared anatomical regions or phenotypes could contribute to SUDEP. Ultimately, the overarching goal of research into SUDEP is the identification of reliable biomarkers and therapeutics that can protect those with epilepsy from this devastating phenomenon.

REFERENCES

Agnati, L. F., & Fuxe, K. (2014). Extracellular-vesicle type of volume transmission and tunnelling-nanotube type of wiring transmission add a new dimension to brain neuro-glial networks. *Philosophical Transactions of the Royal Society B: Biological Sciences*, *369*(1652), 20130505. https://doi.org/10.1098/rstb.2013.0505

Aiba, I., & Noebels, J. L. (2015). Spreading depolarization in the brainstem mediates sudden cardiorespiratory arrest in mouse SUDEP models. *Science Translational Medicine*, *7*(282), 282ra46. https://doi.org/10.1126/scitranslmed.aaa4050

Aiba, I., Wehrens, X. H. T., & Noebels, J. L. (2016). Leaky RyR2 channels unleash a brainstem spreading depolarization mechanism of sudden cardiac death. *Proceedings of the National Academy of Sciences*, *113*(33). https://doi.org/10.1073/pnas.1605216113

Ajayi, I. E., McGovern, A. E., Driessen, A. K., Kerr, N. F., Mills, P. C., & Mazzone, S. B. (2018). Hippocampal modulation of cardiorespiratory function. *Respiratory Physiology & Neurobiology*, *252–253*, 18–27. https://doi.org/10.1016/j.resp.2018.03.004

Ákos Szabó, C., Knape, K. D., Michelle Leland, M., Feldman, J., McCoy, K. J. M., Hubbard, G. B., & Williams, J. T. (2009). Mortality in captive baboons with seizures: A new model for SUDEP? *Epilepsia*, *50*(8), 1995–1998. https://doi.org/10.1111/j.1528-1167.2009.02073.x

Al Kury, L. T., Chacar, S., Alefishat, E., Khraibi, A. A., & Nader, M. (2022). Structural and Electrical Remodeling of the Sinoatrial Node in Diabetes: New Dimensions and Perspectives. *Frontiers in Endocrinology*, *13*. https://doi.org/10.3389/fendo.2022.946313

Allen, L. A., Harper, R. M., Lhatoo, S., Lemieux, L., & Diehl, B. (2019). Neuroimaging of Sudden Unexpected Death in Epilepsy (SUDEP): Insights From Structural and Resting-State Functional MRI Studies. *Frontiers in Neurology*, *10*. https://doi.org/10.3389/fneur.2019.00185

Aloi, M. S., Thompson, S. J., Quartapella, N., & Noebels, J. L. (2022). Loss of functional System x-c uncouples aberrant postnatal neurogenesis from epileptogenesis in the hippocampus of Kcna1-KO mice. *Cell Reports*, *41*(8), 111696. https://doi.org/10.1016/j.celrep.2022.111696

Aronica, E., & Crino, P. B. (2011). Inflammation in epilepsy: Clinical observations. *Epilepsia*, *52*(s3), 26–32. https://doi.org/10.1111/j.1528-1167.2011.03033.x

Arrigo, A., Mormina, E., Calamuneri, A., Gaeta, M., Marino, S., Milardi, D., Anastasi, G. P., & Quartarone, A. (2017). Amygdalar and hippocampal connections with brainstem and spinal cord: A diffusion MRI study in human brain. *Neuroscience*, *343*, 346–354. https://doi.org/10.1016/j.neuroscience.2016.12.016

Auerbach, D. S., Jones, J., Clawson, B. C., Offord, J., Lenk, G. M., Ogiwara, I., Yamakawa, K., Meisler, M. H., Parent, J. M., & Isom, L. L. (2013). Altered Cardiac Electrophysiology and SUDEP in a Model of Dravet Syndrome. *PLoS ONE*, *8*(10), e77843. https://doi.org/10.1371/journal.pone.0077843

Azevedo, F. A. C., Carvalho, L. R. B., Grinberg, L. T., Farfel, J. M., Ferretti, R. E. L., Leite, R. E. P., Filho, W. J., Lent, R., & Herculano-Houzel, S. (2009). Equal numbers of neuronal and nonneuronal cells make the human brain an isometrically scaled-up primate brain. *Journal of Comparative Neurology*, *513*(5), 532–541. https://doi.org/10.1002/cne.21974

Bagnall, R. D., Crompton, D. E., & Semsarian, C. (2017). Genetic basis of sudden unexpected death in epilepsy. *Frontiers in Neurology*, *8*. https://doi.org/10.3389/fneur.2017.00348

Barros-Barbosa, A. R., Ferreirinha, F., Oliveira, Â., Mendes, M., Lobo, M. G., Santos, A., Rangel, R., Pelletier, J., Sévigny, J., Cordeiro, J. M., & Correia-de-Sá, P. (2016). Adenosine A2A receptor and ecto-5′-nucleotidase/CD73 are upregulated in hippocampal astrocytes of human patients with mesial temporal lobe epilepsy (MTLE). *Purinergic Signalling*, *12*(4), 719–734. https://doi.org/10.1007/s11302-016-9535-2

Bateman, L. M., Li, C., Lin, T., & Seyal, M. (2010). Serotonin reuptake inhibitors are associated with reduced severity of ictal hypoxemia in medically refractory partial epilepsy. *Epilepsia*, *51*(10), 2211–2214. https://doi.org/10.1111/j.1528-1167.2010.02594.x

Benarroch, E. E. (2020). Physiology and Pathophysiology of the Autonomic Nervous System. *CONTINUUM: Lifelong Learning in Neurology*, *26*(1), 12–24. https://doi.org/10.1212/CON.0000000000000817

Bezanilla, F. (2000). The Voltage Sensor in Voltage-Dependent Ion Channels. *Physiological Reviews*, *80*(2), 555–592. https://doi.org/10.1152/physrev.2000.80.2.555

Bhuyan, R., & Seal, A. (2015). Conformational Dynamics of Shaker-Type Kv1.1 Ion Channel in Open, Closed, and Two Mutated States. *J Membrane Biol*, *248*, 241–255. https://doi.org/10.1007/s00232-014-9764-7

Binder, D. K., Rajneesh, K. F., Lee, D. J., & Reynolds, E. H. (2011). Robert Bentley Todd's Contribution to Cell Theory and The Neuron Doctrine. *Journal of the History of the Neurosciences*, *20*(2), 123–134. https://doi.org/10.1080/0964704X.2010.496611

Blanchi, B., Kelly, L. M., Viemari, J.-C., Lafon, I., Burnet, H., Bévengut, M., Tillmanns, S., Daniel, L., Graf, T., Hilaire, G., & Sieweke, M. H. (2003). MafB deficiency causes defective respiratory rhythmogenesis and fatal central apnea at birth. *Nature Neuroscience*, *6*(10), 1091–1100. https://doi.org/10.1038/nn1129

Boison, D. (2011). *Methylxanthines, Seizures, and Excitotoxicity* (pp. 251–266). https://doi.org/10.1007/978-3-642-13443-2_9

Boison, D. (2012). Adenosine dysfunction in epilepsy. *Glia*, *60*(8), 1234–1243. https://doi.org/10.1002/glia.22285

Bracci, E., Vreugdenhil, M., Hack, S. P., & Jefferys, J. G. R. (2001). Dynamic Modulation of Excitation and Inhibition During Stimulation at Gamma and Beta Frequencies in the CA1

Hippocampal Region. *Journal of Neurophysiology*, *85*(6), 2412–2422. https://doi.org/10.1152/jn.2001.85.6.2412

Brahmajothi, M. V., Morales, M. J., Rasmusson, R. L., Campbell, D. L., & Strauss, H. C. (1997). Heterogeneity in K^+ Channel Transcript Expression Detected in Isolated Ferret Cardiac Myocytes. *Pacing and Clinical Electrophysiology*, *20*(2), 388–396. https://doi.org/10.1111/j.1540-8159.1997.tb06198.x

Briata, P., Blas, E. Di, Gulisano, M., Mallamaci, A., Iannone, R., Boncinelli, E., & Corte, G. (1996). EMXl homeoprotein is expressed in cell nuclei of the developing cortex and in the axons of the olfactory sensory neurons cerebral. *Mechanisms of Development*, *57*, 169–180. https://doi.org/10.1016/0925-4773(96)00544-8

Browne, D. L., Gancher, S. T., Nutt, J. G., Brunt, E. R. P., Smith, E. A., Kramer, P., & Litt, M. (1994). Episodic ataxia/myokymia syndrome is associated with point mutations in the human potassium channel gene, KCNA1. *Nature Genetics*, *8*, 136–140. https://doi.org/doi.org/10.1038/ng1094-136

Bunton-Stasyshyn, R. K. A., Wagnon, J. L., Wengert, E. R., Barker, B. S., Faulkner, A., Wagley, P. K., Bhatia, K., Jones, J. M., Maniaci, M. R., Parent, J. M., Goodkin, H. P., Patel, M. K., & Meisler, M. H. (2019). Prominent role of forebrain excitatory neurons in SCN8A encephalopathy. *Brain*, *142*(2), 362–375. https://doi.org/10.1093/brain/awy324

Canas, P. M., Porciúncula, L. O., Simões, A. P., Augusto, E., Silva, H. B., Machado, N. J., Gonçalves, N., Alfaro, T. M., Gonçalves, F. Q., Araújo, I. M., Real, J. I., Coelho, J. E., Andrade, G. M., Almeida, R. D., Chen, J.-F., Köfalvi, A., Agostinho, P., & Cunha, R. A. (2018). Neuronal Adenosine A2A Receptors Are Critical Mediators of Neurodegeneration Triggered by Convulsions. *Eneuro*, *5*(6), ENEURO.0385-18.2018. https://doi.org/10.1523/ENEURO.0385-18.2018

Catterall, W. A. (2012). *Sodium Channel Mutations and Epilepsy* (4th ed.). National Center for Biotechnology Information.

Centers for Disease Control and Prevention. (2022). *CDC Activities Related to Recommendations of the 2012 IOM Report, Epilepsy Across the Spectrum, 2012–2022: Final Progress Report*.

Chen, H., Von Hehn, C., Kaczmarek, L. K., Ment, L. R., Pober, B. R., & Hisama, F. M. (2007). Functional analysis of a novel potassium channel (KCNA1) mutation in hereditary myokymia. *Neurogenetics*, *8*, 131–135. https://doi.org/10.1007/s10048-006-0071-z

Choi, K.-D., & Choi, J.-H. (2016). Episodic Ataxias: Clinical and Genetic Features. *J Mov Disord*, *9*(3), 129–135. https://doi.org/10.14802/jmd.16028/J

Chou, S.-M., Li, K.-X., Huang, M.-Y., Chen, C., Lin King, Y.-H., Li, G. G., Zhou, W., Teo, C. F., Jan, Y. N., Jan, L. Y., & Yang, S.-B. (2021). Kv1.1 channels regulate early postnatal neurogenesis in mouse hippocampus via the TrkB signaling pathway. *ELife*, *10*. https://doi.org/10.7554/eLife.58779

Chun, K., Ma, S.-C., Oh, H., Rho, J. M., & Kim, D. Y. (2018). Ketogenic diet-induced extension of longevity in epileptic Kcna1 -null mice is influenced by gender and age at treatment onset. *Epilepsy Research*, *140*, 53–55. https://doi.org/10.1016/j.eplepsyres.2017.11.005

Clemens, B., Emri, M., Csaba Aranyi, S., Fekete, I., & Fekete, K. (2021). Resting-state EEG theta activity reflects degree of genetic determination of the major epilepsy syndromes. *Clinical Neurophysiology*, *132*(9), 2232–2239. https://doi.org/10.1016/j.clinph.2021.06.012

Clemens, B., Emri, M., Fekete, I., & Fekete, K. (2023). Epileptic diathesis: An EEG-LORETA study. *Clinical Neurophysiology*, *145*, 54–61. https://doi.org/10.1016/j.clinph.2022.11.004

Coleman, S. K., Newcombe, J., Pryke, J., & Oliver Dolly, J. (1999). Subunit Composition of Kv1 Channels in Human CNS. *Journal of Neurochemistry*, *73*(2), 849–858. https://doi.org/10.1046/j.1471-4159.1999.0730849.x

Corcoran, A. E., & Milsom, W. K. (2009). Maturational changes in pontine and medullary alpha-adrenoceptor influences on respiratory rhythm generation in neonatal rats. *Respiratory Physiology & Neurobiology*, *165*(2–3), 195–201. https://doi.org/10.1016/j.resp.2008.11.009

D'Adamo, M. C., Hasan, S., Guglielmi, L., Servettini, I., Cenciarini, M., Catacuzzeno, L., & Franciolini, F. (2015). New insights into the pathogenesis and therapeutics of episodic ataxia type 1. *Frontiers in Cellular Neuroscience*, *9*. https://doi.org/10.3389/fncel.2015.00317

Dailey, J. W., & Naritoku, D. K. (1996). Antidepressants and seizures: Clinical anecdotes overshadow neuroscience. *Biochemical Pharmacology*, *52*(9), 1323–1329. https://doi.org/10.1016/S0006-2952(96)00509-6

Deboer, T., Ross, R. J., Morrison, A. R., Sanford, L. D., Ross, R. J., Morrison, A. R., & Sanford, L. D. (1999). Electrical Stimulation of the Amygdala Increases the Amplitude of Elicited Ponto-geniculo-occipital Waves. *Physiology & Behavior*, *66*(1), 119–124.

DeGiorgio, C. M., Curtis, A., Hertling, D., & Moseley, B. D. (2018). Sudden unexpected death in epilepsy: Risk factors, biomarkers, and prevention. *Acta Neurologica Scandinavica*, ane.13049. https://doi.org/10.1111/ane.13049

Deng, H., Xiu, X., & Song, Z. (2014). The Molecular Biology of Genetic-Based Epilepsies. *Molecular Neurobiology*, *49*(1), 352–367. https://doi.org/10.1007/s12035-013-8523-6

Deodhar, M., Matthews, S. A., Thomas, B., Adamian, L., Mattes, S., Wells, T., Zieba, B., Simeone, K. A., & Simeone, T. A. (2021). Pharmacoresponsiveness of spontaneous recurrent seizures and the comorbid sleep disorder of epileptic Kcna1-null mice. *European Journal of Pharmacology*, *913*, 174656. https://doi.org/10.1016/j.ejphar.2021.174656

Devinsky, O. (2011). Sudden, Unexpected Death in Epilepsy. *New England Journal of Medicine*, *365*(19), 1801–1811. https://doi.org/10.1056/NEJMra1010481

Devinsky, O., Marsh, E., Friedman, D., Thiele, E., Laux, L., Sullivan, J., Miller, I., Flamini, R., Wilfong, A., Filloux, F., Wong, M., Tilton, N., Bruno, P., Bluvstein, J., Hedlund, J., Kamens, R., Maclean, J., Nangia, S., Singhal, N. S., … Cilio, M. R. (2016). Cannabidiol in patients with treatment-resistant epilepsy: an open-label interventional trial. *The Lancet Neurology*, *15*(3), 270–278. https://doi.org/10.1016/S1474-4422(15)00379-8

Dhaibar, H. A., Hamilton, K. A., & Glasscock, E. (2021). Kv1.1 subunits localize to cardiorespiratory brain networks in mice where their absence induces astrogliosis and microgliosis. *Molecular and Cellular Neuroscience*, *113*. https://doi.org/10.1016/j.mcn.2021.103615

Dhaibar, H., Gautier, N. M., Chernyshev, O. Y., Dominic, P., & Glasscock, E. (2019). Cardiorespiratory profiling reveals primary breathing dysfunction in Kcna1-null mice: Implications for sudden unexpected death in epilepsy. *Neurobiology of Disease*, *127*, 502–511. https://doi.org/10.1016/j.nbd.2019.04.006

Dias, N., & Stain, C. A. (2002). Antisense Oligonucleotides: Basic Concepts and Mechanisms. *Molecular Cancer Therapeutics*, *1*, 347–355.

Dixit, R., Ross, J. L., Goldman, Y. E., & Holzbaur, E. L. F. (2008). Differential regulation of dynein and kinesin motor proteins by tau. *Science*, *319*(5866), 1086–1089. https://doi.org/10.1126/science.1152993

Dixon, J. E., & McKinnon, D. (1994). Quantitative analysis of potassium channel mRNA expression in atrial and ventricular muscle of rats. *Circulation Research*, *75*(2), 252–260. https://doi.org/10.1161/01.RES.75.2.252

Dlouhy, B. J., Gehlbach, B. K., Kreple, C. J., Kawasaki, H., Oya, X., Buzza, C., Granner, M. A., Welsh, M. J., Howard, M. A., Wemmie, J. A., George, X., & Richerson, B. (2015). Breathing Inhibited When Seizures Spread to the Amygdala and upon Amygdala Stimulation. *Neurobiology of Disease*, *35*(28), 10281–10289. https://doi.org/10.1523/JNEUROSCI.0888-15.2015

Dogra, D., Meza-Santoscoy, P. L., Gavrilovici, C., Rehak, R., de la Hoz, C. L. R., Ibhazehiebo, K., Rho, J. M., & Kurrasch, D. M. (2023). *kcna1a* mutant zebrafish model episodic ataxia type 1 (EA1) with epilepsy and show response to first-line therapy carbamazepine. *Epilepsia*, *64*(8), 2186–2199. https://doi.org/10.1111/epi.17659

Dosumu-Johnson, R. T., Cocoran, A. E., Chang, Y., Nattie, E., & Dymecki, S. M. (2018). Acute perturbation of Pet1-neuron activity in neonatal mice impairs cardiorespiratory homeostatic recovery. *ELife*, *7*. https://doi.org/10.7554/eLife.37857

Dubreuil, V., Barhanin, J., Goridis, C., & Brunet, J.-F. (2009). Breathing with Phox2b. *Phil. Trans. R. Soc. B*, *364*, 2477–2483. https://doi.org/10.1098/rstb.2009.0085

Dubreuil, V., Ramanantsoa, N., Trochet, D., Vaubourg, V., Amiel, J., Gallego, J., Brunet, J.-F., & Goridis, C. (2008). A human mutation in Phox2b causes lack of CO2 chemosensitivity, fatal central apnea, and specific loss of parafacial neurons. *PNAS*, *105*(3), 1067–1072. https://doi.org/10.1073/pnas.0709115105

During, M. J., & Spencer, D. D. (1992). Adenosine: A potential mediator of seizure arrest and postictal refractoriness. *Annals of Neurology*, *32*(5), 618–624. https://doi.org/10.1002/ana.410320504

Epilepsy Foundation of America. (n.d.). *The Legal Rights of Persons with Epilepsy. An Overview of Legal Issues and Laws Affecting Persons with Epilepsy, 6th edition* (6th ed.). Epilepsy Foundation of America.

Espinosa, P. S., Lee, J. W., Tedrow, U. B., Bromfield, E. B., & Dworetzky, B. A. (2009). Sudden Unexpected Near Death In Epilepsy: Malignant Arrhythmia From A Partial Seizure. *Neurology*, *72*(19), 1702–1703. https://doi.org/10.1212/WNL.0b013e3181a55f90

Feigin, V. L., Vos, T., Alahdab, F., Amit, A. M. L., Bärnighausen, T. W., Beghi, E., Beheshti, M., Chavan, P. P., Criqui, M. H., Desai, R., Dhamminda Dharmaratne, S., Dorsey, E. R., Wilder Eagan, A., Elgendy, I. Y., Filip, I., Giampaoli, S., Giussani, G., Hafezi-Nejad, N., Hole, M. K., … Murray, C. J. L. (2021). Burden of Neurological Disorders Across the US From 1990-2017. *JAMA Neurology*, *78*(2), 165. https://doi.org/10.1001/jamaneurol.2020.4152

Feinstein, J. S., Gould, D., & Khalsa, S. S. (2022). Amygdala-driven apnea and the chemoreceptive origin of anxiety. *Biological Psychology*, *170*, 108305. https://doi.org/10.1016/j.biopsycho.2022.108305

Feng, H.-J., & Faingold, C. L. (2017). Abnormalities of serotonergic neurotransmission in animal models of SUDEP. *Epilepsy & Behavior*, *71*, 174–180. https://doi.org/10.1016/j.yebeh.2015.06.008

Fenoglio-Simeone, K. A., Wilke, J. C., Milligan, H. L., Allen, C. N., Rho, J. M., & Maganti, R. K. (2009). Ketogenic diet treatment abolishes seizure periodicity and improves diurnal rhythmicity in epileptic Kcna1-null mice. *Epilepsia*, *50*(9), 2027–2034. https://doi.org/10.1111/j.1528-1167.2009.02163.x

Ferland, R. (2017). The Repeated Flurothyl Seizure Model in Mice. *BIO-PROTOCOL*, *7*(11). https://doi.org/10.21769/bioprotoc.2309

Fisher, R. S., Acevedo, C., Arzimanoglou, A., Bogacz, A., Cross, J. H., Elger, C. E., Engel, J., Forsgren, L., French, J. A., Glynn, M., Hesdorffer, D. C., Lee, B. I., Mathern, G. W., Moshé, S. L., Perucca, E., Scheffer, I. E., Tomson, T., Watanabe, M., & Wiebe, S. (2014). ILAE Official Report: A practical clinical definition of epilepsy. *Epilepsia*, *55*(4), 475–482. https://doi.org/10.1111/epi.12550

Fletcher, C. F., Lutz, C. M., Hawkes, R., Frankel, W. N., Copeland, N. G., & Jenkins, N. A. (1996). Absence Epilepsy in Tottering Mutant Mice Is Associated with Calcium Channel Defects. *Cell*, *87*, 607–617.

Foley, J., Burnham, V., Tedoldi, M., Danial, N. N., & Yellen, G. (2018). BAD knockout provides metabolic seizure resistance in a genetic model of epilepsy with sudden unexplained death in epilepsy. *Epilepsia*, *59*(1), e1–e4. https://doi.org/10.1111/epi.13960

Fu, X. C., Shi, L., Wei, Z., Yu, H., Hao, Y., Tian, Y., Liu, Y., Zhang, Y., Zhang, X., Yuan, F., & Wang, X. S. (2019). Activation of Phox2b-Expressing Neurons in the Nucleus Tractus Solitarii Drives Breathing in Mice. *The Journal of Neuroscience*, *39*(15), 2837–2846. https://doi.org/10.1523/JNEUROSCI.2048-18.2018

Gallego, J., & Dauger, S. (2008). PHOX2B mutations and ventilatory control. *Respiratory Physiology & Neurobiology*, *164*(1–2), 49–54. https://doi.org/10.1016/j.resp.2008.07.003

García-Medina, N. E., & Miranda, M. I. (2013). Nucleus of the solitary tract chemical stimulation induces extracellular norepinephrine release in the lateral and basolateral amygdala. *Brain Stimulation*, *6*(2), 198–201. https://doi.org/10.1016/j.brs.2012.03.020

Gasbarri, A., Packard, M. G., Campana, E., & Pacitti, C. (1994). Anterograde and retrograde tracing of projections from the ventral tegmental area to the hippocampal formation in the rat. *Brain Research Bulletin*, *33*(4), 445–452. https://doi.org/10.1016/0361-9230(94)90288-7

Gautier, N. M., & Glasscock, E. (2015). Spontaneous seizures in Kcna 1-null mice lacking voltage-gated Kvl.1 channels activate Fos expression in select limbic circuits. *J Neurochem*, *135*(1), 157–164. https://doi.org/10.1111/jnc.13206

Gilliam, F. G., Hecimovic, H., & Gentry, M. S. (2021). Serotonergic therapy in epilepsy. *Current Opinion in Neurology*, *34*(2), 206–212. https://doi.org/10.1097/WCO.0000000000000901

Glasscock, E. (2019). *Kv1.1 channel subunits in the control of neurocardiac function*. https://doi.org/10.1080/19336950.2019.1635864

Glasscock, E., Qian, J., Yoo, J. W., & Noebels, J. L. (2007). Masking epilepsy by combining two epilepsy genes. *Nature Neuroscience*, *10*(12), 1554–1558. https://doi.org/10.1038/nn1999

Glasscock, E., Voigt, N., Mccauley, M. D., Sun, Q., Li, N., Chiang, D. Y., Zhou, X.-B., Molina, C. E., Thomas, D., Schmidt, C., Skapura, D. G., Noebels, J. L., Dobrev, D., & Wehrens, X. H. T. (2015). Expression and function of Kv1.1 potassium channels in human atria from patients with atrial fibrillation. *Basic Res Cardiol*, *110*(47). https://doi.org/10.1007/s00395-015-0505-6

Glasscock, E., Yoo, J. W., Chen, T. T., Klassen, T. L., & Noebels, J. L. (2010). Kv1.1 potassium channel deficiency reveals brain-driven cardiac dysfunction as a candidate mechanism for sudden unexplained death in epilepsy. *Journal of Neuroscience*, *30*(15), 5167–5175. https://doi.org/10.1523/JNEUROSCI.5591-09.2010

Goridis, C., Dubreuil, V., Thoby-Brisson, M., Fortin, G., & Brunet, J.-F. (2010). Phox2b, congenital central hypoventilation syndrome and the control of respiration. *Seminars in Cell & Developmental Biology*, *21*(8), 814–822. https://doi.org/10.1016/j.semcdb.2010.07.006

Gorski, J. A., Talley, T., Qiu, M., Puelles, L., Rubenstein, J. L. R., & Jones, K. R. (2002). Cortical excitatory neurons and glia, but not GABAergic neurons, are produced in the Emx1-expressing lineage. *The Journal of Neuroscience*, *22*(15), 6309–6314. https://doi.org/10.1523/JNEUROSCI.22-15-06309.2002

Graves, T. D., Cha, Y.-H., Hahn, A. F., Barohn, R., Salajegheh, M. K., Griggs, R. C., Bundy, B. N., Jen, J. C., Baloh, R. W., & Hanna, M. G. (2014). Episodic ataxia type 1: clinical characterization, quality of life and genotype-phenotype correlation. *Brain*, *137*, 1009–1018. https://doi.org/10.1093/brain/awu012

Guan, D., Lee, J. C. F., Tkatch, T., Surmeier, D. J., Armstrong, W. E., & Foehring, R. C. (2006). Expression and biophysical properties of Kv1 channels in supragranular neocortical pyramidal neurones. *The Journal of Physiology*, *571*(2), 371–389. https://doi.org/10.1113/jphysiol.2005.097006

Guyenet, P. G., Stornetta, R. L., Souza, G. M. P. R., Abbott, S. B. G., Shi, Y., & Bayliss, D. A. (2019). The Retrotrapezoid Nucleus: Central Chemoreceptor and Regulator of Breathing Automaticity. *Trends in Neurosciences*, *42*(11), 807–824. https://doi.org/10.1016/j.tins.2019.09.002

Harden, C., Tomson, T., Gloss, D., Buchhalter, J., Cross, J. H., Donner, E., French, J. A., Gil-Nagel, A., Hesdorffer, D. C., Smithson, W. H., Spitz, M. C., Walczak, T. S., Sander, J. W., & Ryvlin, P. (2016). Practice Guideline Summary: Sudden Unexpected Death in Epilepsy Incidence Rates and Risk Factors: Report of the Guideline Development, Dissemination, and Implementation Subcommittee of the American Academy of Neurology and the American Epilepsy Society. *Epilepsy Currents*, *17*(3), 180–187. https://doi.org/10.5698/1535-7511.17.3.180

Harmata, G. I. S., Rhone, A. E., Kovach, C. K., Kumar, S., Mowla, M. R., Sainju, R. K., Nagahama, Y., Oya, H., Gehlbach, B. K., Ciliberto, M. A., Mueller, R. N., Kawasaki, H., Pattinson, K. T. S., Simonyan, K., Davenport, P. W., Howard, M. A., Steinschneider, M., Chan, A. C., Richerson, G. B., … Dlouhy, B. J. (2023). Failure to breathe persists without air hunger or alarm following amygdala seizures. *JCI Insight*, *8*(22). https://doi.org/10.1172/jci.insight.172423

Harper, R. M., Kumar, R., Macey, P. M., Harper, R. K., & Ogren, J. A. (2015). Impaired neural structure and function contributing to autonomic symptoms in congenital central hypoventilation syndrome. *Frontiers in Neuroscience*, *9*(415). https://doi.org/10.3389/fnins.2015.00415

Harrell, M. D., Harbi, S., Hoffman, J. F., Zavadil, J., & Coetzee, W. A. (2007). Large-scale analysis of ion channel gene expression in the mouse heart during perinatal development. *Physiological Genomics*, *28*(3), 273–283. https://doi.org/10.1152/physiolgenomics.00163.2006

Healy, B., & Peck, J. (1997). Bradycardia induced from stimulation of the left versus right central nucleus of the amygdala. *Epilepsy Research*, *28*(2), 101–104. https://doi.org/10.1016/S0920-1211(97)00035-1

Helmuth, L. (2001). Glia Tell Neurons to Build Synapses. *Science*, *291*(5504), 569–570. https://doi.org/10.1126/science.291.5504.569A

Herson, P. S., Virk, M., Rustay, N. R., Bond, C. T., Crabbe, J. C., Adelman, J. P., & Maylie, J. (2003). A mouse model of episodic ataxia type-1. *Nature Neuroscience*, *6*(4), 378–383. https://doi.org/10.1038/nn1025

Hill, S. F., Ziobro, J. M., Jafar-Nejad, P., Rigo, F., & Meisler, M. H. (2022). Genetic interaction between *Scn8a* and potassium channel genes *Kcna1* and *Kcnq2*. *Epilepsia*, *63*(10). https://doi.org/10.1111/epi.17374

Hirtz, D., Thurman, D. J., Gwinn-Hardy, K., Mohamed, M., Chaudhuri, A. R., & Zalutsky, R. (2007). How common are the "common" neurologic disorders? *Neurology*, *68*(5), 326–337. https://doi.org/10.1212/01.wnl.0000252807.38124.a3

Holt, M. K., & Rinaman, L. (2022). The role of nucleus of the solitary tract glucagon-like peptide-1 and prolactin-releasing peptide neurons in stress: anatomy, physiology and

cellular interactions. *British Journal of Pharmacology*, *179*(4), 642–658. https://doi.org/10.1111/bph.15576

Holth, J. K., Bomben, V. C., Graham Reed, J., Inoue, T., Younkin, L., Younkin, S. G., Pautler, R. G., Botas, J., & Noebels, J. L. (2013). Tau loss attenuates neuronal network hyperexcitability in mouse and drosophila genetic models of epilepsy. *Journal of Neuroscience*, *33*(4), 1651–1659. https://doi.org/10.1523/JNEUROSCI.3191-12.2013

Hoshi, T., Zagotta, W., & Aldrich, R. (1990). Biophysical and molecular mechanisms of Shaker potassium channel inactivation. *Science*, *250*, 533–538. https://doi.org/https://doi.org/10.1126/science.2122519

Huang, J., Gadotti, V. M., Chen, L., Souza, I. A., Huang, S., Wang, D., Ramakrishnan, C., Deisseroth, K., Zhang, Z., & Zamponi, G. W. (2019). A neuronal circuit for activating descending modulation of neuropathic pain. *Nature Neuroscience*, *22*(10), 1659–1668. https://doi.org/10.1038/s41593-019-0481-5

Imbrici, P., Altamura, C., Gualandi, F., Mangiatordi, G. F., Neri, M., De Maria, G., Ferlini, A., Padovani, A., D'Adamo, M. C., Nicolotti, O., Pessia, M., Conte, D., Filosto, M., & Desaphy, J. F. (2017). A novel KCNA1 mutation in a patient with paroxysmal ataxia, myokymia, painful contractures and metabolic dysfunctions. *Molecular and Cellular Neuroscience*, *83*, 6–12. https://doi.org/10.1016/j.mcn.2017.06.006

Indumathy, J., Pruitt, A., Gautier, N. M., Crane, K., & Glasscock, E. (2021). Kv1.1 deficiency alters repetitive and social behaviors in mice and rescues autistic-like behaviors due to *Scn2a* haploinsufficiency. *Brain and Behavior*. https://doi.org/10.1002/brb3.2041

Inman, C. S., Bijanki, K. R., Bass, D. I., Gross, R. E., Hamann, S., & Willie, J. T. (2020). Human amygdala stimulation effects on emotion physiology and emotional experience. *Neuropsychologia*, *145*, 106722. https://doi.org/10.1016/j.neuropsychologia.2018.03.019

Irizarry, R., Sukato, D., Kollmar, R., Schild, S., Silverman, J., Sundaram, K., Stephenson, S., & Stewart, M. (2020). Seizures induce obstructive apnea in DBA/2J audiogenic seizure-prone mice: Lifesaving impact of tracheal implants. *Epilepsia*, *61*(2). https://doi.org/10.1111/epi.16431

Ishida, S., Sakamoto, Y., Nishio, T., Baulac, S., Kuwamura, M., Ohno, Y., Takizawa, A., Kaneko, S., Serikawa, T., & Mashimo, T. (2012). Kcna1-mutant rats dominantly display myokymia, neuromyotonia and spontaneous epileptic seizures. *Brain Research*, *1435*, 154–166. https://doi.org/10.1016/j.brainres.2011.11.023

Iyer, S. H., Aggarwal, A., Warren, T. J., Hallgren, J., Abel, P. W., Simeone, T. A., & Simeone, K. A. (2020). Progressive cardiorespiratory dysfunction in Kv1.1 knockout mice may provide temporal biomarkers of pending sudden unexpected death in epilepsy (SUDEP): The contribution of orexin. *Epilepsia*, *61*(3), 572–588. https://doi.org/10.1111/epi.16434

Jan, L. Y., & Jan, Y. N. (2012). Voltage-gated potassium channels and the diversity of electrical signalling. *The Journal of Physiology*, *590*, 2591–2599. https://doi.org/10.1113/jphysiol.2011.224212

Jane, D. E., Lodge, D., & Collingridge, G. L. (2009). Kainate receptors: Pharmacology, function and therapeutic potential. *Neuropharmacology*, *56*(1), 90–113. https://doi.org/10.1016/j.neuropharm.2008.08.023

Jobe, P. C., & Browning, R. A. (2005). The serotonergic and noradrenergic effects of antidepressant drugs are anticonvulsant, not proconvulsant. *Epilepsy & Behavior*, *7*(4), 602–619. https://doi.org/10.1016/j.yebeh.2005.07.014

Johannessen Landmark, C., Henning, O., & Johannessen, S. I. (2016). Proconvulsant effects of antidepressants — What is the current evidence? *Epilepsy & Behavior*, *61*, 287–291. https://doi.org/10.1016/j.yebeh.2016.01.029

Kaculini, C. M., Tate-Looney, A. J., & Seifi, A. (2021). The History of Epilepsy: From Ancient Mystery to Modern Misconception. *Cureus*. https://doi.org/10.7759/cureus.13953

Kadam, S. D., D'Ambrosio, R., Duveau, V., Roucard, C., Garcia-Cairasco, N., Ikeda, A., de Curtis, M., Galanopoulou, A. S., & Kelly, K. M. (2017). Methodological standards and interpretation of video-electroencephalography in adult control rodents. A TASK 1- WG 1 report of the AES/ILAE Translational Task Force of the ILAE. *Epilepsia*, *58*(S4), 10–27. https://doi.org/10.1111/epi.13903

Kadiyala, S. B., & Ferland, J. (2017). Dissociation of spontaneous seizures and brainstem seizure thresholds in mice exposed to eight flurothyl-induced generalized seizures. *Epilepsia Open*, *2*(1), 48–58. https://doi.org/10.1002/epi4.12031

Kahn, I., & Shohamy, D. (2013). Intrinsic connectivity between the hippocampus, nucleus accumbens, and ventral tegmental area in humans. *Hippocampus*, *23*(3), 187–192. https://doi.org/10.1002/hipo.22077

Kalume, F., Westenbroek, R. E., Cheah, C. S., Yu, F. H., Oakley, J. C., Scheuer, T., & Catterall, W. A. (2013). Sudden unexpected death in a mouse model of Dravet syndrome. *Journal of Clinical Investigation*, *123*(4), 1798–1808. https://doi.org/10.1172/JCI66220

Kanner, A. M. (2016). Psychiatric comorbidities in epilepsy: Should they be considered in the classification of epileptic disorders? *Epilepsy & Behavior*, *64*, 306–308. https://doi.org/10.1016/j.yebeh.2016.06.040

Kao, H., Yao, Y., Yang, T., Ziobro, J., Zylinski, M., Mir, M. Y., Hu, S., Cao, R., Borna, N. N., Banerjee, R., Parent, J. M., Wang, S., Leventhal, D. K., Li, P., & Wang, Y. (2023). Sudden Unexpected Death in Epilepsy and Respiratory Defects in a Mouse Model of <scp>DEPDC5</scp> -Related Epilepsy. *Annals of Neurology*, *94*(5), 812–824. https://doi.org/10.1002/ana.26773

Kearney, J. A. (2012). Advances in epilepsy genetics and genomics. *Epilepsy Currents*, *12*(4), 143–146.

Keifer, O. P., Hurt, R. C., Ressler, K. J., & Marvar, P. J. (2015). The Physiology of Fear: Reconceptualizing the Role of the Central Amygdala in Fear Learning. *Physiology*, *30*(5), 389–401. https://doi.org/10.1152/physiol.00058.2014

Kim, J., Hu, C., Moufawad El Achkar, C., Black, L. E., Douville, J., Larson, A., Pendergast, M. K., Goldkind, S. F., Lee, E. A., Kuniholm, A., Soucy, A., Vaze, J., Belur, N. R., Fredriksen,

K., Stojkovska, I., Tsytsykova, A., Armant, M., DiDonato, R. L., Choi, J., … Yu, T. W. (2019). Patient-Customized Oligonucleotide Therapy for a Rare Genetic Disease. *New England Journal of Medicine*, *381*(17), 1644–1652. https://doi.org/10.1056/NEJMoa1813279

Kim, Y., Bravo, E., Thirnbeck, C. K., Smith-Mellecker, L. A., Kim, S. H., Gehlbach, B. K., Laux, L. C., Zhou, X., Nordli, D. R., & Richerson, G. B. (2018). Severe peri-ictal respiratory dysfunction is common in Dravet syndrome. *Journal of Clinical Investigation*, *128*(3), 1141–1153. https://doi.org/10.1172/JCI94999

Kline, D. D., Buniel, M. C. F., Glazebrook, P., Peng, Y.-J., Ramirez-Navarro, A., Prabhakar, N. R., & Kunze, D. L. (2005). Kv1.1 Deletion Augments the Afferent Hypoxic Chemosensory Pathway and Respiration. *The Journal of Neuroscience*, *25*(13), 3389–3399. https://doi.org/10.1523/JNEUROSCI.4556-04.2005

Kohwi, M., Petryniak, M. A., Long, J. E., Ekker, M., Obata, K., Yanagawa, Y., Rubenstein, J. L. R., & Alvarez-Buylla, A. (2007). A subpopulation of olfactory bulb GABAergic interneurons is derived from Emx1- and Dlx5/6-expressing progenitors. *Journal of Neuroscience*, *27*(26), 6878–6891. https://doi.org/10.1523/JNEUROSCI.0254-07.2007

Kondziella, D., & Asztely, F. (2009). Don't be afraid to treat depression in patients with epilepsy! *Acta Neurologica Scandinavica*, *119*(2), 75–80. https://doi.org/10.1111/j.1600-0404.2008.01088.x

Krohn, F., Novello, M., van der Giessen, R. S., De Zeeuw, C. I., Pel, J. J., & Bosman, L. W. (2023). The integrated brain network that controls respiration. *ELife*, *12*. https://doi.org/10.7554/eLife.83654

Labat, R. (1951). *Traité akkadien de diagnostics et pronostics médicaux*. Academie Internationale d'Histoire des Sciences.

Lacuey, N., Martins, R., Vilella, L., Hampson, J. P., Rani, M. R. S., Strohl, K., Zaremba, A., Hampson, J. S., Sainju, R. K., Friedman, D., Nei, M., Scott, C., Gehlbach, B. K., Hupp, N. J., Schuele, S., Ogren, J., Harper, R. M., Allen, L., Diehl, B., … Lhatoo, S. (2019). The association of serotonin reuptake inhibitors and benzodiazepines with ictal central apnea. *Epilepsy & Behavior*, *98*, 73–79. https://doi.org/10.1016/j.yebeh.2019.06.029

Lacuey, N., Vilella, L., Hampson, J. P., Sahadevan, J., & Lhatoo, S. D. (2018). Ictal laryngospasm monitored by video-EEG and polygraphy: a potential SUDEP mechanism. *Epileptic Disorders*, *20*(2), 146–150. https://doi.org/10.1684/epd.2018.0964

Lacuey, N., Zonjy, B., Londono, L., & Lhatoo, S. D. (2017). Amygdala and hippocampus are symptomatogenic zones for central apneic seizures. *Neurology*, *88*(7), 701–705. https://doi.org/10.1212/WNL.0000000000003613

Lado, F. A., & Moshé, S. L. (2008). How do seizures stop? *Epilepsia*, *49*(10), 1651–1664. https://doi.org/10.1111/j.1528-1167.2008.01669.x

Lai, M. H., Wu, Y., Gao, Z., Anderson, M. E., Dalziel, J. E., & Meredith, A. L. (2014). BK channels regulate sinoatrial node firing rate and cardiac pacing in vivo. *American Journal of*

Physiology-Heart and Circulatory Physiology, *307*(9), H1327–H1338. https://doi.org/10.1152/ajpheart.00354.2014

Lazarevic, V., Pothula, S., Andres-Alonso, M., & Fejtova, A. (2013). Molecular mechanisms driving homeostatic plasticity of neurotransmitter release. *Frontiers in Cellular Neuroscience*, *7*. https://doi.org/10.3389/fncel.2013.00244

Leonard, A. S., Hyder, S. N., Kolls, B. J., Arehart, E., W. Ng, K. C., Veerapandiyan, A., & Mikati, M. A. (2013). Seizure predisposition after perinatal hypoxia: Effects of subsequent age and of an epilepsy predisposing gene mutation. *Epilepsia*, *54*(10), 1789–1800. https://doi.org/10.1111/epi.12347

Leoni, A.-L., Marionneau, C., Demolombe, S., Bouter, S. Le, Mangoni, M. E., Escande, D., & Charpentier, F. (2006a). Chronic heart rate reduction remodels ion channel transcripts in the mouse sinoatrial node but not in the ventricle. *Physiological Genomics*, *24*(1), 4–12. https://doi.org/10.1152/physiolgenomics.00161.2005

Leoni, A.-L., Marionneau, C., Demolombe, S., Bouter, S. Le, Mangoni, M. E., Escande, D., & Charpentier, F. (2006b). Chronic heart rate reduction remodels ion channel transcripts in the mouse sinoatrial node but not in the ventricle. *Physiological Genomics*, *24*(1), 4–12. https://doi.org/10.1152/physiolgenomics.00161.2005

Letts, V. A., Felix, R., Biddlecome, G. H., Arikkath, J., Mahaffey, C. L., Valenzuela, A., Bartlett, F. S., Mori, Y., Campbell, K. P., & Frankel, W. N. (1998). The mouse stargazer gene encodes a neuronal Ca2+-channel γ subunit. *Nature Genetics*, *19*(4), 340–347. https://doi.org/10.1038/1228

Lhatoo, S. D., Faulkner, H. J., Dembny, K., Trippick, K., Johnson, C., & Bird, J. M. (2010). An electroclinical case-control study of sudden unexpected death in epilepsy. *Annals of Neurology*, *68*(6), 787–796. https://doi.org/10.1002/ana.22101

Li, M., Jan, Y., & Jan, L. (1992). Specification of subunit assembly by the hydrophilic amino-terminal domain of the Shaker potassium channel. *Science*, *257*(5074), 1225–1230.

Li, R., & Buchanan, G. F. (n.d.). *Current Review Scurrying to Understand Sudden Expected Death in Epilepsy: Insights From Animal Models*. https://doi.org/10.1177/1535759719874787

Liddell, B. J., Brown, K. J., Kemp, A. H., Barton, M. J., Das, P., Peduto, A., Gordon, E., & Williams, L. M. (2005). A direct brainstem-amygdala-cortical “alarm” system for subliminal signals of fear. *NeuroImage*, *24*(1), 235–243. https://doi.org/10.1016/j.neuroimage.2004.08.016

Liu, N., Fu, C., Yu, H., Wang, Y., Shi, L., Hao, Y., Yuan, F., Zhang, X., & Wang, S. (2021). Respiratory Control by Phox2b-expressing Neurons in a Locus Coeruleus–preBötzinger Complex Circuit. *Neuroscience Bulletin*, *37*(1), 31–44. https://doi.org/10.1007/s12264-020-00519-1

Liu, Y., Qi, S., Thomas, F., Correia, B. L., Taylor, A. P., Sillitoe, R. V., & Heck, D. H. (2020). Loss of cerebellar function selectively affects intrinsic rhythmicity of eupneic breathing. *Biology Open*. https://doi.org/10.1242/bio.048785

London, B., Guo, W., Pan, X., Lee, J. S., Shusterman, V., Rocco, C. J., Logothetis, D. A., Nerbonne, J. M., & Hill, J. A. (2001). Targeted Replacement of Kv1.5 in the Mouse Leads to Loss of the 4-Aminopyridine–Sensitive Component of $I_{K,slow}$ and Resistance to Drug-Induced QT Prolongation. *Circulation Research*, *88*(9), 940–946. https://doi.org/10.1161/hh0901.090929

Lopantsev, V., Tempel, L., & Schwartzkroin, P. A. (2003). Hyperexcitability of CA3 Pyramidal Cells in Mice Lacking the Potassium Channel Subunit Kv1. In *Epilepsia* (Vol. 44, Issue 12). http://depts.washington.edu/tempelab/

Lopez-Santiago, L. F., Yuan, Y., Wagnon, J. L., Hull, J. M., Frasier, C. R., O'Malley, H. A., Meisler, M. H., & Isom, L. L. (2017). Neuronal hyperexcitability in a mouse model of *SCN8A* epileptic encephalopathy. *Proceedings of the National Academy of Sciences*, *114*(9), 2383–2388. https://doi.org/10.1073/pnas.1616821114

Lorincz, A., & Nusser, Z. (2008). Cell-Type-Dependent Molecular Composition of the Axon Initial Segment. *The Journal of Neuroscience*, *28*(53), 14329–14340. https://doi.org/10.1523/JNEUROSCI.4833-08.2008

MacDonald, E. A., Rose, R. A., & Quinn, T. A. (2020). Neurohumoral Control of Sinoatrial Node Activity and Heart Rate: Insight From Experimental Models and Findings From Humans. In *Frontiers in Physiology* (Vol. 11). Frontiers Media S.A. https://doi.org/10.3389/fphys.2020.00170

Magiorkinis, E., Sidiropoulou, K., & Diamantis, A. (2010). Hallmarks in the history of epilepsy: Epilepsy in antiquity. *Epilepsy & Behavior*, *17*(1), 103–108. https://doi.org/10.1016/j.yebeh.2009.10.023

Manolis, T. A., Manolis, A. A., & Manolis, A. S. (2019). Cardiovascular Safety of Psychiatric Agents: A Cautionary Tale. *Angiology*, *70*(2), 103–129. https://doi.org/10.1177/0003319718780145

Manville, R. W., & Abbott, G. W. (2020). Isoform-Selective KCNA1 Potassium Channel Openers Built from Glycine. *Journal of Pharmacology and Experimental Therapeutics*, *373*(3), 391–401. https://doi.org/10.1124/jpet.119.264507

Marionneau, C., Couette, B., Liu, J., Li, H., Mangoni, M. E., Nargeot, J., Lei, M., Escande, D., & Demolombe, S. (2005). Specific pattern of ionic channel gene expression associated with pacemaker activity in the mouse heart. *The Journal of Physiology*, *562*(1), 223–234. https://doi.org/10.1113/jphysiol.2004.074047

Matos, L., Duarte, A., Ribeiro, D., Chaves, J., Amaral, O., & Alves, S. (2018). Correction of a Splicing Mutation Affecting an Unverricht-Lundborg Disease Patient by Antisense Therapy. *Genes*, *9*(9), 455. https://doi.org/10.3390/genes9090455

Mazzola, L., Mauguière, F., & Chouchou, F. (2023). Central control of cardiac activity as assessed by intra-cerebral recordings and stimulations. *Neurophysiologie Clinique*, *53*(2), 102849. https://doi.org/10.1016/j.neucli.2023.102849

Menuet, C., Connelly, A. A., Bassi, J. K., Melo, M. R., Le, S., Kamar, J., Kumar, N. N., McDougall, S. J., McMullan, S., & Allen, A. M. (2020). Prebötzinger complex neurons

drive respiratory modulation of blood pressure and heart rate. *ELife*, *9*, 1–30. https://doi.org/10.7554/eLife.57288

Mesraoua, B., Tomson, T., Brodie, M., & Asadi-Pooya, A. A. (2022). Sudden unexpected death in epilepsy (SUDEP): Definition, epidemiology, and significance of education. *Epilepsy & Behavior*, *132*, 108742. https://doi.org/10.1016/j.yebeh.2022.108742

Miceli, F., Guerrini, R., Nappi, M., Soldovieri, M. V., Cellini, E., Gurnett, C. A., Parmeggiani, L., Mei, D., & Taglialatela, M. (2022). Distinct epilepsy phenotypes and response to drugs in *KCNA1* gain- and loss-of function variants. *Epilepsia*, *63*(1). https://doi.org/10.1111/epi.17118

Miceli, F., Soldovieri, M. V., Ambrosino, P., De Maria, M., Manocchio, L., Medoro, A., & Taglialatela, M. (2015). Molecular pathophysiology and pharmacology of the voltage-sensing module of neuronal ion channels. *Frontiers in Cellular Neuroscience*, *9*. https://doi.org/10.3389/fncel.2015.00259

Mishra, V., Gautier, N. M., & Glasscock, E. (2018). Simultaneous Video-EEG-ECG Monitoring to Identify Neurocardiac Dysfunction in Mouse Models of Epilepsy. *Journal of Visualized Experiments*, *131*. https://doi.org/10.3791/57300

Mishra, V., Karumuri, B. K., Gautier, N. M., Liu, R., Hutson, T. N., Vanhoof-Villalba, S. L., Vlachos, I., Iasemidis, L., & Glasscock, E. (2017). Scn2a deletion improves survival and brain-heart dynamics in the Kcna1-null mouse model of sudden unexpected death in epilepsy (SUDEP). *Human Molecular Genetics*, *26*(11), 2091–2103. https://doi.org/10.1093/hmg/ddx104

Moore, B. M., Jou, C. J., Tatalovic, M., Kaufman, E. S., Kline, D. D., & Kunze, D. L. (2014). The Kv1.1 null mouse, a model of sudden unexpected death in epilepsy (SUDEP). *Epilepsia*, *55*(11), 1808–1816. https://doi.org/10.1111/epi.12793

Moseley, B. D., Britton, J. W., Nelson, C., Lee, R. W., & So, E. (2012). Periictal cerebral tissue hypoxemia: A potential marker of SUDEP risk. *Epilepsia*, *53*(12). https://doi.org/10.1111/j.1528-1167.2012.03707.x

Mueller, S. G., Bateman, L. M., & Laxer, K. D. (2014). Evidence for brainstem network disruption in temporal lobe epilepsy and sudden unexplained death in epilepsy. *NeuroImage: Clinical*, *5*, 208–216. https://doi.org/10.1016/j.nicl.2014.06.010

Mueller, S. G., Nei, M., Bateman, L. M., Knowlton, R., Laxer, K. D., Friedman, D., Devinsky, O., & Goldman, A. M. (2018). Brainstem network disruption: A pathway to sudden unexplained death in epilepsy? *Human Brain Mapping*, *39*(12), 4820–4830. https://doi.org/10.1002/hbm.24325

Müller, P., Takacs, D. S., Hedrich, U. B. S., Coorg, R., Masters, L., Glinton, K. E., Dai, H., Cokley, J. A., Riviello, J. J., Lerche, H., & Cooper, E. C. (2023). *KCNA1* gain-of-function epileptic encephalopathy treated with 4-aminopyridine. *Annals of Clinical and Translational Neurology*. https://doi.org/10.1002/acn3.51742

Murray, R. C., Powell, D., Curry, J. M., Sperling, M. R., Evans, J. J., & Spiegel, J. R. (2010). Epileptic Laryngospasm Presenting as a Primary Sleep Disturbance. *Archives of*

Otolaryngology–Head & Neck Surgery, *136*(10), 1025. https://doi.org/10.1001/archoto.2010.174

Nashef, L., Elson, L. S., Philippe, R., & Tomson, T. (2012). Unifying the definitions of sudden unexpected death in epilepsy. *Epilepsia*, *53*(2), 227–233. https://doi.org/10.1111/j.1528-1167.2011.03358.x

Nei, M. (2009). Cardiac Effects of Seizures. *Epilepsy Currents*, *9*(4), 91–95. https://doi.org/10.1111/j.1535-7511.2009.01303.x

Nerbonne, J. M. (2016). Molecular Basis of Functional Myocardial Potassium Channel Diversity. *Cardiac Electrophysiology Clinics*, *8*(2), 257–273. https://doi.org/10.1016/j.ccep.2016.01.001

Nerbonne, J. M., & Kass, R. S. (2005). Molecular Physiology of Cardiac Repolarization. *Physiological Reviews*, *85*(4), 1205–1253. https://doi.org/10.1152/physrev.00002.2005

Nieuwenhuys, R., Veening, J. G., & van Domburg, P. (n.d.). Core and paracores; some new chemoarchitectural entities in the mammalian neuraxis. *Acta Morphologica Neerlando-Scandinavica*, *26*(2–3), 131–163.

Nishiyama, A., Yang, Z., & Butt, A. (2005). Astrocytes and NG2-glia: what's in a name? *Journal of Anatomy*, *207*(6), 687–693. https://doi.org/10.1111/j.1469-7580.2005.00489.x

Nobis, W. P., González Otárula, K. A., Templer, J. W., Gerard, E. E., Vanhaerents, S., Lane, G., Zhou, G., Rosenow, J. M., Zelano, C., & Schuele, S. (2019). The effect of seizure spread to the amygdala on respiration and onset of ictal central apnea. *J Neurosurg*, *132*(5), 1313–1323. https://doi.org/10.3171/2019.1.JNS183157

Nobis, W. P., Schuele, S., Templer, J. W., Zhou, G., Lane, G., Rosenow, J. M., & Zelano, C. (2018). Amygdala-stimulation-induced apnea is attention and nasal-breathing dependent. *Annals of Neurology*, *83*(3), 460–471. https://doi.org/10.1002/ana.25178

Noebels, J. L., & Sidman, R. L. (1979). Inherited Epilepsy: Spike-Wave and Focal Motor Seizures in the Mutant Mouse Tottering. *Science*, *204*(4399), 1334–1336.

Ovsepian, S. V., Leberre, M., Steuber, V., O'Leary, V. B., Leibold, C., & Oliver Dolly, J. (2016). Distinctive role of KV1.1 subunit in the biology and functions of low threshold K+ channels with implications for neurological disease. *Pharmacology and Therapeutics*, *159*, 93–101. https://doi.org/10.1016/j.pharmthera.2016.01.005

Parcej D.N., Scott V.E., & Dolly J.O. (1992). Oligomeric properties of alpha-dendrotoxin-sensitive potassium ion channels purified from bovine brain. *Biochemistry*, *31*(45), 11084–11088. https://doi.org/10.1021/bi00160a018

Patodia, S., Somani, A., Liu, J., Cattaneo, A., Paradiso, B., Garcia, M., Othman, M., Diehl, B., Devinsky, O., Mills, J. D., Foong, J., & Thom, M. (2022). Serotonin transporter in the temporal lobe, hippocampus and amygdala in <scp>SUDEP</scp>. *Brain Pathology*, *32*(5). https://doi.org/10.1111/bpa.13074

Patodia, S., Somani, A., & Thom, M. (2021). Review: Neuropathology findings in autonomic brain regions in SUDEP and future research directions. *Autonomic Neuroscience*, *235*, 102862. https://doi.org/10.1016/j.autneu.2021.102862

Paulhus, K., Ammerman, L., & Glasscock, E. (2020). Clinical spectrum of KCNA1 mutations: New insights into episodic ataxia and epilepsy comorbidity. *International Journal of Molecular Sciences*, *21*(8). https://doi.org/10.3390/ijms21082802

Paulhus, K., & Glasscock, E. (2023). Novel Genetic Variants Expand the Functional, Molecular, and Pathological Diversity of KCNA1 Channelopathy. *International Journal of Molecular Sciences*, *24*(10), 8826. https://doi.org/10.3390/ijms24108826

Peng, W., Danison, J. L., & Seyal, M. (2017). Postictal generalized <scp>EEG</scp> suppression and respiratory dysfunction following generalized tonic–clonic seizures in sleep and wakefulness. *Epilepsia*, *58*(8), 1409–1414. https://doi.org/10.1111/epi.13805

Peng, W., Wu, Z., Song, K., Zhang, S., Li, Y., & Xu, M. (2020). Regulation of sleep homeostasis mediator adenosine by basal forebrain glutamatergic neurons. *Science*, *369*(6508). https://doi.org/10.1126/science.abb0556

Persson, A.-S., Klement, G., Almgren, M., Sahlholm, K., Nilsson, J., Petersson, S., Århem, P., Schalling, M., & Lavebratt, C. (2005). A truncated Kv1.1 protein in the brain of the megencephaly mouse: expression and interaction. *BMC Neuroscience*, *6*(65). https://doi.org/10.1186/1471-2202-6-65

Persson, A.-S., Westman, E., Wang, F.-H., Khan, F. H., Spenger, C., & Lavebratt, C. (2007). Kv1.1 null mice have enlarged hippocampus and ventral cortex. *BMC Neuroscience*, *8*(1), 10. https://doi.org/10.1186/1471-2202-8-10

Petersson, S., Persson, A.-S., Johansen, J. E., Ingvar, M., Nilsson, J., Ran Klement, G. È., Rhem, P. A. Ê., Schalling, M., & Lavebratt, C. (2003). Truncation of the Shaker-like voltage-gated potassium channel, Kv1.1, causes megencephaly. *European Journal of Neuroscience2*, *18*, 3231–3240. https://doi.org/10.1046/j.1460-9568.2003.03044.x

Petrucci, A. N., Joyal, K. G., Purnell, B. S., & Buchanan, G. F. (2020). Serotonin and sudden unexpected death in epilepsy. *Experimental Neurology*, *325*, 113145. https://doi.org/10.1016/j.expneurol.2019.113145

Poh, M.-Z., Loddenkemper, T., Reinsberger, C., Swenson, N. C., Goyal, S., Madsen, J. R., & Picard, R. W. (2012). Autonomic changes with seizures correlate with postictal EEG suppression. *Neurology*, *78*(23), 1868–1876. https://doi.org/10.1212/WNL.0b013e318258f7f1

Pongs, O., & Schwarz, J. R. (2010). Ancillary Subunits Associated With Voltage-Dependent K Channels. *Physiol Rev*, *90*, 755–796. https://doi.org/10.1152/physrev.00020.2009

Purnell, B., Murugan, M., Jani, R., & Boison, D. (2021). The Good, the Bad, and the Deadly: Adenosinergic Mechanisms Underlying Sudden Unexpected Death in Epilepsy. *Frontiers in Neuroscience*, *15*. https://doi.org/10.3389/fnins.2021.708304

Purnell, B. S., Alves, M., & Boison, D. (2023). Astrocyte-neuron circuits in epilepsy. *Neurobiology of Disease*, *179*, 106058. https://doi.org/10.1016/j.nbd.2023.106058

Rae Donahue, L., Cook, S. A., Johnson, K. R., Bronson, R. T., & Davissen, M. T. (1996). Megencephaly: a new mouse mutation on chromosome 6 that causes hypertrophy of the brain. *Mammalian Genome*, *7*(12), 871–876. https://doi.org/10.1007/s003359900259

Rajakulendran, S., Kaski, D., & Hanna, M. G. (2012). Neuronal P/Q-type calcium channel dysfunction in inherited disorders of the CNS. *Nature Reviews Neurology*, *8*(2), 86–96. https://doi.org/10.1038/nrneurol.2011.228

Ranjan, R., Logette, E., Marani, M., Herzog, M., Tache, V., Scantamburlo, E., Buchillier, V., & Markram, H. (2019). A Kinetic Map of the Homomeric Voltage-Gated Potassium Channel (Kv) Family. *Frontiers in Cellular Neuroscience*, *13*, 358. https://doi.org/10.3389/fncel.2019.00358

Ravindran, K., Powell, K. L., Todaro, M., & O'Brien, T. J. (2016). The pathophysiology of cardiac dysfunction in epilepsy. *Epilepsy Research*, *127*, 19–29. https://doi.org/10.1016/j.eplepsyres.2016.08.007

Rea, R., Spauschus, A., Eunson, L. H., Hanna, M. G., & Kullman, D. M. (2002). Variable K+ channel subunit dysfunction in inherited mutations of KCNA1. *Journal of Physiology*, *538*(1), 5–23. https://doi.org/10.1013/jphysiol.2001.013242

Reynolds, E. H. (2005a). *Atlas, Epilepsy Care in the World*. World Health Organization.

Reynolds, E. H. (2005b). The John Hughlings Jackson 1935 Centenary Congress Medal. *Journal of Neurology, Neurosurgery & Psychiatry*, *76*(6), 858–859. https://doi.org/10.1136/jnnp.2004.056184

Rho, J. M., Szot, P., Tempel, B. L., & Schwartzkroin, P. A. (1999). Developmental Seizure Susceptibility of Kv1.1 Potassium Channel Knockout Mice. *Developmental Neuroscience*, *21*(3–5), 320–327. https://doi.org/10.1159/000017381

Rhone, A. E., Kovach, C. K., Harmata, G. I. S., Sullivan, A. W., Tranel, D., Ciliberto, M. A., Howard, M. A., Richerson, G. B., Steinschneider, M., Wemmie, J. A., & Dlouhy, B. J. (2020). A human amygdala site that inhibits respiration and elicits apnea in pediatric epilepsy. *JCI Insight*, *5*(6), 1–16. https://doi.org/10.1172/jci.insight.134852

Ritz, T., Kroll, J. L., Aslan, S., Janssens, T., Khan, D. A., Pinkham, A. E., & Brown, E. S. (2020). Subcortical gray matter volumes in asthma: associations with asthma duration, control, and anxiety. *Brain Imaging and Behavior*, *14*(6), 2341–2350. https://doi.org/10.1007/s11682-019-00188-3

Riva, A., Golda, A., Balagura, G., Amadori, E., Vari, M. S., Piccolo, G., Iacomino, M., Lattanzi, S., Salpietro, V., Minetti, C., & Striano, P. (2021). New Trends and Most Promising Therapeutic Strategies for Epilepsy Treatment. *Frontiers in Neurology*, *12*, 753753. https://doi.org/10.3389/fneur.2021.753753

Rizvi, T. A., Ennis, M., Behbehani, M. M., & Shipley, M. T. (1991). Connections between the central nucleus of the amygdala and the midbrain periaqueductal gray: Topography and reciprocity. *The Journal of Comparative Neurology*, *303*(1), 121–131.

Robbins, C. A., & Tempel, B. L. (2012). Kv1.1 and Kv1.2: Similar channels, different seizure models. *Epilepsia*, *53*(SUPPL. 1), 134–141. https://doi.org/10.1111/j.1528-1167.2012.03484.x

Roberds, S. L., & Tamkun, M. M. (1991). Cloning and tissue-specific expression of five voltage-gated potassium channel cDNAs expressed in rat heart. *Proceedings of the National Academy of Sciences*, *88*(5), 1798–1802. https://doi.org/10.1073/pnas.88.5.1798

Ryvlin, P., Nashef, L., Lhatoo, S. D., Bateman, L. M., Bird, J., Bleasel, A., Boon, P., Crespel, A., Dworetzky, B. A., Høgenhaven, H., Lerche, H., Maillard, L., Malter, M. P., Marchal, C., Murthy, J. M. K., Nitsche, M., Pataraia, E., Rabben, T., Rheims, S., … Tomson, T. (2013). Incidence and mechanisms of cardiorespiratory arrests in epilepsy monitoring units (MORTEMUS): A retrospective study. *The Lancet Neurology*, *12*(10), 966–977. https://doi.org/10.1016/S1474-4422(13)70214-X

Ryvlin, P., Rheims, S., & Lhatoo, S. D. (2019). Risks and predictive biomarkers of SUDEP. *Current Opinion in Neurology*, *32*(2), 205–212. https://doi.org/10.1097/WCO.0000000000000668

Saha, S. (2005). Role Of The Central Nucleus Of The Amygdala In The Control Of Blood Pressure: Descending Pathways To Medullary Cardiovascular Nuclei. *Clinical and Experimental Pharmacology and Physiology*, *32*(5–6), 450–456. https://doi.org/10.1111/j.1440-1681.2005.04210.x

Scantlebury, M. H., Chun, K.-C., Ma, S.-C., Rho, J. M., & Kim, D. Y. (2017). Adrenocorticotropic hormone protects learning and memory function in epileptic Kcna1 -null mice. *Neuroscience Letters*, *645*, 14–18. https://doi.org/10.1016/j.neulet.2017.02.069

Scharfman, H. E. (2007). The neurobiology of epilepsy. *Current Neurology and Neuroscience Reports*, *7*(4), 348–354. https://doi.org/10.1007/s11910-007-0053-z

Schimitel, F. G., de Almeida, G. M., Pitol, D. N., Armini, R. S., Tufik, S., & Schenberg, L. C. (2012). Evidence of a suffocation alarm system within the periaqueductal gray matter of the rat. *Neuroscience*, *200*, 59–73. https://doi.org/10.1016/j.neuroscience.2011.10.032

Scott, M. M., Lee, C. E., & Elmquist, J. K. (2011). Leptin receptor expression in hindbrain Glp-1 neurons regulates food intake and energy balance in mice. *J Clin Invest*, *121*(6), 2413–2421. https://doi.org/10.1172/JCI43703

Scott, V. E. S., Muniz, Z. M., Sewing, S., Lichtinghagen, R., Parcej, D. N., Pongs, O., & Dolly, J. O. (1994). Antibodies Specific for Distinct Kv Subunits Unveil a Hetero-Oligomeric Basis for Subtypes of α-Dendrotoxin-Sensitive K+ Channels in Bovine Brain. *Biochemistry*, *33*(7), 1617–1623. https://doi.org/10.1021/bi00173a001

Serdyuk, S., Davtyan, K., Burd, S., Drapkina, O., Boytsov, S., Gusev, E., & Topchyan, A. (2021). Cardiac arrhythmias and sudden unexpected death in epilepsy: Results of long-term monitoring. *Heart Rhythm*, *18*(2), 221–228. https://doi.org/10.1016/j.hrthm.2020.09.002

Seyal, M., Hardin, K. A., & Bateman, L. M. (2012). Postictal generalized EEG suppression is linked to seizure-associated respiratory dysfunction but not postictal apnea. *Epilepsia*, *53*(5), 825–831. https://doi.org/10.1111/j.1528-1167.2012.03443.x

Shankar, R., Donner, E. J., McLean, B., Nashef, L., & Tomson, T. (2017). Sudden unexpected death in epilepsy (SUDEP): what every neurologist should know. *Epileptic Disorders*, *19*(1), 1–9. https://doi.org/10.1684/epd.2017.0891

Shen, H., Li, T., & Boison, D. (2010). A novel mouse model for sudden unexpected death in epilepsy (SUDEP): Role of impaired adenosine clearance. *Epilepsia*, *51*(3), 465–468. https://doi.org/10.1111/j.1528-1167.2009.02248.x

Si, M., Trosclair, K., Hamilton, K. A., & Glasscock, E. (2019). Genetic ablation or pharmacological inhibition of Kv1.1 potassium channel subunits impairs atrial repolarization in mice. *Am J Physiol Cell Physiol*, *316*, 154–161. https://doi.org/10.1152/ajpcell.00335.2018

Simeone, K. A., Hallgren, J., Bockman, C. S., Aggarwal, A., Kansal, V., Netzel, L., Iyer, S. H., Matthews, S. A., Deodhar, M., Oldenburg, P. J., Abel, P. W., & Simeone, T. A. (2018). Respiratory dysfunction progresses with age in Kcna1-null mice, a model of sudden unexpected death in epilepsy. *Epilepsia*, *59*(2), 345–357. https://doi.org/10.1111/epi.13971

Simeone, K. A., Matthews, S. A., Rho, J. M., & Simeone, T. A. (2016). Ketogenic Diet Treatment Increases Longevity in Kcna1-null Mice, a Model of Sudden Unexpected Death in Epilepsy. *Epilepsia*, *57*(8), e178–e182. https://doi.org/10.1111/epi.13444

Simeone, K. A., Wilke, J. C., Matthews, S. A., Simeone, T. A., & Rho, J. M. (2021). Ketogenic diet–mediated seizure reduction preserves CA1 cell numbers in epileptic *Kcna1* -null mice: An unbiased stereological assessment. *Epilepsia*, *62*(8). https://doi.org/10.1111/epi.16983

Simeone, T. A., Simeone, K. A., Samson, K. K., Kim, D. Y., & Rho, J. M. (2013). Loss of the Kv1.1 potassium channel promotes pathologic sharp waves and high frequency oscillations in in vitro hippocampal slices. *Neurobiology of Disease*, *54*, 68–81. https://doi.org/10.1016/j.nbd.2013.02.009

Simon, R. P. (1997). Epileptic Sudden Death: Animal Models. *Epilepsia*, *38*(s11). https://doi.org/10.1111/j.1528-1157.1997.tb06124.x

Singh, V., Ryan, J. M., & Auerbach, D. S. (2023). It is premature for a unified hypothesis of sudden unexpected death in epilepsy: A great amount of research is still needed to understand the multisystem cascade. *Epilepsia*, *64*(8), 2006–2010. https://doi.org/10.1111/epi.17636

Sivathamboo, S., Nhu, D., Piccenna, L., Yang, A., Antonic-Baker, A., Vishwanath, S., Todaro, M., Yap, L. W., Kuhlmann, L., Cheng, W., O'Brien, T. J., Lannin, N. A., & Kwan, P. (2022). Preferences and User Experiences of Wearable Devices in Epilepsy. *Neurology*, *99*(13). https://doi.org/10.1212/WNL.0000000000200794

Smart, S. L., Lopantsev, V., Zhang, C. L., Robbins, C. A., Wang, H., Chiu, S. Y., Schwartzkroin, P. A., Messing, A., & Tempel, B. L. (1998). Deletion of the K(v)1.1 Potassium channel causes epilepsy in mice. *Neuron*, *20*, 809–819. https://doi.org/10.1016/S0896-6273(00)81018-1

Smith, J., Richerson, G., Kouchi, H., Duprat, F., Mantegazza, M., Bezin, L., & Rheims, S. (2024). Are we there yet? A critical evaluation of sudden and unexpected death in epilepsy models. *Epilepsia*, *65*(1), 9–25. https://doi.org/10.1111/epi.17812

Staley, K. (2015). Molecular mechanisms of epilepsy. *Nature Neuroscience*, *18*(3), 367–372. https://doi.org/10.1038/nn.3947

Stewart, C. E., Holt, A. G., Altschuler, R. A., Cacace, A. T., Hall, C. D., Murnane, O. D., King, W. M., & Akin, F. W. (2020). Effects of Noise Exposure on the Vestibular System: A Systematic Review. *Frontiers in Neurology*, *11*. https://doi.org/10.3389/fneur.2020.593919

Stornetta, R. L., Moreira, T. S., Takakura, A. C., Kang, B. J., Chang, D. A., West, G. H., Brunet, J. F., Mulkey, D. K., Bayliss, D. A., & Guyenet, P. G. (2006). Neurobiology of Disease Expression of Phox2b by Brainstem Neurons Involved in Chemosensory Integration in the Adult Rat. *The Journal of Neuroscience*, *26*(40), 10305–10314. https://doi.org/10.1523/JNEUROSCI.2917-06.2006

Sveinsson, O., Andersson, T., Mattsson, P., Carlsson, S., & Tomson, T. (2020). Clinical risk factors in SUDEP. *Neurology*, *94*(4). https://doi.org/10.1212/WNL.0000000000008741

Tang, Y., Chen, Q., Yu, X., Xia, W., Luo, C., Huang, X., Tang, H., Gong, Q., & Zhou, D. (2014). A resting-state functional connectivity study in patients at high risk for sudden unexpected death in epilepsy. *Epilepsy & Behavior*, *41*, 33–38. https://doi.org/10.1016/j.yebeh.2014.08.140

Tavee, J., & Morris III, H. (2008). Severe postictal laryngospasm as a potential mechanism for sudden unexpected death in epilepsy: a near-miss in an EMU. *Epilepsia*, *49*(12), 2113–2117. https://doi.org/10.1111/j.1528-1167.2008.01781.x

Teran, F. A., Kim, Y., Crotts, M. S., Bravo, E., Emaus, K. J., & Richerson, G. B. (2019). Time of Day and a Ketogenic Diet Influence Susceptibility to SUDEP in Scn1aR1407X/+ Mice. *Frontiers in Neurology*, *10*. https://doi.org/10.3389/fneur.2019.00278

Thouta, S., Zhang, Y., Garcia, E., & Snutch, T. P. (2021). Kv1.1 channels mediate network excitability and feed-forward inhibition in local amygdala circuits. *Scientific Reports*, *11*(1), 15180. https://doi.org/10.1038/s41598-021-94633-3

Thurman, D. J., Hesdorffer, D. C., & French, J. A. (2014). Sudden unexpected death in epilepsy: Assessing the public health burden. *Epilepsia*, *55*(10), 1479–1485. https://doi.org/10.1111/epi.12666

Trosclair, K., Dhaibar, H. A., Gautier, N. M., Mishra, V., & Glasscock, E. (2020). Neuron-specific Kv1.1 deficiency is sufficient to cause epilepsy, premature death, and cardiorespiratory dysregulation. *Neurobiology of Disease*, *137*, 1–12. https://doi.org/10.1016/j.nbd.2020.104759

Trosclair, K., Si, M., Watts, M., Gautier, N. M., Voigt, N., Traylor, J., Bitay, M., Baczko, I., Dobrev, D., Hamilton, K. A., Bhuiyan, Md. S., Dominic, P., & Glasscock, E. (2021). Kv1.1 potassium channel subunit deficiency alters ventricular arrhythmia susceptibility, contractility, and repolarization. *Physiological Reports*, *9*(1). https://doi.org/10.14814/phy2.14702

Tupal, S., & Faingold, C. L. (2006). Evidence Supporting a Role of Serotonin in Modulation of Sudden Death Induced by Seizures in DBA/2 Mice. *Epilepsia*, *47*(1), 21–26. https://doi.org/10.1111/j.1528-1167.2006.00365.x

van der Lende, M., Surges, R., Sander, J. W., & Thijs, R. D. (2015). Cardiac arrhythmias during or after epileptic seizures. *Journal of Neurology, Neurosurgery & Psychiatry*, jnnp-2015-310559. https://doi.org/10.1136/jnnp-2015-310559

Van Dyke, D. (1975). Hereditary Myokymia and Periodic Ataxia. *Journal of the Neurological Sciences*, *25*(1), 109–118. https://doi.org/doi:10.1016/0022-510X(75)90191-4

Vanhoof-Villalba, S. L., Gautier, N. M., Mishra, V., & Glasscock, E. (2018). Pharmacogenetics of KCNQ channel activation in two potassium channelopathy mouse models of epilepsy. *Epilepsia*, *59*(2), 358–368. https://doi.org/10.1111/epi.13978

Veeramah, K. R., Johnstone, L., Karafet, T. M., Wolf, D., Sprissler, R., Salogiannis, J., Barth-Maron, A., Greenberg, M. E., Stuhlmann, T., Weinert, S., Jentsch, T. J., Pazzi, M., Restifo, L. L., Talwar, D., Erickson, R. P., & Hammer, M. F. (2013). Exome sequencing reveals new causal mutations in children with epileptic encephalopathies. *Epilepsia*, *54*(7), 1270–1281. https://doi.org/10.1111/epi.12201

Verrier, R. L., Pang, T. D., Nearing, B. D., & Schachter, S. C. (2020). The Epileptic Heart: Concept and clinical evidence. *Epilepsy & Behavior*, *105*, 106946. https://doi.org/10.1016/j.yebeh.2020.106946

Vilella, L., Lacuey, N., Hampson, J. P., Rani, M. R. S., Loparo, K., Sainju, R. K., Friedman, D., Nei, M., Strohl, K., Allen, L., Scott, C., Gehlbach, B. K., Zonjy, B., Hupp, N. J., Zaremba, A., Shafiabadi, N., Zhao, X., Reick-Mitrisin, V., Schuele, S., … Lhatoo, S. D. (2019). Incidence, Recurrence, and Risk Factors for Peri-ictal Central Apnea and Sudden Unexpected Death in Epilepsy. *Frontiers in Neurology*, *10*. https://doi.org/10.3389/fneur.2019.00166

Wagnon, J. L., Korn, M. J., Parent, R., Tarpey, T. A., Jones, J. M., Hammer, M. F., Murphy, G. G., Parent, J. M., & Meisler, M. H. (2015). Convulsive seizures and SUDEP in a mouse model of SCN8A epileptic encephalopathy. *Human Molecular Genetics*, *24*(2), 506–515. https://doi.org/10.1093/hmg/ddu470

Wang, H., Kunkel, D. D., Martin, T. M., Schwartzkroin, P. A., & Tempel, B. L. (1993). Heteromultimeric K+ channels in terminal and juxtaparanodal regions of neurons. *Nature*, *365*, 75–79. https://doi.org/10.1038/365075a0.

Wang, H., Kunkel, D. D., Schwartzkroin, P. A., & Ternpep, B. L. (1994). Localization of Kvl .I and Kvl.2, Two K Channel Proteins, to Synaptic Terminals, Somata, and Dendrites in the Mouse Brain. *The Journal of Neuroscience*, *14*(8), 4588–4599. https://doi.org/10.1523/JNEUROSCI.14-08-04588.1994

Wang, H. T., Zhu, Z. A., Li, Y. Y., Lou, S. Sen, Yang, G., Feng, X., Xu, W., Huang, Z. L., Cheng, X., & Xiong, Z. Q. (2021). CDKL5 deficiency in forebrain glutamatergic neurons results in recurrent spontaneous seizures. *Epilepsia*, *62*(2), 517–528. https://doi.org/10.1111/EPI.16805

Wang, J. Z., & Liu, F. (2008). Microtubule-associated protein tau in development, degeneration and protection of neurons. In *Progress in Neurobiology* (Vol. 85, Issue 2, pp. 148–175). https://doi.org/10.1016/j.pneurobio.2008.03.002

Wehrwein, E. A., Orer, H. S., & Barman, S. M. (2016). Overview of the Anatomy, Physiology, and Pharmacology of the Autonomic Nervous System. In *Comprehensive Physiology* (pp. 1239–1278). Wiley. https://doi.org/10.1002/cphy.c150037

Weltha, L., Reemmer, J., & Boison, D. (2019). The role of adenosine in epilepsy. *Brain Research Bulletin*, *151*, 46–54. https://doi.org/10.1016/j.brainresbull.2018.11.008

Wenker, I. C., Teran, F. A., Wengert, E. R., Wagley, P. K., Panchal, P. S., Blizzard, E. A., Saraf, P., Wagnon, J. L., Goodkin, H. P., Meisler, M. H., Richerson, G. B., & Patel, M. K. (2021). Postictal Death Is Associated with Tonic Phase Apnea in a Mouse Model of Sudden Unexpected Death in Epilepsy. *Annals of Neurology*, *89*(5), 1023–1035. https://doi.org/10.1002/ana.26053

Wenzel, H. J., Vacher, H., Clark, E., Trimmer, J. S., Lee, A. L., Sapolsky, R. M., Tempel, B. L., & Schwartzkroin, P. A. (2007). Structural Consequences of Kcna1 Gene Deletion and Transfer in the Mouse Hippocampus NIH Public Access. *Epilepsia*, *48*(11), 2023–2046. https://doi.org/10.1111/j.1528-1167.2007.01189.x

Whitney, R., & Donner, E. J. (2019). Risk Factors for Sudden Unexpected Death in Epilepsy (SUDEP) and Their Mitigation. *Current Treatment Options in Neurology*, *21*(2), 7. https://doi.org/10.1007/s11940-019-0547-4

Williams, R. W., & Herrup, K. (1988). The Control of Neuron Number. *Annual Review of Neuroscience*, *11*(1), 423–453. https://doi.org/10.1146/annurev.ne.11.030188.002231

Yang, C. F., Kim, E. J., Callaway, E. M., & Feldman, J. L. (2020). Monosynaptic Projections to Excitatory and Inhibitory preBötzinger Complex Neurons. *Frontiers in Neuroanatomy*, *14*. https://doi.org/10.3389/fnana.2020.00058

Yokoi, N., Fukata, M., & Fukata, Y. (2012). *Synaptic Plasticity Regulated by Protein–Protein Interactions and Posttranslational Modifications* (pp. 1–43). https://doi.org/10.1016/B978-0-12-394308-8.00001-7

Yuan, H., Yuan, H., Wang, Q., Ye, W., Yao, R., Xu, W., & Liu, Y. (2020). Two novel *KCNA1* variants identified in two unrelated Chinese families affected by episodic ataxia type 1 and neurodevelopmental disorders. *Molecular Genetics & Genomic Medicine*, *8*(10). https://doi.org/10.1002/mgg3.1434

Zack, M. M., & Kobau, R. (2017). National and State Estimates of the Numbers of Adults and Children with Active Epilepsy — United States, 2015. *MMWR. Morbidity and Mortality Weekly Report*, *66*(31), 821–825. https://doi.org/10.15585/mmwr.mm6631a1